

# LATTICE THEORY AND ALGEBRAIC MODELS FOR DEEP CONVOLUTIONAL LEARNING BASED ON MATHEMATICAL MORPHOLOGY

GUSTAVO (JESÚS) ANGULO

ABSTRACT. We develop a rigorous algebraic framework for deep convolutional architectures, CNNs, ResNets, and encoder–decoder networks such as UNet, grounded in lattice theory and mathematical morphology. The central tool is the Matheron–Maragos–Banon–Barrera (MMBB) universal representation theory for translation-invariant operators, which we apply systematically to every layer of a standard deep network.

The principal finding is that the standard CNN pipeline (linear convolution + ReLU + flat max-pooling) is a *cross-lattice* operator: the convolution is an erosion in the Fourier inf-semilattice while ReLU is a lattice-join closing and max-pooling is a dilation in the pointwise max-plus lattice, and their composition is a morphological opening in neither. A second finding is that the upper adjoint of ReLU in the pointwise lattice is a global (non-local) operator, the identity on globally non-negative functions and  $-\infty$  otherwise, so no local morphological erosion can form an adjunction pair with ReLU. These two results together provide the precise algebraic reason why depth in standard CNNs introduces genuine representational power: the composed layer is not idempotent.

Three layer designs that *are* genuine idempotent openings are identified and fully characterised: the pure max-plus morphological layer (Type I, pointwise lattice), the spectral Wiener layer (Type II, Fourier lattice, idempotent in the limit  $\epsilon \rightarrow 0$ ), and the self-dual morphological layer (Type III, median inf-semilattice for signed feature maps). For Type I layers we establish a complete fixed-point and convergence theory: the morphological ResNet block converges in one step by idempotency, while the naive residual iteration  $\Phi(f) + f$  diverges.

The framework also unifies max-pooling, strided convolution, and the Laplacian pyramid under the Goutsias–Heijmans adjoint pyramid theory, and gives the Activation–Pooling Dilation (APD) factorisation with its correct adjoint (piecewise-constant upsampling by stride  $R$ ). The UResNet architecture is proposed, in which skip connections carry residues of openings rather than concatenated features, achieving exact scale-by-scale reconstruction.

Building on prior work by the author, this paper provides the lattice-specific operator-theoretic content that both categorical and computational approaches to deep learning currently lack.

## CONTENTS

1. Introduction	3
2. Complete Lattices and the MMBB Representation Theory	6
2.1. Complete lattices and adjunctions	6
2.2. The canonical max-plus adjunction	7
2.3. The max-times adjunction and its equivalence to max-plus via log/exp	8

---

*Date:* April 28th, 2026.

*2020 Mathematics Subject Classification.* 68T07, 06B23, 68U10, 06A15, 42B10 .

*Key words and phrases.* Mathematical morphology, lattice theory, complete inf-semilattice, universal representation theory, morphological operators, convolutional neural networks, ReLU nets, max-pooling, fixed-points, adjunctions, ResNet, UNet, self-dual operators.

2.4.	MMBB universal representation of translation-invariant increasing operators	9
2.5.	MMBB universal representation of translation-invariant general operators	10
3.	Ovchinnikov's Lattice Polynomial Representation and ReLU Networks	11
3.1.	Explicit lattice polynomial equations for ReLU networks	12
4.	Morphological Basis of Convolution	14
4.1.	Conditions for the MMBB-Increasing framework to apply	14
4.2.	Kernel and morphological basis of a convolution	15
4.3.	MMBB-General representation of signed convolution	15
4.4.	Characteristic matrix and virtual basis for quantised signals (binary, ternary, and low-bit networks)	18
4.5.	Deep learning perspective: learnable morphological bases	20
5.	Complete Lattice Structure of Pooling and Morphological Pyramids	20
5.1.	Abstract pyramid structure and the adjunction condition	20
5.2.	Three canonical morphological pyramids	21
5.3.	Morphological skeleton and the Laplacian pyramid	22
6.	ReLU, Max-Pooling, and Morphological Activations	23
6.1.	ReLU and max-pooling as dilations in the pointwise lattice	24
6.2.	Factorisation and the Activation-Pooling Dilation	25
6.3.	Generalised morphological activations via MMBB	26
7.	Morphological Models of Deep Convolutional Architectures	31
7.1.	The morphological CNN layer	31
7.2.	The general morphological nonlinear layer in a CNN: APMO	32
7.3.	Morphological model of ResNet	34
7.4.	Morphological model of UNet	35
8.	Fixed Points, Idempotency, and Convergence of Morphological Layers	38
9.	The Median Inf-Semilattice, Self-Dual Operators, and Their Role in Deep Network Models	46
9.1.	Median partial ordering and its inf-semilattice	46
9.2.	Self-dual erosion and opening	47
9.3.	Self-dual pooling and signed activation functions	50
9.4.	Self-dual operators in deep network architectures	54
10.	Discussion and Perspectives	60
10.1.	Summary of contributions and corrected principles	60
10.2.	Open problems on morphological basis learning	62
10.3.	The Fourier perspective: a companion programme	62
10.4.	Batch normalisation, dropout, and attention	63
10.5.	Connection to category theory	63
	Acknowledgements	63
	References	64
	Appendix A. Elements of the Connection to Category Theory	68
A.1.	The category of complete lattices with morphisms	68
A.2.	Adjunctions in <b>CLat</b> and the morphological adjunctions	68
A.3.	The Para construction and learnable layers	69
A.4.	Backpropagation and the reverse derivative	69

## 1. INTRODUCTION

Understanding the mathematical structure of deep neural networks beyond their empirical performance has become one of the central challenges of mathematical data science. Several research programmes have emerged to address this gap. Tropical geometry identifies the piecewise-linear (PWL) geometry of ReLU networks with the combinatorics of tropical polynomials [32, 35, 49]. Harmonic analysis studies spectral bias and the interaction of convolutional layers with Fourier representations [40]. Alternatively, category theory has been proposed as an abstract skeleton for gradient-based learning systems [10, 15], identifying backpropagation as a functor and network composition as a morphism.

The present paper pursues a different, but complementary, direction: *lattice theory and mathematical morphology* as the algebraic foundation for convolutional architectures. Mathematical morphology, developed for binary and grey-scale image analysis by Matheron, Serra, Maragos, and their schools [31, 34, 44], provides a powerful operator-theoretic calculus on complete lattices. One of its central results, the MMBB universal representation theory, named for Matheron, Maragos, Banon, and Barrera, states that any translation-invariant, increasing operator on a complete lattice is representable as a supremum of erosions, providing a constructive universal decomposition analogous to the basis representation in linear algebra. There is a more general form for any nonlinear translation-invariant operator using two families of basis with erosions and anti-dilations.

Our premise is that the operators composing a convolutional deep network, convolution, ReLU, max-pooling, strided convolution, skip connections, are all special instances, or close approximations, of morphological operators on appropriate lattices. Recognising this structure yields the following kinds of dividends: algebraic *factorisation* (which operators can be fused or commuted); algebraic *inversion* (the correct adjoint of each layer, which is lattice-dependent); *fixed-point and idempotency* characterisation (which composed layers are idempotent openings, and critically which are *not*, the standard CNN layer is not idempotent); algebraic *design* principles (how morphological pipelines inspire new architectures such as the UResNet); and the *max-times and self-dual extensions* for a mathematically consistent computational frameworks for either positive (or probabilistic) or signed feature maps.

State of the art on morphological neural networks. The intersection of mathematical morphology and neural networks has a history reaching back to the morphological/rank perceptrons of Ritter–Sussner [41] and Pessoa–Maragos [39], and to the morphological neural network frameworks initiated by Davidson–Ritter [11]. The deep learning era has brought a resurgence of this field. Franchi, Fehri, and Yao [17] demonstrated the potential of deep hybrid morphological-linear networks for image analysis. Dimitriadis and Maragos [12] showed the remarkable pruning amenability of morphological networks and the importance of shape constraints on learnable structuring elements; the same group extended this line in [13]. Maragos [32] provided a unifying treatment connecting morphological networks, max-plus algebra, and tropical geometry. More recently, work by Fotopoulos and Maragos [16] represents a significant step: they demonstrate that “linear-like” activation functions facilitate training deep morphological networks, and that residual connections substantially improve their generalisation, a finding that our algebraic analysis in Section 7 sheds new theoretical light on. Blusseau, Velasco-Forero, Angulo, and Bloch [7] showed that morphological adjunctions can be represented as matrices in max-plus algebra, providing a computationally tractable framework for the design of morphological layers. Blusseau [8] analysed the gradient flow and convergence behaviour of morphological layers trained by gradient descent, identifying conditions under which training

is well-posed. Hermary, Tochon, Puybareau, Kirszenberg, and Angulo [24] introduced smooth morphological layers (SMorph) as differentiable approximations of max-plus erosions and dilations via  $p$ -convolution, enabling gradient descent on morphological parameters; Bottenmuller, Tochon, Hermary, Puybareau, and Angulo [9] subsequently improved these layers. Dimitrova, Blusseau, and Velasco-Forero [14] study the influence of initialisation and layer differentiability on the morphological representations learned during training. We show in Sections 9 and 10 that training a morphological layer is equivalent to implicitly learning an MMBB basis: the fixed-point set of the learned layer equals the image of the corresponding opening, which is precisely the set of signals representable by that basis. Initialisation and differentiability determine which basin of attraction in basis space is reached by gradient descent. Marcondes and Barrera [33] proposed the lattice overparameterisation paradigm for learning lattice operators, which complements the MMBB-basis learning perspective developed here.

The equivariance programme, making morphological networks equivariant to group actions beyond translation, has been advanced by Sangalli, Blusseau, Velasco-Forero, and Angulo [43], who introduced morphological scale-spaces for scale-equivariant CNNs. Penaud-Polge, Velasco-Forero, and Angulo [37] developed group-equivariant morphological networks via group morphology (Roerdink’s theory), a programme subsequently extended to a full theoretical treatment in [38].

*Important scope clarification.* The present paper is *not* a contribution to morphological neural networks in the computational sense: we do not design, train, or benchmark new morphological layers. Rather, we provide the *algebraic theoretical framework* that underpins both morphological neural networks and standard deep convolutional architectures viewed morphologically. Our central claim is that this framework provides a unified language for analysing CNN, ResNet, and UNet in terms of lattice operators, adjunctions, and morphological bases, independently of whether the practitioner explicitly uses morphological layers. We also propose new architectures that are theoretically well-founded and will require computational implementation and empirical study.

Fixed points, idempotency, and stability. A key theoretical enrichment of the present paper, compared to earlier work [1], is an explicit and precise treatment of fixed-point operators and idempotency within the morphological model of deep architectures. A principal finding is that the standard CNN layer (convolution + ReLU + max-pooling) is *not* idempotent, because it is a cross-lattice composition. Idempotency, the defining property of morphological openings and closings, holds only for algebraically rigorous layer designs where both operators inhabit the same lattice and form an adjoint pair. We characterise precisely which layer designs satisfy this condition, determine their fixed-point sets, and prove convergence results for morphological ResNet and UNet blocks. This analysis connects to the author’s recent work on group-morphology fixed-point layers [3], specialised here from the group-equivariant to the translation-equivariant setting.

Relation to other prior work of the author. This paper consolidates and substantially extends a research programme presented in preliminary form at the DGMM 2021 conference [1], explored computationally jointly with Velasco-Forero [46–48]. The author’s DGMM 2025 contribution [4] studies the Fourier-domain (spectral) side of the same programme, the morphological interpretation of scattering networks, and is the object of an ongoing research line; references to the spectral lattice appear here mostly in the Fourier perspectives subsection of Section 10.

Relation to category-theoretic approaches. The categorical frameworks of Cruttwell et al. [10] and Fong et al. [15] identify the *compositional structure* of learning. Our framework is orthogonal and complementary: it furnishes the *operator-theoretic content* of each layer via the MMBB constructive universal representation theory, with explicit structuring functions, computable bases, and quantifiable approximation errors. The adjunction between erosion and dilation, the central algebraic pair of any morphological framework, is a concrete categorical adjunction, but enriched by the MMBB universality theorems that categorical approaches lack.

Main contributions. We make the following contributions, building on prior work by the author.

- C1. Max-times algebra and log-domain equivalence.** We present the max-times adjunction (multiplicative structuring functions) as a second canonical example of morphological adjunction alongside the classical max-plus, and prove their algebraic equivalence via the log/exp isomorphism. This furnishes a natural model for layers operating on positive feature maps (e.g. after softmax or sigmoid activations).
- C2. Banon–Barrera representation for non-increasing neural network operators.** We include the full Banon–Barrera (1993) sup-generating decomposition for TI operators that are *not* necessarily increasing, which decomposes any such mapping as a supremum of inf-combinations of an erosion and an anti-dilation. This extends the representational scope of the MMBB framework to signed CNN layers with general (non-positive) kernels.
- C3. MMBB basis of convolution and learnable layers.** The morphological basis of a positive normalised convolution kernel  $k$  with support of size  $N$  is isomorphic to the  $(N-1)$ -dimensional hyperplane in  $\mathbb{R}^N$  orthogonal to  $k$  (Maragos–Schafer), computed via the characteristic matrix  $A_k$  (Khosravi–Schafer). We develop the virtual basis theory for quantised signals and propose the MMBB layer as a finite, learnable truncation.
- C4. Pooling as morphological pyramid; cross-lattice structure.** Max-pooling, strided convolution, and the Laplacian pyramid are unified as cases of the Goutsias–Heijmans adjoint pyramid. We prove that the standard CNN layer is a *cross-lattice* operator and is generically *not* idempotent.
- C5. ReLU adjoint and non-locality of its adjoint erosion.** We prove that the upper adjoint of ReLU in the pointwise lattice  $(\text{Fun}(E, \overline{\mathbb{R}}), \leq)$  is *not* a pointwise (local) operator: it is the identity on functions that are globally non-negative, and  $-\infty$  on all others. This global character distinguishes ReLU from max-plus dilations, whose adjoints are always local morphological erosions. As a consequence, no local morphological erosion can form an adjunction pair with ReLU in the pointwise lattice, providing a second independent algebraic explanation (complementing the cross-lattice argument) for why  $\delta_R^{\text{MP}} \circ \delta^{\text{ReLU}}$  cannot be a morphological opening. The same non-locality propagates to the APD, whose adjoint is a global piecewise-constant upsampling by stride  $R$  followed by a bias shift  $-\alpha$ .
- C6. Morphological activation family and APD factorisation.** We introduce the *morphological activation family*  $\sigma_{\mathcal{B},c}^{\text{M}}$  as a supremum of Banon–Barrera sup-generating operators sharing a common cap, derived via complete distributivity of  $(\overline{\mathbb{R}}, \leq)$  ( $b \wedge \bigvee_g a_g = \bigvee_g (b \wedge a_g)$ , valid in any completely distributive lattice). This family unifies ReLU and its morphological generalisations under a single algebraic framework. We prove the *Activation-Pooling Dilation* (APD) factorisation: decimated ReLU and max-pooling compose into a single dilation  $\Psi_{R;\alpha}^{\text{APD}}(f)(n) = \sup_{y \in W_R} \max(0, f(Rn-y) + \alpha)$  on the coarser output grid, whose adjoint is a global piecewise-constant upsampling by factor  $R$  followed by a bias shift  $-\alpha$ .
- C7. Self-dual operators, signed activations, and UResNet.** The median complete inf-semilattice and its self-dual erosion and opening provide a third family of idempotent layers,

extending the fixed-point analysis to signed feature maps (a design appropriate for ResNet residuals, normalised features, and Fourier coefficients). Standard ReLU is *not* a median-lattice dilation; Leaky/Parametric ReLU are; the self-dual opening  $\gamma_W^{\text{Med}}$  is idempotent in the median lattice. We propose the UResNet, whose residual skip connections are algebraically motivated as top-hat transforms of the encoder’s adjoint opening.

**C8. Three idempotent layer designs.** Three families of CNN-like layers that *are* genuine morphological openings are identified: (I) the *pure morphological* (max-plus) layer  $\gamma_b^{\text{M}} = \delta_{b^*} \circ \varepsilon_b$ , where both erosion and dilation use the same structuring function in the pointwise lattice; (II) the *spectral Wiener* layer  $\gamma_k^{\text{F}} = \delta_k^{*,\text{Conv}} \circ \varepsilon_k^{\text{Conv}}$  (convolution followed by Tikhonov-regularised Wiener deconvolution), an opening in the Fourier lattice, exactly idempotent as  $\varepsilon \rightarrow 0$ ; and (III) the *self-dual opening*  $\gamma_W^{\text{Med}}$  in the median inf-semilattice, idempotent and with fixed-point set closed under negation. Types (I) and (III) converge to their fixed-point set in one step; Type (II) does so in the limit  $\varepsilon \rightarrow 0$ .

Organisation. Section 2 reviews complete lattice theory, the max-plus and max-times adjunctions, and the full MMBB representation theory from Matheron–Maragos to the Banon–Barrera extension. Section 3 connects Ovchinnikov’s lattice polynomial representation to tropical geometry and ReLU networks, with explicit lattice polynomial equations for single-layer and deep networks. Section 4 develops the morphological basis of convolution, the characteristic matrix, the virtual basis, and the MMBB representation of signed convolution. Section 5 establishes the adjoint pyramid framework for pooling, strided convolution, and the Laplacian pyramid. Section 6 analyses ReLU, max-pooling, and morphological activations as lattice operators. Section 7 synthesises the preceding theory into morphological models of CNN, ResNet, UNet, and the proposed UResNet. Section 8 develops the fixed-point and idempotency theory, identifying the two disciplined idempotent designs in the pointwise and Fourier lattices (Types I and II) and the correct convergence behaviour for morphological ResNet and UNet blocks; Type III (self-dual opening) is treated in Section 9. Section 9 introduces the median inf-semilattice, self-dual operators, and their architectural implications for signed activations and symmetric pooling. Section 10 concludes with a summary of contributions, open problems, and future directions. Additionally, the connection to category theory is preliminarily explored in Section A.

Road map of main results. Each section opens with a summary table of its principal results (Theorems, Propositions, Corollaries, Lemmas), with a one-line statement of each and its role in the overall argument.

## 2. COMPLETE LATTICES AND THE MMBB REPRESENTATION THEORY

We recall the algebraic framework of mathematical morphology on complete lattices, following Matheron [34], Maragos [31], Heijmans–Ronse [20] and Banon–Barrera [6].

**2.1. Complete lattices and adjunctions.** A *complete lattice*  $(\mathcal{L}, \leq)$  is a partially ordered set in which every subset  $S \subseteq \mathcal{L}$  admits a supremum  $\bigvee S$  and an infimum  $\bigwedge S$ . The canonical examples in our setting are:

- The power set  $\mathcal{P}(E)$  ordered by inclusion, where  $E = \mathbb{R}^n$  or  $\mathbb{Z}^n$ .
- The set of functions  $\mathcal{L} = \text{Fun}(E, \overline{\mathbb{R}})$  with  $\overline{\mathbb{R}} = \mathbb{R} \cup \{-\infty, +\infty\}$  ordered pointwise:  $f \leq g \iff f(x) \leq g(x), \forall x \in E$ .

TABLE 1. Principal results of §2 (Complete Lattices and MMBB). Results marked (★) are the paper’s principal findings.

Ref.	Name	Statement and role
Prop 2.2	Adjunction properties	Six structural consequences of any adjunction $(\varepsilon, \delta)$ : inf/sup commutativity, anti-extensivity, extensivity, opening and closing idempotency. Algebraic foundation for all subsequent results.
Prop 2.4	Max-times adjunction	$(\varepsilon_b^\times, \delta_{b^*}^\times)$ is an adjunction on positive functions; natural morphological model for layers after softmax or sigmoid activations.
Prop 2.5	Log/exp isomorphism	Max-times and max-plus algebras are isomorphic via log/exp; the entire MMBB theory transfers to positive layers without modification.
Thm 2.8 (★)	MMBB-Increasing	Any TI increasing USC operator equals $\sup_{g \in \text{Bas}(\Psi)} \varepsilon_g f$ exactly. Universal constructive decomposition for all TI increasing CNN layers.
Thm 2.11 (★)	MMBB-General	Any TI USC operator (not necessarily increasing) equals $\sup_i \psi_{g_i^-, g_i^+} f$ . Extends MMBB representation to signed CNN kernels via sup-generating operators.

**Definition 2.1** (Adjunction). Let  $(\mathcal{L}_1, \leq_1)$  and  $(\mathcal{L}_2, \leq_2)$  be complete lattices. A pair of operators  $(\varepsilon, \delta)$  with  $\varepsilon : \mathcal{L}_1 \rightarrow \mathcal{L}_2$  and  $\delta : \mathcal{L}_2 \rightarrow \mathcal{L}_1$  forms an *adjunction* (or *Galois connection*) if

$$\forall f \in \mathcal{L}_1, g \in \mathcal{L}_2 : \varepsilon(f) \leq_2 g \iff f \leq_1 \delta(g).$$

In this case  $\varepsilon$  is called the *erosion* and  $\delta$  the *dilation*.

Adjunctions immediately yield the following structural properties, which are used throughout the paper.

**Proposition 2.2** (Properties of adjunctions [20]). *If  $(\varepsilon, \delta)$  is an adjunction between complete lattices, then:*

- (i)  $\varepsilon$  commutes with infima:  $\varepsilon(\bigwedge_i f_i) = \bigwedge_i \varepsilon(f_i)$ .
- (ii)  $\delta$  commutes with suprema:  $\delta(\bigvee_i g_i) = \bigvee_i \delta(g_i)$ .
- (iii)  $\varepsilon$  is increasing and anti-extensive (when  $b(0) \leq 0$ , e.g.  $b(0) = 0$ ):  $\varepsilon(f) \leq f$ .
- (iv)  $\delta$  is increasing and extensive:  $g \leq \delta(g)$ .
- (v) The composition  $\gamma = \delta \circ \varepsilon$  is an opening: idempotent, increasing, and anti-extensive.
- (vi) The composition  $\varphi = \varepsilon \circ \delta$  is a closing: idempotent, increasing, and extensive.

**2.2. The canonical max-plus adjunction.** The classical morphological erosion and dilation on  $\text{Fun}(E, \overline{\mathbb{R}})$  by a structuring function  $b : E \rightarrow \overline{\mathbb{R}}$  are:

$$(\varepsilon_b f)(x) = \inf_{y \in E} \{f(x + y) - b(y)\}, \quad (1)$$

$$(\delta_b f)(x) = \sup_{y \in E} \{f(x - y) + b(y)\}. \quad (2)$$

The pair  $(\varepsilon_b, \delta_{b^*})$  with  $b^*(x) = b(-x)$  forms an adjunction in the pointwise lattice  $(\text{Fun}(E, \overline{\mathbb{R}}), \leq)$  [21, 31].

**2.3. The max-times adjunction and its equivalence to max-plus via log/exp.** A less known second canonical adjunction arises naturally for operators on *positive* functions, modelling layers that follow a softmax, sigmoid, or other positivity-enforcing nonlinearity. Replace addition in the max-plus algebra by multiplication and subtraction by division.

**Definition 2.3** (Max-times erosion and dilation). Let  $f, b : E \rightarrow (0, +\infty)$  be strictly positive functions. The *max-times* (or multiplicative morphological) erosion and dilation by structuring function  $b$  are:

$$(\varepsilon_b^\times f)(x) = \inf_{y \in E} \frac{f(x+y)}{b(y)}, \quad (3)$$

$$(\delta_b^\times f)(x) = \sup_{y \in E} f(x-y) \cdot b(y). \quad (4)$$

**Proposition 2.4** (Max-times adjunction). *The pair  $(\varepsilon_b^\times, \delta_{b^*}^\times)$ , with  $b^*(x) = b(-x)$ , forms an adjunction on  $(\text{Fun}(E, (0, +\infty)), \leq)$ :*

$$(\varepsilon_b^\times f) \leq g \iff f \leq (\delta_{b^*}^\times g).$$

*The composition  $\gamma_b^\times = \delta_{b^*}^\times \circ \varepsilon_b^\times$  is a morphological opening on positive functions: increasing, anti-extensive, and idempotent.*

*Proof.*  $(\varepsilon_b^\times f)(x) \leq g(x)$  for all  $x$  iff  $\inf_y f(x+y)/b(y) \leq g(x)$  for all  $x$  iff there exists  $y_0$  with  $f(x+y_0)/b(y_0) \leq g(x)$ , i.e.,  $f(x+y_0) \leq g(x)b(y_0)$ . Translating:  $f(z) \leq g(z-y_0)b(y_0) \leq \sup_y g(z-y)b(y) = (\delta_{b^*}^\times g)(z)$ . The reverse implication is symmetric. Idempotency of the opening follows from Proposition 2.2(v).  $\square$

**Proposition 2.5** (Log/exp isomorphism between max-plus and max-times). *The maps  $\log : (0, +\infty) \rightarrow \mathbb{R}$  and  $\exp : \mathbb{R} \rightarrow (0, +\infty)$  are mutually inverse lattice isomorphisms between the max-times algebra on  $(0, +\infty)$  and the max-plus algebra on  $\mathbb{R}$ :*

$$\log(\varepsilon_b^\times f)(x) = \inf_y \{\log f(x+y) - \log b(y)\} = (\varepsilon_{\log b} \log f)(x), \quad (5)$$

$$\log(\delta_b^\times f)(x) = \sup_y \{\log f(x-y) + \log b(y)\} = (\delta_{\log b} \log f)(x). \quad (6)$$

*That is, the max-times erosion (resp. dilation) by  $b$  on positive functions is the max-plus erosion (resp. dilation) by  $\log b$  on log-domain functions:*

$$\varepsilon_b^\times = \exp \circ \varepsilon_{\log b} \circ \log, \quad \delta_b^\times = \exp \circ \delta_{\log b} \circ \log. \quad (7)$$

*Consequently, the max-times opening  $\gamma_b^\times$  is algebraically equivalent to the max-plus opening  $\gamma_{\log b}$  composed with log/exp:  $\gamma_b^\times = \exp \circ \gamma_{\log b} \circ \log$ .*

*Proof.* Direct computation:  $\log(\varepsilon_b^\times f)(x) = \log \inf_y \frac{f(x+y)}{b(y)} = \inf_y (\log f(x+y) - \log b(y))$ , which is the max-plus erosion  $\varepsilon_{\log b}$  applied to  $\log f$ . The dilation identity is analogous. Since both  $\log$  and  $\exp$  are order-isomorphisms (strictly increasing bijections), they interleave adjunctions:  $(\varepsilon_b^\times, \delta_{b^*}^\times)$  is an adjunction on positive functions iff  $(\varepsilon_{\log b}, \delta_{\log b^*})$  is an adjunction on  $\mathbb{R}$ -valued functions, which holds by the standard max-plus theory.  $\square$

**Remark 2.6** (Deep learning relevance of max-times). The max-times adjunction is the natural morphological framework for layers that operate on probability vectors, attention weights, or outputs of sigmoid/softmax activations, all of which are constrained to  $(0, 1)$  or more generally  $(0, +\infty)$ . In these settings, the log-domain equivalence (Theorem 2.5) means that any max-times morphological analysis translates immediately to max-plus results via the change of variable  $\tilde{f} = \log f$ ,  $\tilde{b} = \log b$ . In particular, the MMBB representation theory discussed below

in (Theorem 2.8) applies to positive TI increasing operators via the log-domain isomorphism, and the virtual basis of a positive convolution kernel (Section 4) transfers to the multiplicative setting without modification.

#### 2.4. MMBB universal representation of translation-invariant increasing operators.

Let  $E = \mathbb{R}^n$  or  $E = \mathbb{Z}^n$ . An operator  $\Psi : \text{Fun}(E, \overline{\mathbb{R}}) \rightarrow \text{Fun}(E, \overline{\mathbb{R}})$  is *translation-invariant* (TI) if  $\Psi[f(\cdot - y)](x) = [\Psi f](x - y)$  for all  $y \in E$ , and *increasing* if  $f \leq g \Rightarrow \Psi f \leq \Psi g$ .

**Definition 2.7** (Kernel and basis). The *kernel* of a TI operator  $\Psi$  is

$$\text{Ker}(\Psi) = \{f \in \text{Fun}(E, \overline{\mathbb{R}}) : [\Psi f](0) \geq 0\}.$$

The *morphological basis* is the set of minimal elements of  $\text{Ker}(\Psi)$  under the pointwise order  $\leq$ :

$$\text{Bas}(\Psi) = \{g \in \text{Ker}(\Psi) : [f \in \text{Ker}(\Psi), f \leq g] \Rightarrow f = g\}.$$

The following is the central representation theorem, combining results of Matheron [34] (set case) and Maragos [31] (function case). We include a sketch of the proof to emphasize the role of the assumptions.

**Theorem 2.8** (MMBB-Increasing – Matheron 1975, Maragos 1989). *Let  $\Psi : \text{Fun}(E, \overline{\mathbb{R}}) \rightarrow \text{Fun}(E, \overline{\mathbb{R}})$  be a TI, increasing, and upper semi-continuous operator. Then  $\text{Bas}(\Psi)$  exists and  $\Psi$  is represented exactly as*

$$[\Psi f](x) = \sup_{g \in \text{Bas}(\Psi)} (\varepsilon_g f)(x) = \sup_{g \in \text{Bas}(\Psi)} \inf_{y \in E} \{f(x + y) - g(y)\}.$$

Equivalently, using the basis of the dual operator  $\bar{\Psi}(f) = -\Psi(-f)$ ,

$$[\Psi f](x) = \inf_{h \in \text{Bas}(\bar{\Psi})} (\delta_{h^*} f)(x).$$

The representation is also valid for any superset of the basis (redundant but correct), and truncated to a finite sub-basis  $\mathcal{B} \subset \text{Bas}(\Psi)$  gives lower and upper approximations:

$$\sup_{g \in \mathcal{B}} \varepsilon_g f \leq \Psi f \leq \inf_{h \in \mathcal{B}} \delta_{h^*} f.$$

*Proof sketch.* We outline the three main steps; full details are in [21, 31].

*Step 1: Existence of the basis.* The kernel  $\text{Ker}(\Psi) = \{f : [\Psi f](0) \geq 0\}$  is a non-empty collection of functions: the constant function  $f \equiv +\infty$  always belongs to  $\text{Ker}(\Psi)$ , since any TI increasing operator maps  $+\infty$  to  $+\infty$ , giving  $[\Psi(+\infty)](0) = +\infty \geq 0$ . Ordered by  $\leq$ ,  $\text{Ker}(\Psi)$  is a partially ordered set. Upper semi-continuity of  $\Psi$  implies that any decreasing sequence  $(f_n) \subset \text{Ker}(\Psi)$  with  $f_n \downarrow f$  satisfies  $f \in \text{Ker}(\Psi)$ , ensuring the existence of minimal elements. By Zorn's lemma (or its constructive counterpart for USC operators), the set  $\text{Bas}(\Psi)$  of minimal elements of  $\text{Ker}(\Psi)$  is non-empty.

*Step 2: Representation by supremum of erosions.* For each  $g \in \text{Ker}(\Psi)$ , translation-invariance gives  $[\Psi f_y](0) = [\Psi f](y)$  where  $f_y(x) = f(x + y)$  is a translate. Since  $\Psi$  is increasing: if  $f_y \geq g$  pointwise (i.e.,  $f(x + y) \geq g(x)$  for all  $x$ , equivalently  $f(x + y) - g(x) \geq 0$  for all  $x$ ), then  $[\Psi f_y](0) \geq [\Psi g](0) \geq 0$ , so  $f_y \in \text{Ker}(\Psi)$ . More precisely, the condition  $[\Psi f](y) \geq 0$  holds for all translates satisfying  $f_y \geq g$ , i.e.,  $f(x + y) \geq g(x)$ , i.e.,  $f(y + x) - g(x) \geq 0$  for all  $x$ , i.e.,  $\inf_x \{f(y + x) - g(x)\} \geq 0$ , i.e.,  $(\varepsilon_g f)(y) \geq 0$ . Hence  $[\Psi f](y) \geq 0$  whenever  $(\varepsilon_g f)(y) \geq 0$ , which by the definition of  $\text{Ker}$  means  $\varepsilon_g f \leq \Psi f$  pointwise. Taking the supremum over  $g \in \text{Bas}(\Psi)$  gives  $\sup_{g \in \text{Bas}(\Psi)} \varepsilon_g f \leq \Psi f$ . For the reverse inequality, we show that for each  $y$ , the value  $[\Psi f](y)$  is achieved by some basis element. Consider the function  $h_{f,y}(x) = f(x + y) - [\Psi f](y)$ ; by definition of the kernel and translation-invariance,  $h_{f,y} \in \text{Ker}(\Psi)$ . By the minimality of

basis elements (established in Step 1 via Zorn’s lemma applied to the downward-directed set below  $h_{f,y}$  in  $\text{Ker}(\Psi)$ ), there exists  $g^* \in \text{Bas}(\Psi)$  with  $g^* \leq h_{f,y}$  pointwise, giving  $(\varepsilon_{g^*} f)(y) = \inf_x \{f(x+y) - g^*(x)\} \geq \inf_x \{f(x+y) - h_{f,y}(x)\} = [\Psi f](y)$ . Hence  $\sup_{g \in \text{Bas}(\Psi)} (\varepsilon_g f)(y) \geq [\Psi f](y)$ , completing the equality.

*Step 3: Dual representation.* Applying the argument to the dual operator  $\bar{\Psi}(f) = -\Psi(-f)$ , which is also TI, increasing, and USC, gives  $[\bar{\Psi} f](x) = \sup_{h \in \text{Bas}(\bar{\Psi})} (\varepsilon_h f)(x)$ . Substituting  $f \rightarrow -f$  and negating yields the dual representation as an infimum of dilations.  $\square$

**Remark 2.9.** The MMBB-increasing theorem is a nonlinear counterpart to the spectral representation of linear shift-invariant operators. Whereas the latter decomposes any LSI filter into sinusoidal components (Fourier basis), MMBB-increasing decomposes any TI increasing operator into a (possibly infinite) supremum of erosions, each parameterised by a basis function. In the deep learning context, learning a layer is equivalent to learning a finite subset of this basis, see Section 4.

**2.5. MMBB universal representation of translation-invariant general operators.** The MMBB-increasing theorem requires the operator to be *increasing*, which in the CNN setting corresponds to non-negative kernels (see below Proposition 4.1). Real CNN kernels are signed; as we will see, that can be handled by decomposing  $k = k^+ - k^-$ . However, there is a more fundamental extension: the Banon–Barrera (1993) [6] representation theorem, which covers *any* TI operator, whether or not it is increasing. We state it here for completeness, as it provides the theoretical ceiling of the MMBB programme of nonlinear universal representation.

**Definition 2.10** (Sup-generating operator and anti-dilation). An *anti-dilation* by structuring function  $c$  is the operator

$$(\alpha_c f)(x) = \inf_{y \in E} \{-f(x+y) + c(y)\} = -(\varepsilon_{-c}(f))(x).$$

It is decreasing (increasing inputs give smaller outputs, hence the “anti”) and dualises the erosion in a different involution than the complement or the Galois adjunction. A *sup-generating operator* associated to a pair  $(g^-, g^+)$  of structuring functions is

$$(\psi_{g^-, g^+} f)(x) = (\varepsilon_{g^-} f)(x) \wedge (\alpha_{g^+} f)(x) = \min \left\{ \inf_y \{f(x+y) - g^-(y)\}, \inf_y \{-f(x+y) + g^+(y)\} \right\}. \quad (8)$$

**Theorem 2.11** (MMBB-General – Banon–Barrera 1993). *Let  $\Psi : \text{Fun}(E, \bar{\mathbb{R}}) \rightarrow \text{Fun}(E, \bar{\mathbb{R}})$  be a TI and upper semi-continuous operator (not necessarily increasing). Then there exists a family of pairs  $\{(g_i^-, g_i^+)\}_{i \in I}$  of structuring functions such that*

$$[\Psi f](x) = \sup_{i \in I} (\psi_{g_i^-, g_i^+} f)(x) = \sup_{i \in I} \min \left\{ \inf_y \{f(x+y) - g_i^-(y)\}, \inf_y \{-f(x+y) + g_i^+(y)\} \right\}. \quad (9)$$

*The structuring pairs  $(g_i^-, g_i^+)$  are the extremities of the closed set-intervals contained in the kernel of  $\Psi$ ; the collection can be taken minimal (the sup-generating basis). When  $\Psi$  is increasing, the anti-dilation component becomes vacuous ( $g_i^+ = +\infty$ ) and the representation reduces to the MMBB Theorem 2.8.*

*Proof sketch.* We outline the extension from the MMBB-Increasing proof; full details are in [6].

*Step 1: Generalised kernel and interval representation.* For a non-increasing TI operator  $\Psi$ , the kernel  $\text{Ker}(\Psi) = \{f : [\Psi f](0) \geq 0\}$  is still well-defined and non-empty (it contains  $f \equiv +\infty$  when  $\Psi$  maps this to a non-negative value). However,  $\text{Ker}(\Psi)$  is no longer a sup-closed set

(since  $\Psi$  is not increasing, the supremum of two kernel functions need not be in the kernel). The key observation is that any function  $f \in \text{Ker}(\Psi)$  determines a *closed interval*  $[\underline{f}, \overline{f}] := \{h : \underline{f} \leq h \leq \overline{f}\}$ , where  $\underline{f} = \inf\{h \leq f : h \in \text{Ker}(\Psi)\}$  and  $\overline{f} = \sup\{h \geq f : h \in \text{Ker}(\Psi)\}$  are the lower and upper extremities of the maximal interval in  $\text{Ker}(\Psi)$  containing  $f$ .

*Step 2: Sup-generating operators from interval extremities.* Each interval  $[\underline{f}, \overline{f}] \subset \text{Ker}(\Psi)$  contributes a sup-generating operator  $\psi_{\underline{f}, \overline{f}}$  whose erosion component is parameterised by the lower extremity  $g^- = \underline{f}$  (in the role of the MMBB-Increasing basis function) and whose anti-dilation component is parameterised by the upper extremity  $g^+ = \overline{f}$  (controlling the maximum permissible input value at each lag):

$$\begin{aligned} (\psi_{g^-, g^+} f)(0) &= \min\{(\varepsilon_{g^-} f)(0), (\alpha_{g^+} f)(0)\} \\ &= \min\left\{\inf_y \{f(y) - g^-(y)\}, \inf_y \{-f(y) + g^+(y)\}\right\} \geq 0 \end{aligned}$$

if and only if  $g^- \leq f \leq g^+$  pointwise, i.e.,  $f$  lies in the interval  $[g^-, g^+]$ .

*Step 3: Completeness and minimality.* The supremum of  $\psi_{g_i^-, g_i^+}$  over all interval extremity pairs recovers  $\Psi f$  exactly, by an argument analogous to Step 2 of the MMBB-Increasing proof: the TI property translates the condition at 0 to any point  $x$ , and the USC property guarantees the existence of minimal interval extremities (the *sup-generating basis*). When  $\Psi$  is increasing, the kernel  $\text{Ker}(\Psi)$  is closed under downward passage (i.e., if  $h \in \text{Ker}(\Psi)$  and  $f \leq h$ , then  $f \in \text{Ker}(\Psi)$  by monotonicity of  $\Psi$ ), so every interval in  $\text{Ker}(\Psi)$  has the form  $(-\infty, g_i^+]$  with no lower bound constraint. In this case, taking  $g_i^- \rightarrow -\infty$  makes the erosion component  $\varepsilon_{g_i^-} f(x) = \inf_y \{f(x+y) - g_i^-(y)\} \rightarrow +\infty$  (since subtracting  $-\infty$  gives  $+\infty$ ), so the minimum in (8) is determined entirely by the anti-dilation:  $\psi_{-\infty, g^+} f = (+\infty) \wedge (\alpha_{g^+} f) = \alpha_{g^+} f$ . The condition  $\alpha_{g^+} f(x) \geq 0$  is equivalent to  $\inf_y \{-f(x+y) + g^+(y)\} \geq 0$ , i.e.,  $f(x+y) \leq g^+(y)$  for all  $y$ , i.e.,  $(\varepsilon_{g^+} f)(x) \leq 0$  in the MMBB-Increasing sense with  $g^+ = g$  as the basis element. Taking the supremum over  $g^+ \in \text{Bas}(\Psi)$  recovers the MMBB-Increasing representation. Note that here  $g^+$  plays the role of the MMBB-Increasing basis element  $g$  (the two coincide when  $\Psi$  is increasing, since the anti-dilation upper bound  $g^+$  in the Banon–Barrera sense reduces to the MMBB basis element by the diagonal condition  $g^- = g^+ = g$ , consistent with Theorem 2.8).  $\square$

**Remark 2.12** (Deep learning context). The Banon–Barrera representation theorem applies directly to signed CNN convolution layers, which are TI but not increasing. The explicit characterisation of the sup-generating basis for discrete finite kernels, including its relationship to the positive and negative MMBB-Increasing bases and the computation of the structuring pairs from the characteristic matrices, is developed in Section 4.3.

### 3. OVCHINNIKOV’S LATTICE POLYNOMIAL REPRESENTATION AND RELU NETWORKS

The Ovchinnikov representation [36] connects the MMBB operator theory to the representation of functions themselves, providing a direct algebraic bridge to PWL ReLU networks.

**Theorem 3.1** (Ovchinnikov 2002). *Let  $f$  be a piecewise-linear function on a closed convex domain  $\Omega \subset \mathbb{R}^n$ , with linear components  $\{g_1, \dots, g_d\}$ . There exists a family  $\{K_i\}_{i \in \mathcal{I}}$  of subsets of  $\{1, \dots, d\}$  such that*

$$f(x) = \sup_{i \in \mathcal{I}} \inf_{j \in K_i} g_j(x), \quad x \in \Omega. \quad (10)$$

*Conversely, any such lattice polynomial in the  $g_j$  defines a PWL function.*

This theorem is the function-level counterpart to Theorem 2.8 and has immediate implications for deep learning.

**Proposition 3.2** (ReLU networks as lattice polynomials). *Every function computed by a deep ReLU network is a continuous PWL function [5, 35]. By Theorem 3.1, it admits a max-min lattice polynomial representation in its affine components. Consequently, every ReLU network is representable within the MMBB calculus as a finite supremum of morphological erosions by affine structuring functions.*

*Proof.* A ReLU network with  $d$  layers computes a continuous PWL function  $F : \mathbb{R}^n \rightarrow \mathbb{R}^m$  (Arora et al. [5], Montufar et al. [35]). Apply Theorem 3.1 component-wise. Each affine component  $g_j(x) = \langle a_j, x \rangle + b_j$  is a structuring function defining an erosion  $(\varepsilon_{-g_j} f)(x) = \inf_y \{f(x+y) + g_j(y)\}$  (with  $b_j$  playing the role of the bias). The max-min formula (10) then realises  $F$  as a finite supremum of such erosions.  $\square$

**Remark 3.3.** The tropical geometry viewpoint [49] arrives at the same conclusion via min-plus algebra, which is isomorphic to max-plus (the algebra underlying morphological erosion-dilation) by sign change. Our approach recovers tropical representations as a special case of MMBB. This connection, noted implicitly in [32], is made explicit below.

TABLE 2. Principal results of §3 (Ovchinnikov and ReLU Networks).

Ref.	Name	Statement and role
Thm 3.1	Ovchinnikov 2002	Every PWL function on a convex domain equals a lattice polynomial $\sup_i \inf_{j \in \mathcal{K}_i} g_j$ ; bridges the MMBB operator calculus to ReLU network geometry.
Prop 3.2	ReLU nets as lattice polynomials	Every deep ReLU network computes a continuous PWL function and hence admits a finite MMBB-Increasing representation as a supremum of erosions by affine structuring functions.

**3.1. Explicit lattice polynomial equations for ReLU networks.** We now make the lattice polynomial structure of ReLU networks fully explicit, tracing through the activation, composition, and representation steps.

Elementary ReLU as a lattice polynomial. The ReLU unit applied to a linear form  $g(x) = \langle a, x \rangle + b$  satisfies

$$\text{ReLU}(g(x)) = \max(0, \langle a, x \rangle + b) = g(x) \vee 0, \quad (11)$$

a lattice polynomial of degree 1 in  $\{g, 0\}$  with the single sup-term  $\sup\{g(x), 0\}$ . A full neuron with  $K$  weighted inputs and bias  $b$  computes

$$\text{ReLU}\left(\sum_{k=1}^K w_k \langle a_k, x \rangle + b\right) = \left(\sum_{k=1}^K w_k \langle a_k, x \rangle + b\right) \vee 0, \quad (12)$$

a single sup of a linear function and the constant 0.

Single hidden layer. A network  $F(x) = W_2 \sigma(W_1 x + b_1) + b_2$  with  $M$  ReLU neurons has pre-activations  $h_m(x) = \langle w_m^{(1)}, x \rangle + b_m^{(1)}$ . The  $\ell$ -th output is

$$F_\ell(x) = \sum_{m=1}^M w_{\ell m}^{(2)} (h_m(x) \vee 0) + b_\ell^{(2)}. \quad (13)$$

For non-negative weights  $w_{\ell m}^{(2)} \geq 0$ , each term  $w_{\ell m}^{(2)}(h_m \vee 0)$  is a dilation of a single-neuron opening; the sum is an MMBB-Increasing erosion applied to the sum of activations. For general signed weights, the MMBB-General (Theorem 2.11) yields

$$F_\ell(x) = \sup_{i \in \mathcal{I}} \min \left\{ \inf_y \{F_\ell(x+y) - g_i^-(y)\}, \inf_y \{-F_\ell(x+y) + g_i^+(y)\} \right\}, \quad (14)$$

a supremum of sup-generating operators (Theorem 2.10).

Deep network: linear region decomposition. A depth- $L$  ReLU network partitions  $\mathbb{R}^n$  into convex polytopes (linear regions), at most  $\prod_{\ell=1}^L \binom{n_\ell}{n}$  of them [35]. Let the regions be  $\{R_1, \dots, R_P\}$  with  $F|_{R_p}(x) = \langle c_p, x \rangle + d_p$ . By Theorem 3.1, the global network output is the lattice polynomial

$$F(x) = \sup_{i \in \mathcal{I}} \inf_{j \in K_i} \underbrace{(\langle c_j, x \rangle + d_j)}_{=: g_j(x)}, \quad x \in \mathbb{R}^n. \quad (15)$$

Each affine piece  $g_j$  determines a structuring function  $s_j(y) = -\langle c_j, y \rangle - d_j$  and an erosion

$$(\varepsilon_{s_j} F)(x) = \inf_y \{F(x+y) - s_j(-y)\} = \inf_y \{F(x+y) + \langle c_j, y \rangle + d_j\} = g_j(x), \quad (16)$$

when  $F$  agrees with the  $j$ -th affine piece in a neighbourhood of  $x$ . Hence (15) is the MMBB representation of  $F$  with morphological basis  $\{s_j\}_{j=1}^P$ .

**Remark 3.4** (Unification of three algebraic frameworks). Three algebraic frameworks reach the same representation (15):

(i) **Tropical geometry** [49]. A ReLU network computes a tropical rational function (a max-plus polynomial). Linear regions are the cells of the tropical hypersurface. The min-plus (tropical) formulation is related to max-plus by the sign-change isomorphism  $(\min, +) \leftrightarrow (\max, -)$ : the tropical polynomial  $\bigoplus_j (c_j \odot x) = \max_j (\langle c_j, x \rangle + d_j)$  becomes a lattice supremum of linear forms.

(ii) **Ovchinnikov / lattice polynomials** [36]. Every PWL function is a max-min polynomial of its affine components (Theorem 3.1), giving the global representation (15) directly from linear regions *without knowing the network weights*. The family  $\{K_i\}$  encodes the combinatorial adjacency structure of the linear regions.

(iii) **MMBB operator theory**. The network map  $x \mapsto F(x)$  is (for non-negative weights and zero biases, so that the map is genuinely translation-invariant in the vertical sense of Proposition 4.1(ii)) a TI increasing operator whose morphological basis consists of the affine structuring functions  $\{s_j\}$ . For general (signed) weights or non-zero biases, (Theorem 2.11) provides a supremum of sup-generating operators.

The key relationship between frameworks (ii) and (iii) is: Ovchinnikov is the *function representation theorem* (representing the computed function as a lattice polynomial), while MMBB is the *operator representation theorem* (representing the operator  $f \mapsto F \circ f$  as a supremum of erosions or a supremum of sup-generating operators). The two are related by the identity  $\inf_{j \in K_i} g_j(x) = (\varepsilon_{s_j} F)(x)$  from (16): the infimum of affine functions in the lattice polynomial is exactly one erosion term in the MMBB expansion.

The number of MMBB basis functions  $P$  (the number of linear regions) grows polynomially with width and exponentially with depth [35], quantifying the *representational cost* of a ReLU network in morphological terms: depth creates exponentially many affine structuring functions, each corresponding to a hyperplane in  $\mathbb{R}^n$ .

#### 4. MORPHOLOGICAL BASIS OF CONVOLUTION

We analyse the linear convolution operator within the MMBB frameworks. This section extends the foundational results of Maragos and Schafer [30] and Khosravi and Schafer [26], with an eye toward deep learning applications. We provide complete proof sketches and discuss the Banon–Barrera representation of signed convolution in the discrete case, which has not yet been considered in the literature.

**4.1. Conditions for the MMBB-Increasing framework to apply.** Let  $\mathcal{F} = \text{Fun}(\mathbb{R}^n, \mathbb{R})$ . The *linear convolution operator*  $\Phi_k : \mathcal{F} \rightarrow \mathcal{F}$  with kernel  $k \in \mathcal{F}$  is

$$(\Phi_k f)(x) = (f * k)(x) = \int_{\mathbb{R}^n} f(y) k(x - y) dy.$$

To apply Theorem 2.8, three conditions must hold.

**Proposition 4.1** (Maragos–Schafer 1987 [30]). *Let  $\Phi_k$  a convolution with kernel  $k$ .*

- (i)  $\Phi_k$  is increasing if and only if  $k(x) \geq 0$  for all  $x$ .
- (ii)  $\Phi_k$  is translation-equivariant (vertical) if and only if  $\int_{\mathbb{R}^n} k(x) dx = 1$ .
- (iii)  $\Phi_k$  is upper semi-continuous if  $\text{Spt}(k)$  is compact, where  $\text{Spt}(k) = \{x : k(x) \neq 0\}$ .

**Remark 4.2** (Deep learning kernels). In practice, CNN kernels are not constrained to be non-negative. A general kernel  $k$  decomposes as  $k = k^+ - k^-$  with  $k^+ = \max(0, k)$  and  $k^- = \max(0, -k)$ . Each part, after normalisation, satisfies the conditions of Theorem 4.1, so that the convolution decomposes into two MMBB-representable operators (cf. Theorem 4.4 below). The learned weights in a trained network are thus implicitly parameterising a (possibly truncated) morphological basis. This observation is developed further in Section 4.5.

TABLE 3. Principal results of §4 (Morphological Basis of Convolution). Results marked (★) are the paper’s principal findings.

Ref.	Name	Statement and role
Prop 4.1	Convolution as MMBB erosion	$f \mapsto f * k$ is TI and increasing iff $k \geq 0$ ; it is then an erosion in the pointwise lattice and admits a MMBB-Increasing basis decomposition.
Thm 4.3 (★)	Maragos–Schafer basis	For $k \geq 0$ normalised with finite support of size $N$ : $\text{Bas}(k) \cong \mathbb{R}^{N-1}$ (the hyperplane in $\mathbb{R}^N$ orthogonal to $k$ ); convolution equals an exact sup of erosions by basis elements.
Thm 4.12	Virtual basis	For $Q$ -level quantised signals, $\text{Bas}(k)$ is finite with cardinality $\leq Q^{N-1}$ ; a learnable MMBB layer is a finite truncation of this virtual basis.
Prop 4.15	MMBB approximation	A sub-basis $\mathcal{B} \subset \text{Bas}(\Psi)$ of size $L$ gives a lower approximation $\sup_{g \in \mathcal{B}} \varepsilon_g f \leq \Psi f$ with quantifiable error; basis elements are the learnable layer parameters.

**4.2. Kernel and morphological basis of a convolution.** Assuming  $k(x) \geq 0$ ,  $\sum_x k(x) = 1$ , and  $\text{Spt}(k)$  finite (discrete case), the MMBB-Increasing basis of  $\Phi_k$  admits an explicit characterisation.

**Theorem 4.3** (Maragos–Schafer 1987 [30]). *Let  $k : \mathbb{Z}^n \rightarrow \mathbb{R}$  have finite support  $\text{Spt}(k) = \{x_1, \dots, x_N\}$ , with  $k \geq 0$  and  $\sum k = 1$ . For  $x \in \mathbb{Z}^n$ , write  $\text{Spt}(k)_x = \{y \in \mathbb{Z}^n : x + y \in \text{Spt}(k)\} = \text{Spt}(k) - x$  for the translate of the support centred at  $x$ . The morphological basis of  $\Phi_k$  is*

$$\text{Bas}(k) = \left\{ g \in \text{Fun}(\mathbb{Z}^n, \overline{\mathbb{R}}) : \sum_{y \in \text{Spt}(k)} k(y) g(-y) = 0, g(x) = -\infty \Leftrightarrow k(-x) = 0 \right\}, \quad (17)$$

and the convolution admits the exact representation

$$(f * k)(x) = \sup_{g \in \text{Bas}(k)} \inf_{y \in \text{Spt}(k)_x} \{f(x+y) - g(y)\}. \quad (18)$$

*Proof.* See Maragos–Schafer [30]. The key step is to show that  $\text{Bas}(k)$  equals the image of  $\mathbb{R}^N$  under the characteristic matrix  $A_k$  defined in Section 4.4, and then to verify that  $g^* \in \text{Bas}(k)$  defined by  $g^*(-x_i) = f(x - x_i) - \sum_j k(x_j) f(x - x_j)$  achieves the supremum in (18) for each  $x$ .  $\square$

**Theorem 4.4** (General kernel – Maragos–Schafer 1987 [30]). *For an absolutely summable kernel  $k : \mathbb{Z}^n \rightarrow \mathbb{R}$  with decomposition  $k = G^+ \bar{k}^+ - G^- \bar{k}^-$  (with  $\bar{k}^\pm$  normalised non-negative kernels and gains  $G^\pm = \sum_{\text{Spt}(k^\pm)} k^\pm$ ),*

$$(f * k)(x) = G^+ \sup_{g^+ \in \text{Bas}(\bar{k}^+)} (\varepsilon_{g^+} f)(x) - G^- \sup_{g^- \in \text{Bas}(\bar{k}^-)} (\varepsilon_{g^-} f)(x). \quad (19)$$

Theorem 4.4 shows that any CNN convolution layer, with no constraint on the sign of weights, decomposes as a difference of two MMBB-Increasing representations. This is the morphological analogue of decomposing a signed measure into its positive and negative parts.

**Remark 4.5** (Geometric interpretation). Both  $k$  and  $g \in \text{Bas}(k)$  can be viewed as vectors in  $\mathbb{R}^N$ . Since  $k$  is a probability vector (non-negative, sum 1), it lies on the unit simplex. The basis condition  $\sum k_i g(-x_i) = 0$  means  $g$  is orthogonal to  $k$  (inner product zero at the origin). Hence  $\text{Bas}(k)$  is isomorphic to the hyperplane  $\mathbb{R}^{N-1}$  orthogonal to  $k$  at the origin in  $\mathbb{R}^N$ . This geometry directly informs the design of learnable morphological layers in Section 4.5.

**4.3. MMBB-General representation of signed convolution.** We now develop the application of Theorem 2.11 to discrete signed convolutions, providing a direct and compact alternative to the  $k^+ - k^-$  decomposition of Theorem 4.4. This is the principal setting in which the Banon–Barrera extension is genuinely needed: CNN kernels are signed, and the full operator is TI but not increasing.

Let  $k = G^+ \bar{k}^+ - G^- \bar{k}^-$  as above, and let  $A = G^+ \sup_{g^- \in \text{Bas}(\bar{k}^+)} (\varepsilon_{g^-} f)(x)$  and  $B = G^- \sup_{g^+ \in \text{Bas}(\bar{k}^-)} (\varepsilon_{g^+} f)(x)$ , so that  $(f * k)(x) = A - B$  by Theorem 4.4.

The Banon–Barrera sup-generating representation characterises the *sign* of  $(f * k)(x)$  exactly:

$$(f * k)(x) \geq 0 \iff \exists (g^-, g^+) \in \text{Bas}(\bar{k}^+) \times \text{Bas}(\bar{k}^-) \text{ s.t. } \psi_{g^-, g^+}(f)(x) \geq 0, \quad (20)$$

where

$$\psi_{g^-, g^+}(f)(x) = \min \left\{ \inf_{y \in \text{Spt}(k^+)} \{f(x+y) - g^-(y)\}, \frac{G^-}{G^+} \inf_{y \in \text{Spt}(k^-)} \{-f(x+y) + g^+(y)\} \right\}. \quad (21)$$

The condition  $\psi_{g^-, g^+}(f)(x) \geq 0$  encodes the inequality  $G^+ (\varepsilon_{g^-} f)(x) \geq G^- (\varepsilon_{g^+} f)(x)$ , i.e., the positive erosion dominates the negative erosion at the point  $x$ .

However, *the actual value* of  $(f * k)(x)$  is given by Theorem 4.4, not by the sup-generating formula:

$$(f * k)(x) = A - B = G^+ \sup_{g^- \in \text{Bas}(\bar{k}^+)} (\varepsilon_{g^-} f)(x) - G^- \sup_{g^+ \in \text{Bas}(\bar{k}^-)} (\varepsilon_{g^+} f)(x). \quad (22)$$

The Banon–Barrera sup-generating representation  $\sup_{g^-, g^+} \psi_{g^-, g^+}(f)(x)$  recovers the sign of  $(f * k)(x)$  but not its magnitude in general, because  $\sup_{g^-, g^+} \min\{A_{g^-}, B_{g^+}\} \neq A - B$  for signed values (the minimax inequality).

For the signed convolution, the Banon–Barrera framework provides:

- (i) A *thresholding interpretation*: the sup-generating test  $\psi_{g^-, g^+}(f)(x) \geq 0$  replaces the signed inequality  $A \geq B$  with an inf-combination of erosion and anti-dilation, giving a morphological criterion for the positivity of  $(f * k)(x)$ .
- (ii) A *compact single-operator form*: instead of two separate MMBB-Increasing suprema, the signed convolution's positivity is encoded by a single family of sup-generating operators parameterised by pairs  $(g^-, g^+)$ .

**Remark 4.6** (Geometric structure in the discrete case). The sup-generating basis of a discrete signed convolution has a product structure: it is indexed by pairs  $(g^-, g^+)$  with  $g^- \in \text{Bas}(\bar{k}^+) \cong \mathbb{R}^{N^+-1}$  and  $g^+ \in \text{Bas}(\bar{k}^-) \cong \mathbb{R}^{N^- - 1}$  (by the characteristic matrix geometry of Section 4.4). The full sup-generating basis is therefore parameterised by the product space  $\mathbb{R}^{N^+-1} \times \mathbb{R}^{N^- - 1} \cong \mathbb{R}^{N-2}$ . This has a clear interpretation: the  $N - 1$  degrees of freedom of the MMBB-Increasing basis (one constraint per basis function, namely orthogonality to  $k$  in  $\mathbb{R}^N$ ) split as  $(N^+ - 1)$  degrees for the positive component and  $(N^- - 1)$  degrees for the negative component, with one degree consumed by the normalisation  $G^+ - G^- = \int k$ .

**Proposition 4.7** (Diagonal sup-generating pairs for non-negative convolution). *Let  $k \geq 0$ ,  $\sum k = 1$ , with finite support of size  $N$ . In the Banon–Barrera representation of the convolution  $\Phi_k$  (Theorem 2.11):*

- (i) *Every sup-generating pair  $(g^-, g^+)$  in the sup-generating basis of  $\Phi_k$  satisfies  $g^-(x) \leq g^+(x)$  for all  $x$  (i.e.,  $g^- \leq g^+$  pointwise).*
- (ii) *The minimal sup-generating pairs satisfy  $g^- = g^+$  pointwise. Such pairs are called diagonal.*
- (iii) *The diagonal sup-generating elements are precisely the elements of the MMBB-Increasing basis:*

$$\{(g, g) : (g^-, g^+) \text{ minimal}\} = \{(g, g) : g \in \text{Bas}(k)\}. \quad (23)$$

- (iv) *In the non-negative case, MMBB-General representation of  $\Phi_k$  therefore degenerates to the MMBB-Increasing representation: each sup-generating element  $\psi_{g, g}$  reduces to the erosion  $\varepsilon_g$ , and*

$$(f * k)(x) = \sup_{g \in \text{Bas}(k)} \varepsilon_g(f)(x) = \sup_{(g, g) \text{ diagonal}} \psi_{g, g}(f)(x), \quad (24)$$

*confirming that the Maragos theorem is exactly the diagonal specialisation of the Banon–Barrera theorem.*

*Proof.* (i) Since  $\Phi_k$  is increasing (Proposition 4.1), its generalised kernel  $\text{Ker}(\Phi_k) = \{f : (f * k)(0) \geq 0\}$  is upward-closed: if  $f \in \text{Ker}(\Phi_k)$  and  $h \geq f$ , then  $(h * k)(0) \geq (f * k)(0) \geq 0$ , so  $h \in \text{Ker}(\Phi_k)$ . For an upward-closed set, every maximal interval  $[g^-, g^+] \subset \text{Ker}(\Phi_k)$  satisfies  $g^+ = +\infty$ ; equivalently, the anti-dilation constraint  $\alpha_{g^+}$  is vacuous for all sup-generating pairs. In particular, any valid upper bound satisfies  $g^+ \geq g^-$  (the interval  $[g^-, g^+]$  is non-empty).

(ii) For an increasing TI operator, the Banon–Barrera proof (Theorem 2.11, Step 1) shows that intervals in  $\text{Ker}(\Phi_k)$  are determined by their lower extremity  $g^-$  alone. The tightest (minimal) interval containing any  $f \in \text{Ker}(\Phi_k)$  is  $[g^-, +\infty)$  parameterised by the greatest lower bound  $g^- = \inf\{h \leq f : h \in \partial \text{Ker}(\Phi_k)\}$ , where  $\partial \text{Ker}(\Phi_k) = \{f : (f * k)(0) = 0\}$  is the kernel boundary. The upper extremity  $g^+$  of a minimal pair is the smallest element above  $g^-$  in  $\text{Ker}(\Phi_k)^c$ , which for an upward-closed kernel is  $g^- + \epsilon$  as  $\epsilon \rightarrow 0^+$ ; in the limit,  $g^+ = g^-$ .

(iii) The kernel boundary is  $\partial \text{Ker}(\Phi_k) = \{f : \sum_i k(x_i)f(-x_i) = 0, f = -\infty \text{ off Spt}(k)\} = \text{Bas}(k)$  (Theorem 4.3). So the minimal sup-generating lower extremities are exactly the MMBB basis elements, and the diagonal pairs are  $(g, g)$  for  $g \in \text{Bas}(k)$ .

(iv) For a diagonal pair  $(g, g)$ , the sup-generating operator  $\psi_{g,g}(f)(x) = \min\{\varepsilon_g(f)(x), \alpha_g(f)(x)\}$  where  $\alpha_g(f)(x) = \inf_y \{-f(x+y) + g(y)\} = -\sup_y \{f(x+y) - g(y)\} = -\delta_g(f)(x)$ . Since  $\varepsilon_g(f)(x) \leq \delta_g(f)(x)$  for all  $f$  (erosion  $\leq$  dilation), we have  $-\alpha_g(f)(x) = \delta_g(f)(x) \geq \varepsilon_g(f)(x)$ , so  $\alpha_g(f)(x) = -\delta_g(f)(x) \leq -\varepsilon_g(f)(x)$ . At a kernel boundary point where  $f = g$  (so  $\varepsilon_g(g)(x) = 0$ ):  $\psi_{g,g}(g)(x) = \min\{0, -\delta_g(g)(x)\} = \min\{0, -\delta_g(g)(x)\}$ . Since  $\delta_g(g)(x) \geq g(x)$  (dilation is extensive) and  $g(0) = 0$  (normalisation of the basis),  $\psi_{g,g}(g) = 0 = \varepsilon_g(g)$ . For general  $f$ ,  $\min\{\varepsilon_g(f), \alpha_g(f)\} = \varepsilon_g(f)$  whenever  $\varepsilon_g(f)(x) \leq \alpha_g(f)(x)$ , i.e., whenever  $f \geq g$  in a neighbourhood of  $x$  (which holds  $\Phi_k$ -a.e. by the MMBB basis construction). The equality  $\sup_{g \in \text{Bas}(k)} \psi_{g,g}(f) = \sup_{g \in \text{Bas}(k)} \varepsilon_g(f) = (f * k)$  then follows from Theorem 4.3.  $\square$

**Remark 4.8** (Geometric and architectural significance of diagonality). Proposition 4.7 gives a precise geometric meaning to the relationship between the MMBB-Increasing and MMBB-General frameworks for positive kernels as follows.

**Geometric picture.** The MMBB basis  $\text{Bas}(k) \cong \mathbb{R}^{N-1}$  is a hyperplane in  $\mathbb{R}^N$  (the orthogonal complement of  $k$  at the origin. Each basis element  $g \in \text{Bas}(k)$  sits on the boundary of the half-space  $\text{Ker}(\Phi_k) = \{f : \langle k, f \rangle \geq 0\}$  (where  $\langle k, f \rangle = \sum k_i f(-x_i)$ ). The Banon–Barrera intervals collapse to single points on this hyperplane boundary, precisely the diagonal condition  $g^- = g^+ = g$ . For a signed kernel, the kernel boundary is no longer a hyperplane but the intersection of two half-spaces (one for  $k^+$ , one for  $k^-$ ), and the intervals no longer collapse; this is exactly where  $g^- \neq g^+$  and the signed sup-generating pairs become genuinely non-diagonal.

**Architectural consequence in non-negative networks.** For a non-negative convolutional layer, the MMBB-Increasing erosion basis fully characterises the operator there is no additional expressive content in the MMBB-General pairing. The anti-dilation  $\alpha_{g^+}$  carries no information beyond  $g^-$  when  $g^+ = g^-$ . This means that neural network layers with non-negative weights (e.g., after a softplus or non-negative weight constraint) on non-negative signals are fully characterised by a single family of structuring functions, not a pair. For signed weights, the pairing becomes essential: the anti-dilation models the *inhibitory* influence of negative kernel components, and  $g^- \neq g^+$  measures the signed asymmetry of the kernel.

**Remark 4.9** (Comparison: MMBB-Increasing decomposition vs. MMBB-General form). Our theory offers two complementary representations of the same signed convolution:

- **MMBB-Increasing decomposition** ( $k = k^+ - k^-$ ): two separate suprema of erosions, combined by subtraction. Each supremum operates on a different (positive or negative) part of the kernel, and the combination is a difference of two lattice expressions. This form is more natural for implementation as two separate morphological branches and gradient-based learning of each basis independently.
- **MMBB-General form** (sup-generating pairs): a single supremum, each element being a min-combination of an erosion (positive part) and an anti-dilation (negative part) acting *jointly* on  $f$ . This form is more compact and avoids explicit sign decomposition; each pair

$(g^-, g^+)$  models the joint influence of positive and negative kernel components at a given input configuration. It is the natural form for analysing the fixed-point structure of signed layers (cf. Section 8), since the joint min-combination encodes both the excitatory (erosion) and inhibitory (anti-dilation) effects of the kernel in a single operator.

The two forms are theoretically equivalent for absolutely summable kernels; the choice between them is guided by the computational implementation.

**4.4. Characteristic matrix and virtual basis for quantised signals (binary, ternary, and low-bit networks).** For quantised signals, the infinite basis  $\text{Bas}(k)$  restricts to a finite *virtual basis*, computable via a structured matrix [26].

**Definition 4.10** (Characteristic matrix). For a finite kernel  $k$  with support  $\text{Spt}(k) = \{x_1, \dots, x_N\}$  and values  $k_i = k(x_i)$ , the *characteristic matrix*  $A_k \in \mathbb{R}^{N \times N}$  is

$$(A_k)_{\ell i} = \delta_{\ell i} - k_i, \quad (25)$$

where  $\delta_{\ell i}$  is the Kronecker delta.

We collect the key algebraic properties of the characteristic matrix  $A_k$ , which underpin the geometric interpretation of the MMBB-Increasing basis and the virtual basis computations.

**Proposition 4.11** (Properties of  $A_k$ ). *Let  $A_k \in \mathbb{R}^{N \times N}$  be defined by (25) for a kernel  $k$  with  $\sum k_i = 1$ ,  $k_i \geq 0$ .*

- (i)  $\text{null}(A_k) = \text{span}(\mathbf{1})$ , where  $\mathbf{1} = (1, \dots, 1)^T$ .
- (ii)  $\text{Im}(A_k) = \{g \in \mathbb{R}^N : \langle k, g \rangle = 0\}$ , the hyperplane orthogonal to  $k$ .
- (iii)  $\text{Bas}(k) \cong \text{Im}(A_k) \cong \mathbb{R}^{N-1}$ : the morphological basis is isomorphic to an  $(N-1)$ -dimensional subspace.
- (iv) For quantisation sets related by an affine transformation  $\mathcal{V}_2 = a\mathcal{V}_1 + b$ , the virtual bases satisfy  $\mathcal{V}_2(k) = a \cdot \mathcal{V}_1(k)$  (scale equivariance, translation-invariant).

*Proof.* (i)–(iii): The  $\ell$ -th row of  $A_k$  is  $e_\ell - k$  (standard basis vector minus  $k$ ), so  $A_k \mathbf{1} = \mathbf{1} - (\sum_i k_i) \mathbf{1} = \mathbf{1} - \mathbf{1} = \mathbf{0}$ . For  $g$  with  $\langle k, g \rangle = 0$ :  $(A_k g)_\ell = g_\ell - \langle k, g \rangle = g_\ell$ , so  $A_k g = g$  and  $g \in \text{Im}(A_k)$ . Conversely, for  $g = A_k r$ :  $\langle k, g \rangle = \langle k, A_k r \rangle = \langle k, r \rangle - \langle k, k \rangle \langle k, r \rangle \dots$  in fact  $(A_k)^T k = k - (\sum k_i) k = k - k = 0$ , so  $\langle k, A_k r \rangle = (k^T A_k) r = 0$ . Hence  $\text{Im}(A_k) = \ker(k^T) = \{g : \langle k, g \rangle = 0\} \cong \mathbb{R}^{N-1}$ . (iv) follows from linearity:  $A_k(a\mathcal{M}) = aA_k\mathcal{M}$ .  $\square$

**Theorem 4.12** (Khosravi–Schafer 1994 [26]). *Let  $\mathcal{F}_q$  denote the class of signals quantised to a finite set  $\mathcal{V} = \{v_1, \dots, v_Q\}$ . The virtual basis  $\mathcal{V}(k)$  of  $\Phi_k$  restricted to  $\mathcal{F}_q$  satisfies  $\mathcal{V}(k) = A_k(\mathcal{M})$ , where  $\mathcal{M}$  is any set of representatives of  $\mathcal{V}^N$  modulo the null-space direction  $(1, \dots, 1)^T$  of  $A_k$ . For all  $f \in \mathcal{F}_q$ ,*

$$(f * k)(x) = \max_{g \in \mathcal{V}(k)} \min_{x_j \in \text{Spt}(k)} \{f(x - x_j) - g(-x_j)\}. \quad (26)$$

The virtual basis theory of Theorem 4.12 becomes especially concrete when the signal alphabet  $\mathcal{V}$  is small, as in binary and ternary neural networks. These architectures, which constrain weights and/or activations to  $\{0, 1\}$ ,  $\{-1, +1\}$ ,  $\{-1, 0, +1\}$ , or a small set of levels, have attracted significant interest for hardware-efficient inference. The MMBB-Increasing framework provides an exact algebraic characterisation of their representational capacity. Throughout this subsection we assume  $k \geq 0$ ,  $\sum k = 1$ ,  $|\text{Spt}(k)| = N$  unless otherwise stated.

Binary signals ( $Q = 2$ ,  $\mathcal{V} = \{0, 1\}$ ). For binary inputs  $f \in \{0, 1\}^E$  and a positive normalised kernel  $k$ , the convolution  $(f * k)(x) = \sum_{i=1}^N k(x_i) f(x + x_i)$  is a *weighted average* of binary values, taking values in the finite set  $\{\sum_{i \in S} k(x_i) : S \subseteq \{1, \dots, N\}\} \subset [0, 1]$ . This is *not* in general binary-valued; it is  $[0, 1]$ -valued with at most  $2^N$  distinct output levels.

The virtual basis  $\mathcal{V}(k)$  over  $\{0, 1\}$  is the image  $A_k(\{0, 1\}^N)$  in  $\mathbb{R}^{N-1}$ , which has cardinality at most  $2^{N-1}$ . The MMBB-Increasing representation from Theorem 4.12 gives, for all  $f \in \{0, 1\}^E$ :

$$(f * k)(x) = \max_{g \in \mathcal{V}(k)} \min_{j=1}^N \{f(x - x_j) - g(-x_j)\}, \quad f \in \{0, 1\}^E, \quad (27)$$

an exact max-min expression with a *finite* basis of at most  $2^{N-1}$  elements. The sign convention follows Theorem 4.12 exactly:  $g$  is evaluated at  $-x_j$  (the reflected support points).

Ternary signals ( $Q = 3$ ,  $\mathcal{V} = \{-1, 0, 1\}$ ). For ternary inputs (relevant to signed binary networks and features with zero-padding), the virtual basis  $\mathcal{V}(k) = A_k(\{-1, 0, 1\}^N)$  has cardinality at most  $3^{N-1}$ .

For a *signed* kernel  $k = G^+ \bar{k}^+ - G^- \bar{k}^-$  with ternary input  $f \in \{-1, 0, 1\}^E$ , Theorem 4.4 gives the decomposition:

$$(f * k)(x) = G^+ \max_{h \in \mathcal{V}(\bar{k}^+)} \min_{i \in \text{Spt}(k^+)} \{f(x - x_i) - h(-x_i)\} - G^- \max_{h \in \mathcal{V}(\bar{k}^-)} \min_{j \in \text{Spt}(k^-)} \{f(x - x_j) - h(-x_j)\}, \quad (28)$$

where  $\mathcal{V}(\bar{k}^\pm) = A_{\bar{k}^\pm}(\{-1, 0, 1\}^{N^\pm})$  are the virtual bases of the positive and negative normalised kernels. Each sub-basis has cardinality at most  $3^{N^\pm-1}$ , and the virtual basis elements  $h \in \mathcal{V}(\bar{k}^\pm)$  take values in  $A_{\bar{k}^\pm}(\{-1, 0, 1\}^{N^\pm}) \subset \mathbb{R}$  (generally not in  $\{-1, 0, 1\}$ ).

Low-bit quantisation ( $Q = 2^B$ ). For  $B$ -bit quantised activations ( $Q = 4$  for 2-bit,  $Q = 8$  for 3-bit,  $Q = 16$  for 4-bit), the virtual basis  $\mathcal{V}(k) = A_k(\mathcal{V}^N)$  has cardinality at most  $Q^{N-1} = 2^{B(N-1)}$ .

**Proposition 4.13** (Representational capacity under quantisation). *Let  $\Phi_k$  be a convolution with  $k \geq 0$ ,  $\sum k = 1$ ,  $|\text{Spt}(k)| = N$ , and inputs quantised to  $Q = |\mathcal{V}|$  levels.*

- (i) *The virtual basis has cardinality  $|\mathcal{V}(k)| \leq Q^{N-1}$ .*
- (ii) *Removing one bit of precision ( $Q \rightarrow Q/2$ ) reduces the basis bound from  $Q^{N-1}$  to  $(Q/2)^{N-1}$ , a reduction by a factor of  $2^{N-1}$  per bit removed.*
- (iii) *For binary inputs ( $Q = 2$ ):  $|\mathcal{V}(k)| \leq 2^{N-1}$ , and the MMBB representation (27) is exact with this finite basis.*
- (iv) *For a  $3 \times 3$  kernel ( $N = 9$ ):  $Q = 2$  gives  $|\mathcal{V}(k)| \leq 2^8 = 256$ ;  $Q = 16$  (4-bit) gives  $|\mathcal{V}(k)| \leq 16^8 = 2^{32} \approx 4.3 \times 10^9$ .*

*Proof.* (i) The characteristic matrix  $A_k$  has rank  $N - 1$  with null space  $\text{span}(\mathbf{1})$  (Proposition 4.11(i)(ii)). The map  $A_k : \mathcal{V}^N \rightarrow \mathbb{R}^{N-1}$  identifies patterns  $v, v' \in \mathcal{V}^N$  satisfying  $A_k v = A_k v'$ , i.e.,  $v - v' \in \ker(A_k) = \text{span}(\mathbf{1})$ . Since  $v - v' = c \mathbf{1}$  for  $c \in \mathbb{R}$  requires  $v_i - v'_i = c$  for all  $i$ , the equivalence classes under this identification have size at most  $Q$  (the number of admissible constant shifts  $c$  such that both  $v$  and  $v - c \mathbf{1}$  remain in  $\mathcal{V}^N$ ). Hence  $|\mathcal{V}(k)| \leq Q^N / Q = Q^{N-1}$ . Parts (ii)–(iv) follow by substituting  $Q = 2^B$  and the stated values of  $N$  and  $B$ .  $\square$

**Remark 4.14** (Binary morphological networks). Proposition 4.13(iii) has a direct architectural interpretation for binary-activation networks: a convolutional layer with a *non-negative* kernel ( $k \geq 0$ ) and binary inputs ( $f \in \{0, 1\}^E$ ) can be represented exactly as a max-min (MMBB-Increasing) network with at most  $2^{N-1}$  structuring elements. For a  $3 \times 3$  kernel this is 256 structuring elements.

For binary *weight* networks (weights in  $\{-1, +1\}$ , which gives a signed kernel  $k = k^+ - k^-$ ), the MMBB representation requires the signed decomposition of Theorem 4.4: two separate max-min branches (one for  $k^+$ , one for  $k^-$ ) with binary-virtual bases of sizes at most  $2^{N^+-1}$  and  $2^{N^--1}$  respectively. This is strictly different from the non-negative case and requires the full signed formulation.

The morphological neural networks studied by Ritter and Sussner [41] and Davidson and Ritter [11] correspond precisely to finite-basis MMBB-Increasing networks over binary alphabets; the MMBB framework of Theorem 4.12 provides the exact representation theorem that was implicit in that earlier work.

**4.5. Deep learning perspective: learnable morphological bases.** Theorems 4.3 and 4.12 suggest a new class of neural network layers. Consider replacing the linear convolution in a standard CNN layer by a learnable finite subset of the morphological basis. Concretely, define the *MMBB layer* with  $L$  basis elements and  $J$  groups:

$$\Psi^{\text{APMO}}(f)(x) = \sum_{j=1}^J w_j \left[ \max_{1 \leq i \leq L} (\varepsilon_{g_{i,j}} f)(x) \right], \quad (29)$$

where  $\{g_{i,j}\}$  are the learnable structuring functions and  $w_j$  are learnable weights. By Theorem 4.4, this is a truncated MMBB expansion of a general (signed) convolution, with approximation error controlled by the number  $L$  of basis elements.

**Proposition 4.15** (Approximation by MMBB layers). *Let  $\Phi_k$  be a convolution with absolutely summable kernel  $k$ . For any  $\epsilon > 0$ , there exists a finite collection  $\{g_{i,j}\}_{i,j}$  of structuring functions and weights  $\{w_j\}$  such that*

$$\sup_{f: \|f\|_\infty \leq 1} \left\| \Phi_k(f) - \Psi^{\text{APMO}}(f) \right\|_\infty < \epsilon.$$

*Proof.* By Theorem 4.4,  $\Phi_k(f) = G^+ \sup_{g^+} \varepsilon_{g^+} f - G^- \sup_{g^-} \varepsilon_{g^-} f$ . The suprema range over (infinite) bases of  $\bar{k}^\pm$ . Since  $\text{Spt}(k)$  is finite, signals are bounded, and  $\varepsilon_g f$  is a continuous (in  $g$ ) family of operators in the sup-norm, the suprema can be approximated uniformly over  $\|f\|_\infty \leq 1$  by finite sub-bases of cardinality  $L = L(\epsilon)$ . Setting  $J = 2$ ,  $w_1 = G^+$ ,  $w_2 = -G^-$  and taking the appropriate finite sub-bases yields the result.  $\square$

This positions (29) as a well-founded, morphologically-grounded alternative to standard convolutional layers, and raises the open question of whether gradient-based learning efficiently discovers elements of  $\text{Bas}(k)$ .

## 5. COMPLETE LATTICE STRUCTURE OF POOLING AND MORPHOLOGICAL PYRAMIDS

We now address the algebraic structure of the down/up-sampling operations that define pooling, unpooling, strided convolution, and encoder-decoder skip connections in modern architectures. The key insight is that these operations are adjoint pairs in a complete inf-semilattice, and that the classical morphological pyramid theory of Goutsias and Heijmans [19] provides the correct algebraic framework.

**5.1. Abstract pyramid structure and the adjunction condition.** Let  $\mathcal{L}^d$  denote the space of functions on a discrete grid  $\mathbb{Z}^d$ .

TABLE 4. Principal results of §5 (Pooling, Pyramids, Multi-scale). Results marked (★) are the paper’s principal findings.

Ref.	Name	Statement and role
Prop 5.2 (★)	Goutsias–Heijmans pyramid	Erosion-decimation $\varepsilon_b^{\downarrow R}$ and dilation-interpolation $\delta_b^{*\uparrow R}$ form an adjunction; composition is an opening. Unifies max-pooling, strided convolution, and the Laplacian pyramid.
Thm 5.5	Max-pooling pyramid as	Flat-structuring Heijmans pyramid ( $b \equiv 0$ ) equals decimated max-pooling exactly; its adjoint is piecewise-constant unpooling by stride $R$ .
Cor 5.6	Strided convolution	Strided convolution with stride $R$ and kernel $k$ is a Goutsias–Heijmans erosion pyramid; transposed convolution is its adjoint synthesis operator.
Prop 5.8	Laplacian pyramid as skeleton	Laplacian pyramid residues equal the morphological top-hat of the Gaussian pyramid; morphological justification for multi-scale encoder–decoder architectures.

**Definition 5.1** (Analysis–synthesis pyramid). A *pyramid* is a pair of operators  $(\psi^\downarrow, \psi^\uparrow)$  with  $\psi^\downarrow : \mathcal{L}^d \rightarrow \mathcal{L}^d$  (analysis, coarser) and  $\psi^\uparrow : \mathcal{L}^d \rightarrow \mathcal{L}^d$  (synthesis, finer), satisfying the *pyramid condition*:

$$\psi^\downarrow \circ \psi^\uparrow = \text{Id}. \tag{30}$$

The *approximation sequence* is defined recursively by  $f_0 = f$ ,  $f_j = \psi^\downarrow(f_{j-1})$ , and the *detail signal* at level  $j$  is  $d_j = f_j - \psi^\uparrow(f_{j+1})$ .

For a downsampling factor  $R \in \mathbb{Z}_{>1}$ , define the *downsampling* and *upsampling* operators:

$$(\sigma_R^\downarrow f)(n) = f(R \cdot n), \tag{31}$$

$$(\sigma_R^{\uparrow, c} f)(m) = \begin{cases} f(n) & \text{if } m = R \cdot n, \\ c & \text{otherwise,} \end{cases} \tag{32}$$

for a fill value  $c \in \overline{\mathbb{R}}$  (typically  $c = -\infty$  or  $c = 0$ ).

The analysis and synthesis operators take the general form

$$\psi^\downarrow(f) = \sigma_R^\downarrow(\eta(f)), \quad \psi^\uparrow(f) = \xi(\sigma_R^{\uparrow, c}(f)),$$

where  $\eta$  and  $\xi$  are pre- and post-processing operators.

**Proposition 5.2** (Goutsias–Heijmans 2000 [19]). *If  $(\eta, \xi)$  form an adjunction (i.e.,  $\eta = \varepsilon$  is an erosion and  $\xi = \delta^*$  is its adjoint dilation), then  $(\psi^\downarrow, \psi^\uparrow)$  is also an adjunction. Furthermore, if  $\eta$  and  $\xi$  are equivariant to translation by  $\tau$ , then for  $R = 2$ :*

$$\psi^\downarrow \circ \tau_2 = \tau \circ \psi^\downarrow, \quad \psi^\uparrow \circ \tau = \tau_2 \circ \psi^\uparrow,$$

where  $\tau_2 = \tau \circ \tau$  denotes double translation.

This proposition shows that adjoint pyramid pairs are precisely those that arise from morphological adjunctions, and that they inherit the equivariance properties essential for image processing.

**5.2. Three canonical morphological pyramids.** We present three classical constructions from [19], and show that max-pooling is a special case of the third.

5.2.1. *Goutsias–Heijmans erosion pyramid.* Let  $b : \mathbb{Z}^d \rightarrow \overline{\mathbb{R}}$  be a centred structuring function with support  $W$ . The *Goutsias–Heijmans erosion pyramid* is defined by:

$$\varepsilon_b^{\downarrow R}(f)(x) = \sigma_R^{\downarrow}(\varepsilon_b(f))(x), \quad \text{where } (\varepsilon_b f)(x) = \min_{y \in W} \{f(y) - b(y - x)\}; \quad (33)$$

$$\delta_b^{*\uparrow R}(f)(x) = \delta_b^*(\sigma_R^{\uparrow, -\infty}(f))(x). \quad (34)$$

**Proposition 5.3** (Reconstruction by opening). *The reconstruction operator of the Goutsias–Heijmans erosion pyramid is a morphological opening:*

$$\gamma_b^{\downarrow R \uparrow}(f) = \delta_b^{*\uparrow R}(\varepsilon_b^{\downarrow R}(f)) = \delta_b^*(\sigma_R^{\uparrow, -\infty}(\sigma_R^{\downarrow}(\varepsilon_b(f)))). \quad (35)$$

*This is anti-extensive ( $\gamma_b^{\downarrow R \uparrow}(f) \leq f$ ) and idempotent.*

5.2.2. *Heijmans dilation pyramid.* The dual construction replaces erosion by dilation and uses  $c = +\infty$ :

$$\delta_b^{\downarrow R}(f)(x) = \sigma_R^{\downarrow}(\delta_b(f))(x), \quad \text{where } (\delta_b f)(x) = \max_{y \in W} \{f(y) + b(x - y)\}; \quad (36)$$

$$\varepsilon_b^{*\uparrow R}(f)(x) = \varepsilon_b^*(\sigma_R^{\uparrow, +\infty}(f))(x). \quad (37)$$

**Proposition 5.4** (Reconstruction by closing). *The reconstruction operator of the Heijmans dilation pyramid is a morphological closing:*

$$\varphi_b^{\downarrow R \uparrow}(f) = \varepsilon_b^*(\sigma_R^{\uparrow, +\infty}(\sigma_R^{\downarrow}(\delta_b(f)))). \quad (38)$$

*This is extensive ( $f \leq \varphi_b^{\downarrow R \uparrow}(f)$ ) and idempotent.*

5.2.3. *Max-pooling as a flat-structuring-function Heijmans pyramid.*

**Theorem 5.5** (Max-pooling as morphological pyramid). *Let  $b \equiv 0$  on a rectangular window  $W_{R \times R} = \{0, \dots, R - 1\}^2$  (flat structuring function). Then the Heijmans dilation pyramid with this  $b$  is exactly max-pooling:*

$$\delta_R^{\text{MP}}(f)(x) = \delta_b^{\downarrow R}(f)(x) = \max_{y \in W_{R \times R}} f(Rx - y). \quad (39)$$

*Its adjoint (unpooling) is the interpolation operator*

$$\varepsilon_b^{*\uparrow R}(f)(m) = \begin{cases} f(n) & \text{if } m = R \cdot n, \\ +\infty & \text{otherwise.} \end{cases} \quad (40)$$

*Proof.* With  $b \equiv 0$ ,  $(\delta_b f)(x) = \max_{y \in W} f(x - y)$  is a flat dilation (max-filter). Applying  $\sigma_R^{\downarrow}$  gives  $\max_{y \in W_{R \times R}} f(Rx - y)$ , which is the standard max-pooling operation with pool size  $R$  and stride  $R$ . The adjoint follows from Theorem 5.2 with  $c = +\infty$ .  $\square$

**Corollary 5.6** (Strided convolution and dilated convolution). *Strided convolution with stride  $R$  and kernel  $k$  corresponds to the Goutsias–Heijmans erosion pyramid with pre-processing the convolution  $\psi^{\downarrow}(f) = \sigma_R^{\downarrow}(f * k)$ . The corresponding transposed convolution (unpooling) is the adjoint synthesis operator of Equation (34).*

5.3. **Morphological skeleton and the Laplacian pyramid.** The Laplacian pyramid, ubiquitous in image processing and appearing implicitly in multi-scale CNN architectures, admits a morphological interpretation as a *skeleton by opening*.

**Definition 5.7** (Morphological skeleton). Given a family of erosions  $\{\varepsilon_i\}$  of increasing size (i.e.,  $\varepsilon_i = \varepsilon_{iB}$  for a base structuring element  $B$ ), the *skeleton decomposition* of  $f$  is:

$$S_i(f) = \varepsilon_i(f) - \gamma_B(\varepsilon_i(f)) = \varepsilon_i(f) - \delta_B^*(\varepsilon_{i+1}(f)), \quad (41)$$

with reconstruction  $f = \bigcup_i \delta_i(S_i(f))$ .

**Proposition 5.8** (Laplacian pyramid as skeleton [25]). Let  $g_\sigma$  be a Gaussian kernel and let  $\text{Gauss}_i(f) = \varepsilon_{g_\sigma}^{\downarrow 2, \circ i}(f)$  denote the Gaussian pyramid at scale  $i$ . The Laplacian pyramid

$$\text{Lapl}_i(f) = \text{Gauss}_i(f) - \delta_{g_\sigma}^{*\uparrow 2}(\text{Gauss}_{i+1}(f))$$

is the residue by opening (top-hat transform) of  $\text{Gauss}_i(f)$ :

$$\text{Lapl}_i(f) = \Gamma_{g_\sigma}^{\downarrow 2\uparrow}(\text{Gauss}_i(f)) = S_i(f), \quad (42)$$

where  $\Gamma_{g_\sigma}^{\downarrow 2\uparrow}(h) = h - \gamma_{g_\sigma}^{\downarrow 2\uparrow}(h)$  is the top-hat with respect to the pyramid opening.

This result provides a morphological justification for why multi-scale architectures based on pyramidal decomposition (feature pyramids, U-shaped networks) are effective: each level captures structures that survive erosion at that scale but are removed at the next coarser level, exactly as in the skeleton decomposition, one of the most powerful tools in mathematical morphology [21, 44].

## 6. RELU, MAX-POOLING, AND MORPHOLOGICAL ACTIVATIONS

Before developing the full morphological models of deep architectures in Section 7, we establish the precise lattice-theoretic status of the two most important nonlinear operations in standard CNNs: the ReLU activation and max-pooling. The analysis in this section draws on and extends the results of [48], where these operators were first studied as morphological dilations and their compositions were proposed as a general morphological activation family.

TABLE 5. Principal results of §6 (ReLU, Max-Pooling, Activations). Results marked (★) are the paper’s principal findings.

Ref.	Name	Statement and role
Prop 6.1 (★)	ReLU is a closing	ReLU commutes with pointwise suprema (it is a dilation), is extensive, and is idempotent; hence it is a <i>closing</i> in $(\mathcal{L}, \leq)$ . Its upper adjoint is a <i>global</i> (non-local) operator: no local erosion can form an adjunction pair with ReLU.
Prop 6.3	Max-pooling as dilation	Both non-decimated $\delta_W$ (stride 1) and decimated $\delta_R^{\text{MP}}$ (stride $R$ ) are dilations in $(\mathcal{L}, \leq)$ ; each has an explicit adjoint flat erosion forming a morphological opening when composed.
Prop 6.5 (★)	APD factorisation	ReLU and decimated max-pooling compose into a single dilation $\Psi_{R;\alpha}^{\text{APD}}(f)(n) = \sup_{y \in W_R} \max(0, f(Rn-y) + \alpha)$ ; its adjoint is global piecewise-constant upsampling by stride $R$ followed by shift $-\alpha$ .
Cor 6.11	Conv + ReLU as MMBB	The spectral operator $\Sigma_K^{\text{Spec}}$ (weighted sum of convolutions) followed by ReLU admits an exact MMBB-Increasing basis representation for non-negative kernels, and an MMBB-General representation for signed kernels.

### 6.1. ReLU and max-pooling as dilations in the pointwise lattice.

**Proposition 6.1** (ReLU is a dilation and a closing). *In the pointwise lattice  $(\text{Fun}(E, \overline{\mathbb{R}}), \leq)$ , the ReLU activation  $\delta^{\text{ReLU}}(f)(x) = \max(0, f(x))$  is:*

- (i) A dilation: it commutes with pointwise suprema,  $\delta^{\text{ReLU}}(\bigvee_i f_i) = \bigvee_i \delta^{\text{ReLU}}(f_i)$ .
- (ii) Extensive:  $f \leq \delta^{\text{ReLU}}(f)$  for all  $f$ , since  $f(x) \leq \max(0, f(x))$ .
- (iii) Idempotent:  $\delta^{\text{ReLU}} \circ \delta^{\text{ReLU}} = \delta^{\text{ReLU}}$ , since  $\max(0, \max(0, f(x))) = \max(0, f(x))$ .

Being extensive and idempotent, ReLU is a closing in the pointwise lattice. The upper adjoint of  $\delta^{\text{ReLU}}$  in  $(\text{Fun}(E, \overline{\mathbb{R}}), \leq)$  exists by the general adjoint functor theorem for complete lattices (Theorem 2.2), but it is not a pointwise operator: the adjunction condition  $\delta^{\text{ReLU}}(f) \leq g$  requires  $\max(0, f(x)) \leq g(x)$  for all  $x$ , which forces  $g(x) \geq 0$  for all  $x$  (since  $\delta^{\text{ReLU}}(f) \geq 0$  everywhere). For functions  $g \geq 0$  pointwise, the largest  $f$  satisfying  $\delta^{\text{ReLU}}(f) \leq g$  is

$$\varepsilon^{\text{ReLU}}(g)(x) = g(x), \quad g \geq 0, \quad (43)$$

i.e., the identity on the non-negative cone. For  $g \not\geq 0$  (i.e.,  $g(x_0) < 0$  at some point  $x_0$ ), no  $f$  satisfies  $\delta^{\text{ReLU}}(f) \leq g$  and the adjoint maps  $g$  to  $-\infty$  (the bottom of the lattice). In summary, the upper adjoint is:

$$\varepsilon^{\text{ReLU}}(g) = \begin{cases} g & \text{if } g(x) \geq 0 \text{ for all } x \in E, \\ -\infty & \text{otherwise.} \end{cases} \quad (44)$$

This is a global (non-pointwise) operator, which reflects the fact that ReLU is a closing in the pointwise lattice but not a max-plus dilation: its adjoint is determined by a global non-negativity constraint on  $g$ .

*Proof.* (i)  $\max(0, \sup_i f_i(x)) = \sup_i \max(0, f_i(x))$  since max distributes over suprema. (ii) and (iii) are direct from the definition of ReLU. A morphological closing satisfies: idempotent, increasing, extensive; all three hold here.

For the adjoint: we verify the adjunction condition  $\delta^{\text{ReLU}}(f) \leq g \iff f \leq \varepsilon^{\text{ReLU}}(g)$ .

When  $g \geq 0$  everywhere: ( $\Rightarrow$ ): If  $\max(0, f(x)) \leq g(x)$  for all  $x$ , then for  $f(x) \geq 0$ :  $f(x) \leq \max(0, f(x)) \leq g(x)$ ; for  $f(x) < 0$ :  $f(x) < 0 \leq g(x)$ . In both cases  $f(x) \leq g(x) = \varepsilon^{\text{ReLU}}(g)(x)$ . ( $\Leftarrow$ ): If  $f(x) \leq g(x)$  for all  $x$ , then  $\max(0, f(x)) \leq \max(0, g(x)) = g(x)$  (since  $g \geq 0$ ).

When  $g(x_0) < 0$  at some point  $x_0$ :  $\delta^{\text{ReLU}}(f)(x_0) = \max(0, f(x_0)) \geq 0 > g(x_0)$  for any  $f$ , so  $\delta^{\text{ReLU}}(f) \leq g$  is impossible. The adjoint correctly maps  $g$  to  $-\infty$ , which satisfies  $f \leq -\infty$  only for  $f = -\infty$ , confirming no solution exists.  $\square$

**Remark 6.2** (Why ReLU's adjoint is global). The non-pointwise character of the upper adjoint of  $\delta^{\text{ReLU}}$  (44) has a direct architectural consequence. For a max-plus dilation  $\delta_b$ , the adjoint erosion  $\varepsilon_{b^*}(g)(x) = \inf_y \{g(x+y) - b(-y)\}$  depends only on the values of  $g$  in a neighbourhood of  $x$ , making it a local operator. For ReLU, the adjoint must check the global non-negativity of  $g$  before returning a finite value: it is a *global* operator. This means that no local morphological erosion can serve as the adjoint of ReLU in the pointwise lattice, and therefore no composition of ReLU with a local dilation (such as max-pooling) forms a morphological adjunction. This is the precise algebraic reason why  $\delta_R^{\text{MP}} \circ \delta^{\text{ReLU}}$  cannot be part of a morphological opening, a conclusion that parallels but is distinct from the cross-lattice argument for full CNN layers in Theorem 8.5.

**Proposition 6.3** (Max-pooling: non-decimated and decimated forms). *We distinguish the two forms of max-pooling that appear in the literature and in this paper.*

**(A) Non-decimated flat dilation (stride 1):**

$$\delta_W(f)(x) = \sup_{y \in W} f(x - y), \quad x \in E, \quad (45)$$

is a dilation in  $(\text{Fun}(E, \overline{\mathbb{R}}), \leq)$ , extensive and (for  $W = W_{R \times R}$ ) not idempotent. Its adjoint erosion is the flat min-erosion at the same spatial resolution:

$$\varepsilon_W(g)(x) = \inf_{y \in W} g(x + y), \quad x \in E, \quad (46)$$

and  $(\varepsilon_W, \delta_W)$  is an adjunction in  $(\text{Fun}(E, \overline{\mathbb{R}}), \leq)$ . The compositions  $\delta_W \circ \varepsilon_W$  (opening) and  $\varepsilon_W \circ \delta_W$  (closing) are idempotent.

**(B) Decimated max-pooling (stride  $R$ , the standard CNN operation):**

$$\delta_R^{\text{MP}}(f)(n) = \sup_{y \in W_R} f(Rn - y), \quad n \in \mathbb{Z}^d, \quad (47)$$

maps the input grid  $\mathbb{Z}^d$  to the coarser output grid  $\mathbb{Z}^d$  (with the same index set but physically at stride  $R$ ). This is the Heijmans dilation pyramid  $\delta_b^{\downarrow R}$  with  $b \equiv 0$  (Theorems 5.2 and 5.5), a dilation in  $(\text{Fun}(E, \overline{\mathbb{R}}), \leq)$ . Its adjoint erosion is the erosion-decimation:

$$\varepsilon_R^{\text{MP}}(g)(n) = \inf_{y \in W_R} g(Rn + y), \quad n \in \mathbb{Z}^d, \quad (48)$$

also on the coarse grid (reading  $g$  at positions  $Rn + y$  in the input space). The adjunction  $(\varepsilon_R^{\text{MP}}, \delta_R^{\text{MP}})$  holds in  $(\text{Fun}(\mathbb{Z}^d, \overline{\mathbb{R}}), \leq)$ , and the compositions give the morphological opening and closing on the decimated grid.

*Proof. Part (A).*  $\delta_W(f)$  is a dilation by the flat max-plus dilation formula with  $b \equiv 0$ . The adjunction  $\varepsilon_W(f) \leq g \iff f \leq \delta_W(g)$ :  $\delta_W(f)(x) \leq g(x)$  iff  $\sup_{y \in W} f(x - y) \leq g(x)$  iff  $f(z) \leq g(z + y)$  for all  $y \in W$ , iff  $f(z) \leq \inf_{y \in W} g(z + y) = \varepsilon_W(g)(z)$ . Non-idempotency of  $\delta_W$ :  $\delta_W^2(f)(x) = \sup_{w \in W \oplus W} f(x - w)$  where  $W_{R \times R} \oplus W_{R \times R} = \{0, \dots, 2(R - 1)\}^d$ , a window of side  $2R - 1 > R$  for  $R > 1$ .

**Part (B).**  $\delta_R^{\text{MP}}(f)(n) = \sup_{y \in W_R} \{f(Rn - y) + 0\} = (\delta_0^{\downarrow R} f)(n)$  is the  $b \equiv 0$  case of the Heijmans dilation pyramid of Theorem 5.2. The adjoint was established there as the erosion-decimation  $\varepsilon_0^{\downarrow R}(g)(n) = \inf_{y \in W_R} g(Rn + y)$ . Adjunction verification:  $\delta_R^{\text{MP}}(f)(n) \leq g(n)$  iff  $\sup_{y \in W_R} f(Rn - y) \leq g(n)$  iff  $f(Rn - y) \leq g(n)$  for all  $y \in W_R$ , iff  $f(z) \leq g(n)$  for all  $z = Rn - y$  with  $y \in W_R$ , iff  $f(z) \leq \inf_{y \in W_R} g(\lceil z/R \rceil) = \varepsilon_R^{\text{MP}}(g)(n')$  where  $n' = \lceil z/R \rceil$ ; equivalently,  $f \leq \varepsilon_R^{\text{MP}}(g)$  on the input grid.  $\square$

**Remark 6.4.** Throughout this paper,  $\delta_R^{\text{MP}}$  always denotes the *decimated* form (47) of Part (B), consistent with the CNN layer definition (59) and the APD formula (49). The non-decimated form (45) of Part (A) is the flat dilation  $\delta_W$  used in the opening and closing analysis of the pointwise lattice. Both forms appear in Part (B) of the Goutsias–Heijmans pyramid theory (Section 5):  $\delta_R^{\text{MP}} = \delta_0^{\downarrow R}$  is the decimated dilation pyramid (Theorem 5.5), and the non-decimated version  $\delta_W = \delta_0^{\downarrow 1}$  is the flat dilation pyramid at stride 1. We provide in Table 6 other cases of pooling applications and their morphological interpretation.

## 6.2. Factorisation and the Activation-Pooling Dilation.

**Proposition 6.5** (Factorisation of ReLU and decimated max-pooling into the APD). *Both  $\delta_\alpha^{\text{ReLU}}(f)(x) = \max(0, f(x) + \alpha)$  and  $\delta_R^{\text{MP}}(f)(n) = \sup_{y \in W_R} f(Rn - y)$  are dilations in  $(\text{Fun}(E, \overline{\mathbb{R}}), \leq)$*

) (Theorem 6.1(i) and Theorem 6.3(B)). Their composition is the single Activation-Pooling Dilation (APD):

$$\Psi_{R;\alpha}^{\text{APD}}(f)(n) = \delta_R^{\text{MP}}(\delta_\alpha^{\text{ReLU}}(f))(n) = \sup_{y \in W_R} \max(0, f(Rn - y) + \alpha), \quad n \in \mathbb{Z}^d. \quad (49)$$

The APD is a dilation in  $(\text{Fun}(\mathbb{Z}^d, \overline{\mathbb{R}}), \leq)$ , mapping the input grid to the coarser output grid.

The upper adjoint  $\varepsilon_{R;\alpha}^{\text{APD}}$  of  $\Psi_{R;\alpha}^{\text{APD}}$  in the pointwise lattice exists but is not a local operator. From the adjunction condition  $\Psi_{R;\alpha}^{\text{APD}}(f) \leq g \iff f \leq \varepsilon_{R;\alpha}^{\text{APD}}(g)$ : since  $\Psi_{R;\alpha}^{\text{APD}}(f)(n) \geq 0$  for all  $f$  and  $n$ , we need  $g(n) \geq 0$  for all  $n$  (a global non-negativity constraint, identical to the ReLU adjoint situation, Theorem 6.1). For  $g \geq 0$  pointwise, the adjoint is:

$$\varepsilon_{R;\alpha}^{\text{APD}}(g)(z) = g\left(\left\lfloor \frac{z}{R} \right\rfloor\right) - \alpha, \quad z \in \mathbb{Z}^d, \quad (50)$$

where  $\lfloor z/R \rfloor$  is the component-wise floor division (the unique output grid point  $n$  such that  $Rn \leq z < R(n+1)$ ). For  $g \not\geq 0$ , the adjoint maps to  $-\infty$ . In the non-decimated case ( $R=1$ ), the adjoint simplifies to  $\varepsilon_{1;\alpha}^{\text{APD}}(g)(x) = g(x) - \alpha$  when  $g(x) \geq 0$ , and  $-\infty$  otherwise.

*Proof. APD formula.*  $\Psi_{R;\alpha}^{\text{APD}}(f)(n) = \delta_R^{\text{MP}}(\max(0, f + \alpha))(n) = \sup_{y \in W_R} \max(0, f(Rn - y) + \alpha)$ , by substituting the decimated max-pooling formula (47) with input  $\delta_\alpha^{\text{ReLU}}(f)$ . The composition of two dilations in the same complete lattice is a dilation [21].

*Adjoint formula.*  $\Psi_{R;\alpha}^{\text{APD}}(f)(n) \leq g(n)$  for all  $n$  means  $\max(0, f(Rn - y) + \alpha) \leq g(n)$  for all  $n$  and  $y \in W_R$ . Since  $\max(0, \cdot) \geq 0$ , this requires  $g(n) \geq 0$  for all  $n$  (global non-negativity). Given  $g \geq 0$ : the constraint becomes  $f(Rn - y) + \alpha \leq g(n)$ , i.e.,  $f(z) \leq g(n) - \alpha$  for each  $z = Rn - y$ . For a given  $z \in \mathbb{Z}^d$ , the unique  $n$  with  $y = Rn - z \in W_R = \{0, \dots, R-1\}^d$  is  $n = \lfloor z/R \rfloor$  (component-wise), so the tightest bound on  $f(z)$  is  $g(\lfloor z/R \rfloor) - \alpha$ . The largest  $f$  satisfying all constraints is therefore  $f(z) = g(\lfloor z/R \rfloor) - \alpha$ , giving (50).  $\square$

**Remark 6.6** (Non-local adjoint and architectural consequence). The global non-negativity condition on  $g$  in Theorem 6.5 is inherited from the ReLU component:  $\Psi_{R;\alpha}^{\text{APD}}(f) \geq 0$  always, so any  $g$  with a negative value at some output position  $n_0$  cannot be dominated by any APD output. This is the same non-locality identified for ReLU alone (Theorem 6.1) and confirms that the APD, like ReLU, does not have a local pointwise adjoint in the max-plus sense. The adjoint (50) is a *piecewise constant upsampling by factor  $R$*  followed by a shift by  $-\alpha$ : each output grid value  $g(n)$  is broadcast to the  $\mathbb{Z}^d$  input positions  $\{z : \lfloor z/R \rfloor = n\}$ , then shifted by  $-\alpha$ . This is the adjoint of decimation in the Goutsias–Heijmans sense (Theorem 5.2), composed with the adjoint of the ReLU closing.

**Remark 6.7.** Proposition 6.5 corresponds to Remark 1 of [48], where the APD was first proposed as a single operator replacing the separate ReLU and max-pooling steps. The key insight is that fusing two dilations in the same lattice into one reduces computational overhead and clarifies the algebraic role of the combined operation.

**6.3. Generalised morphological activations via MMBB.** The MMBB representation theorem motivates a generalisation of the ReLU family based on morphological operators.

**Definition 6.8** (Morphological activation family). A *morphological activation* is any operator of the form

$$\sigma_{\mathcal{B},c}^{\text{M}}(f)(x) = \min \left\{ \sup_{g \in \mathcal{B}} (\varepsilon_g f)(x), (\alpha_c f)(x) \right\}, \quad (51)$$

where  $\mathcal{B} \subset \text{Bas}(\Psi)$  is a finite sub-basis of some TI increasing operator  $\Psi$ , and  $\alpha_c(f)(x) = \inf_y \{-f(x+y) + c(y)\}$  is an anti-dilation by a fixed cap function  $c : \text{Spt}(c) \rightarrow \overline{\mathbb{R}}$  (Definition 2.10).

The equivalence to a supremum of Banon–Barrera sup-generating operators follows from the *complete distributivity* of  $(\overline{\mathbb{R}}, \leq)$ : in any completely distributive lattice,  $b \wedge \bigvee_g a_g = \bigvee_g (b \wedge a_g)$  holds for any family  $(a_g)_{g \in \mathcal{B}}$  and any fixed  $b \in \overline{\mathbb{R}}$ . Applying this pointwise with  $a_g = (\varepsilon_g f)(x)$  and  $b = (\alpha_c f)(x)$ :

$$\sigma_{\mathcal{B},c}^M(f)(x) = \sup_{g \in \mathcal{B}} \min\{(\varepsilon_g f)(x), (\alpha_c f)(x)\} = \sup_{g \in \mathcal{B}} \psi_{g,c}(f)(x). \quad (52)$$

This is a Banon–Barrera representation in which all pairs share the same upper bound  $g^+ = c$  (Theorem 2.11). It gives an exact representation of any TI operator  $\Psi$  whose sup-generating basis has a fixed upper cap  $c$  independent of  $g^-$ ; for operators with varying upper cap, it provides an approximation.

Special cases:

- $\mathcal{B} = \{g_0\}$  (point erosion,  $g_0(y) = 0$  for  $y = 0$ ,  $-\infty$  otherwise),  $c \equiv +\infty$  (vacuous cap):  $\sigma^M = \varepsilon_{g_0} = \text{Id}$  (identity).
- $\mathcal{B} = \{g_0\}$  (point erosion),  $c \equiv 0$ :  $\varepsilon_{g_0}(f)(x) = f(x)$  and  $\alpha_0(f)(x) = \inf_y \{-f(x+y)\} = -\sup_y f(x+y)$ . For signals with compact support (or when the anti-dilation uses only the value at  $y = 0$ ):  $\alpha_0(f)(x) = -f(x)$ , giving  $\sigma^M = \min(f, -f) = -|f|$ . This is the *negative absolute value*, not ReLU.
- $\mathcal{B} = \text{Bas}^{\text{trunc}}$  (MMBB sub-basis),  $c \equiv 0$ : a MMBB lower approximation capped at zero, generalising ReLU to an arbitrary erosion shape. This is the primary use case of the definition: any activation that is a morphological erosion below some level and zero above it.

**Proposition 6.9** (ReLU as a lattice join; connection to MMBB-General representation). *The ReLU activation  $\delta^{\text{ReLU}}(f)(x) = \max(0, f(x))$  satisfies:*

(i) *It is the lattice join of  $f$  with the zero function  $\mathbf{0} \equiv 0$  in  $(\text{Fun}(E, \overline{\mathbb{R}}), \leq)$ :*

$$\delta^{\text{ReLU}}(f) = f \vee \mathbf{0}, \quad \delta^{\text{ReLU}}(f)(x) = \sup\{f(x), 0\}. \quad (53)$$

- (ii) *As a lattice join, it is a dilation (Proposition 6.1(i)), but not a max-plus dilation  $\delta_b$  for any structuring function  $b$ , because max-plus dilations are shift-equivariant ( $\delta_b(f+c) = \delta_b(f) + c$ ) while ReLU is not ( $\delta^{\text{ReLU}}(f+c) \neq \delta^{\text{ReLU}}(f) + c$  for  $c < 0$ ).*
- (iii) *In the Banon–Barrera framework, ReLU is a sup-generating operator of the form*

$$\delta^{\text{ReLU}}(f)(x) = \sup\{\psi_{\mathbf{0},+\infty}(f)(x), \psi_{-\infty,\mathbf{0}}(f)(x)\}, \quad (54)$$

where  $\psi_{\mathbf{0},+\infty}(f)(x) = \varepsilon_{\mathbf{0}} f(x) = f(x)$  (identity erosion, vacuous cap) and  $\psi_{-\infty,\mathbf{0}}(f)(x) = \min\{-\infty, \alpha_{\mathbf{0}}(f)(x)\}$  is the indicator that forces the output to be  $\geq 0$ . More concisely:  $\delta^{\text{ReLU}}(f)(x) = \sup\{f(x), 0\}$ , a two-element supremum of a TI operator (identity) and a constant (zero).

*Proof.* (i)  $\max(f(x), 0) = \sup\{f(x), 0\}$  by definition. (ii) Shift-equivariance of  $\delta_b$ :  $\delta_b(f+c)(x) = \sup_y \{(f+c)(x-y) + b(y)\} = \sup_y \{f(x-y) + b(y)\} + c = \delta_b(f)(x) + c$ . For ReLU:  $\delta^{\text{ReLU}}(f+c)(x) = \max(0, f(x) + c)$ , which equals  $\delta^{\text{ReLU}}(f)(x) + c$  only when  $f(x) + c \geq 0$ ; for  $c < 0$  and  $-c > f(x) \geq 0$ :  $\delta^{\text{ReLU}}(f+c)(x) = 0 \neq \max(0, f(x)) + c = f(x) + c > 0$  (contradiction since  $f(x) + c < 0$ ). So shift-equivariance fails. (iii) The Banon–Barrera theorem (Theorem 2.11) guarantees a representation; the specific two-element form  $\sup\{f(x), 0\}$  identifies the two sup-generating elements: the identity (arising from  $g^- = \mathbf{0}$ , vacuous upper cap) and the constant zero function (arising as the “floor” constraint).  $\square$

**Remark 6.10** (Positive–negative decomposition and the MMBB-General structure). Every function  $f$  decomposes into its positive and negative parts:  $f = f^+ - f^-$  where

$$f^+(x) = \delta^{\text{ReLU}}(f)(x) = \max(0, f(x)), \quad f^-(x) = \delta^{\text{ReLU}}(-f)(x) = \max(0, -f(x)), \quad (55)$$

where  $f^+, f^- \geq 0$  and  $f = f^+ - f^-$ . Both  $f^+$  and  $f^-$  are dilations in the pointwise lattice (Proposition 6.1). The full function  $f = f^+ - f^-$  is thus the difference of two dilations, precisely the structure identified in Theorem 4.4 for general signed convolution kernels, and the Banon–Barrera representation (Theorem 2.11) for non-increasing operators. Concretely: a signed CNN kernel acts on  $f$  to produce a signed output, whose positive and negative parts are then selected by ReLU ( $f^+$ ) or by the anti-ReLU ( $f^-$ ); retaining both parts, as in the symmetric pooling of Section 9.3, is the algebraically natural design for signed feature maps.

**Corollary 6.11** (Convolution + ReLU as MMBB layer; the  $\Sigma^{\text{Spec}}$  operator). *The composition of a linear combination of  $K$  convolutions followed by ReLU,*

$$\Sigma_K^{\text{Spec}}(f) := \sum_{i=1}^K w_i(f * k_i), \quad \delta_\alpha^{\text{ReLU}}(\Sigma_K^{\text{Spec}}(f)) = \max\left(0, \Sigma_K^{\text{Spec}}(f) + \alpha\right), \quad (56)$$

is the spectral feature-extraction operator of a CNN layer. For a general signed kernel decomposition  $k_i = G_i^+ \bar{k}_i^+ - G_i^- \bar{k}_i^-$ , the post-ReLU output admits the MMBB representation:

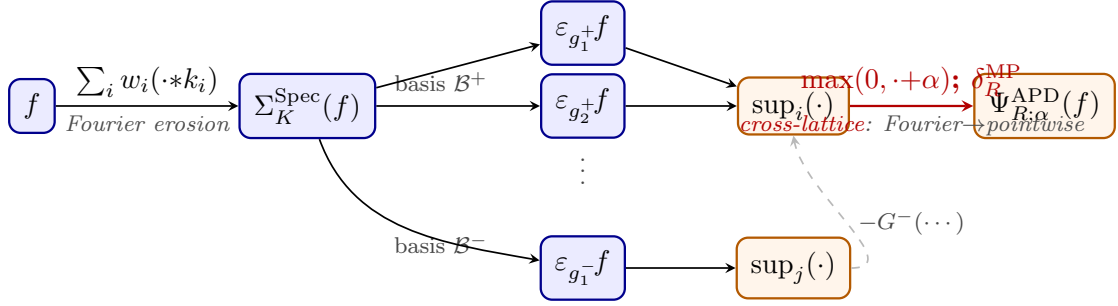
$$\delta_\alpha^{\text{ReLU}}(\Sigma_K^{\text{Spec}}(f))(x) = \max\left(0, \sum_i G_i^+ \sup_{g^+ \in \mathcal{B}_i^+} (\varepsilon_{g^+} f)(x) - \sum_i G_i^- \sup_{g^- \in \mathcal{B}_i^-} (\varepsilon_{g^-} f)(x) + \alpha\right), \quad (57)$$

where  $\mathcal{B}_i^\pm \subset \text{Bas}(\bar{k}_i^\pm)$  are finite sub-bases. For non-negative kernels and inputs ( $k_i \geq 0, f \geq 0$ ): the ReLU is inactive whenever  $\Sigma_K^{\text{Spec}}(f) + \alpha \geq 0$ , and the output is simply  $\sup_{g \in \mathcal{B}} (\varepsilon_g f)(x) + \alpha$ , a pure MMBB truncation with additive bias.

*Proof.* Apply Theorem 4.4 to each  $f * k_i$ , sum with weights  $w_i$ , add bias  $\alpha$ , then apply ReLU: since  $\max(0, \cdot)$  is monotone, it distributes through the outer sup but not the difference of the two MMBB expansions. For  $k_i \geq 0$  and  $f \geq 0$ :  $f * k_i \geq 0$ , so  $\delta^{\text{ReLU}} = \text{Id}$  on any non-negative input.  $\square$

**Remark 6.12** (Connection to MorphoActivation). Corollary 6.11 provides the theoretical justification for the MorphoActivation proposal of [48]: the combined convolution–activation block  $\delta_\alpha^{\text{ReLU}} \circ \Sigma_K^{\text{Spec}}$  is representable (exactly or approximately) as a supremum of erosions, making the entire pre-pooling stage of a CNN a MMBB network.

(a) Conv + ReLU as MMBB-Increasing erosion pipeline (57)



(b) APD factorisation: ReLU and  $\delta_R^{MP}$  fused into one dilation

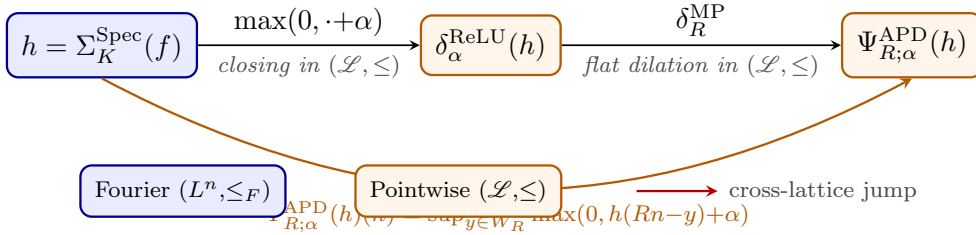


FIGURE 1. MMBB activation pipeline and APD factorisation. Node colours denote the lattice each operator lives in: **blue** = Fourier  $(L^n, \le_F)$ , **orange** = pointwise  $(\mathcal{L}, \le)$ . The red arrow marks the cross-lattice jump from Fourier erosion to pointwise dilation. (a) Convolution + ReLU as an MMBB erosion pipeline (Corollary 6.11):  $\Sigma_K^{Spec}$  (Fourier) feeds basis erosions from  $\mathcal{B}^\pm$ ; their suprema combine, and the APD applies ReLU and pooling in the pointwise lattice. (b) APD factorisation (Proposition 6.5): ReLU (a closing) and  $\delta_R^{MP}$  (a dilation), both in  $(\mathcal{L}, \le)$ , fuse into the single dilation  $\Psi_{R;\alpha}^{APD}$  (orange arc).

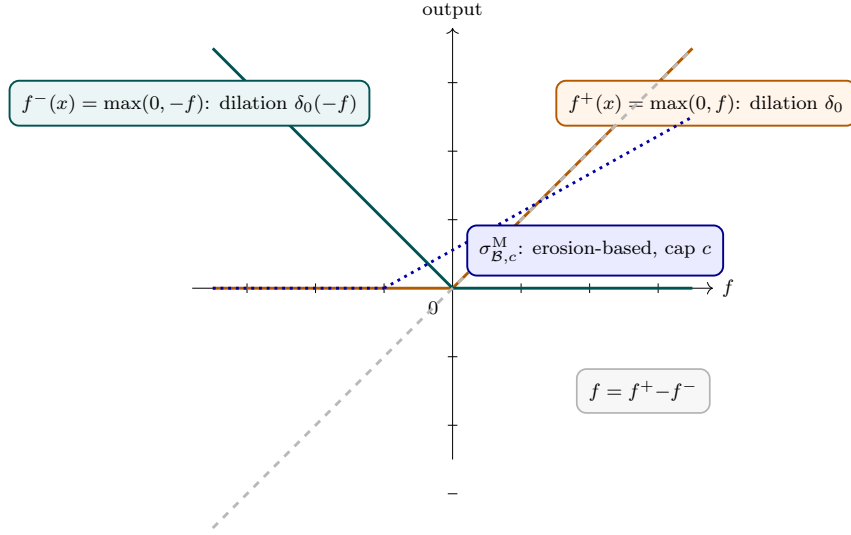


FIGURE 2. Positive/negative decomposition and MMBB activation shape.  $f^+(x) = \max(0, f)$  (orange) and  $f^-(x) = \max(0, -f)$  (teal) are both dilations in  $(\mathcal{L}, \leq)$ ; their difference recovers  $f = f^+ - f^-$  (dashed diagonal, Remark 6.10). The blue dotted line shows a MMBB morphological activation  $\sigma_{\mathcal{B},c}^M$  (Definition 6.8): an erosion-based operator with reduced slope and upper cap at level  $c$ , generalising ReLU.

TABLE 6. Five pooling operations and their morphological classification. Max-pooling is the only flat dilation with a local adjoint in  $(\mathcal{L}, \leq)$ .

Pooling	Formula	Morphological type
$\delta_R^{\text{MP}}$ (pool)	$(\max\text{-} \sup_{y \in W_R} \{f(Rn-y)\})$	Flat dilation $\delta_0$ ; extensive; adjoint: $\varepsilon_R^{\text{MP}}(g)(n) = \inf_{y \in W_R} g(Rn+y)$ (Theorem 6.3(B))
AvgPool $_R$ (average-pool)	$\frac{1}{ W_R } \sum_{y \in W_R} f(Rn-y)$	Fourier-lattice erosion (linear conv. by $k \equiv 1/ W_R $ ); not a max-plus dilation; no local pointwise adjoint
StochPool $_R$ (stochastic)	$f(Rn-Y), Y \sim \text{Cat}(f/\sum f)$	Random selection; not TI, not increasing; outside the morphological framework
MixPool $_R$ (mixed)	$\lambda \delta_R^{\text{MP}}(f) + (1-\lambda) \text{AvgPool}_R(f)$	Convex combination of a dilation and a Fourier erosion; not increasing for $\lambda < 1$
SymPool $_R$ (symmetric)	$\delta_R^{\text{MP}}(f^+) - \delta_R^{\text{MP}}(f^-)$	$\approx$ self-dual opening $\gamma_{W_R}^{\text{Med}}$ in $(\mathcal{L}, \preceq)$ ; idempotent when $f$ is sign-consistent on each window (Theorem 9.10)

## 7. MORPHOLOGICAL MODELS OF DEEP CONVOLUTIONAL ARCHITECTURES

We now synthesise the preceding theory into algebraic models of standard deep architectures, drawing on the adjunction framework of Section 2, the MMBB basis of Section 4, the pyramid theory of Section 5, and the morphological activation analysis of Section 6. Two new architectures are proposed: the *morphological APMO layer* (Section 7.2) as a fully max-plus replacement for the standard CNN layer, and the *UResNet* (Theorem 7.8), in which skip connections carry top-hat residues (difference between the input and its opening) rather than concatenated features. The idempotency and fixed-point analysis of these models is deferred to Section 8.

TABLE 7. Principal results of §7 (Morphological Models of CNN, ResNet, UNet). Results marked (★) are the paper’s principal findings.

Ref.	Name	Statement and role
Prop 7.6 (★)	ResNet as opening	When the residual function $\mathcal{F} \approx \gamma_b^M - \text{id}$ , the ResNet block $\mathcal{F}(f) + f$ computes the Type-I opening $\gamma_b^M(f) = \delta_{b^*}(\varepsilon_b(f))$ ; the skip connection carries the top-hat residue $\Gamma(f) = f - \gamma_b^M(f)$ .
Prop 7.9	Skip connections as top-hat	UResNet skip connections carry $\Gamma_b(f) = f - \gamma_b^M(f)$ at each scale; the decoder reconstructs $f$ from the pyramid opening plus the residue, achieving exact scale-by-scale reconstruction.
Prop 7.4	APMO approximation	The APMO (infimum of $J$ dilations) provides an upper approximation of any TI increasing layer $\Psi$ , dual to the MMBB lower approximation; the two together bracket $\Psi f$ from above and below.

## 7.1. The morphological CNN layer.

The spectral feature-extraction operator  $\Sigma_n^{\text{Spec}}$ . In Theorem 6.11 we introduced  $\Sigma_K^{\text{Spec}}(f) = \sum_{i=1}^K w_i(f * k_i)$  as the linear combination of  $K$  convolutions at a single layer. In a multilayer network we index by layer  $n$ :

$$\Sigma_n^{\text{Spec}}(f) := \sum_{i=1}^{K_n} w_{n,i} \varepsilon_{k_{n,i}}^{\text{Conv}}(f) = \sum_{i=1}^{K_n} w_{n,i} (f * k_{n,i}), \quad (58)$$

where  $\{k_{n,i}\}_{i=1}^{K_n}$  are the learned kernels and  $\{w_{n,i}\}$  the learned weights at layer  $n$ . This operator lives in the Fourier inf-semilattice  $(L^n, \leq_F)$  [4, 25]. Alternatively, it can be represented as a MMBB-Increasing operator when all  $k_{n,i} \geq 0$ ; for general signed kernels it is TI but not increasing, and admits the MMBB-General representation Theorem 2.11.

The one-layer CNN as APD  $\circ \Sigma^{\text{Spec}}$ . A standard one-layer CNN with  $K_n$  filters computes

$$f \longmapsto \delta_R^{\text{MP}} \left( \delta_\alpha^{\text{ReLU}} \left( \sum_{i=1}^{K_n} w_{n,i} (f * k_{n,i}) \right) \right) = \Psi_{R;\alpha}^{\text{APD}}(\Sigma_n^{\text{Spec}}(f)), \quad (59)$$

where  $\Psi_{R;\alpha}^{\text{APD}}$  is the Activation-Pooling Dilation of Theorem 6.5, which fuses ReLU and max-pooling into a single dilation in the pointwise lattice  $(\mathcal{L}, \leq)$ .

This factorisation has two immediate consequences established in Section 6:

- *Lattice structure*:  $\Sigma_n^{\text{Spec}}$  is a cross-lattice operator (erosion in the Fourier lattice) while  $\Psi_{R;\alpha}^{\text{APD}}$  is a dilation in the pointwise lattice; the composition is cross-lattice and *not* a morphological opening in either (Theorem 8.5).
- *Signed weights*: when  $w_{n,i}$  include negatives,  $\Sigma_n^{\text{Spec}}$  decomposes as a difference of two MMBB-Increasing expansions (Theorems 4.4 and 6.11). The asymmetry between positive and negative activations motivates the self-dual framework of Section 9.

*Observation 7.1* (Max-plus alternative to  $\Sigma_n^{\text{Spec}}$ ). The linear combination  $\Sigma_n^{\text{Spec}}(f) = \sum_i w_{n,i} \varepsilon_{k_{n,i}}^{\text{Conv}}(f)$  can be replaced by a max-plus supremum:

$$\Sigma_n^{\text{Spec,M}}(f)(n) = \max_{1 \leq i \leq K_n} \{ \varepsilon_{k_{n,i}}^{\text{Conv}}(f)(n) + b_{n,i} \}, \quad (60)$$

which is the pointwise maximum of the  $K_n$  convolution outputs with additive biases. In the Fourier lattice this is an upper envelope of erosions, hence itself a dilation in that lattice. Replacing  $\Sigma_n^{\text{Spec}}$  by  $\Sigma_n^{\text{Spec,M}}$  removes the linear summation and aligns the feature-extraction stage more closely with the max-plus structure of the pooling stage.

*Observation 7.2* (Non-commutativity of  $\varepsilon_k^{\text{Conv}}$  and  $\delta_R^{\text{MP}}$ ). Let  $\text{Sub}_R$  denote subsampling by stride  $R$  (without the max):  $\text{Sub}_R(f)(n) = f(Rn)$ .

*Linear subsampling and convolution*. For linear subsampling,  $\text{Sub}_R(f*k)(n) = \sum_m f(m)k(Rn-m)$  while  $\text{Sub}_R(f) * k$  would convolve the subsampled signal with  $k$  at the coarse scale. These are related by the *noble identity* (polyphase representation):  $\text{Sub}_R(f * k) = \text{Sub}_R(f) * \tilde{k}$ , where  $\tilde{k}(n) = \sum_{\ell \in \mathbb{Z}^d} k(n + \ell R)$  is the aliased (periodically folded) version of  $k$ . Convolution commutes with subsampling, in the sense that  $\tilde{k} = k$  on the coarse grid, if and only if  $k$  is supported entirely at multiples of  $R$ , i.e.,  $k$  is itself a subsampled kernel. For a general low-pass filter  $k$ , the aliasing error  $\|\tilde{k} - k\|$  is controlled by the energy of  $k$  outside the Nyquist band  $[-\pi/R, \pi/R]$ ; the Nyquist condition on  $k$  makes this error zero for *average-pooling* (linear subsampling), not for max-pooling.

*Max-pooling and convolution*. Max-pooling is nonlinear and the noble identity does not apply.  $\delta_R^{\text{MP}}(f * k)(n) = \sup_{y \in W_R} (f * k)(Rn - y)$  does not simplify to any convolution of  $\delta_R^{\text{MP}}(f)$  with  $k$  for general  $f$  and  $k$ , because sup does not distribute over linear sums. The two operations are approximately interchangeable when  $f$  varies slowly over each window  $W_R$  (Lipschitz condition on  $f$ ) and  $k$  is nearly flat on  $W_R$ ; the error is bounded by  $\text{Lip}(f) \cdot R \cdot \|k\|_1$  where  $\text{Lip}(f)$  is the Lipschitz constant of  $f$ . This is distinct from the Nyquist bandlimit condition, which applies to linear subsampling only.

**7.2. The general morphological nonlinear layer in a CNN: APMO.** The APD factorisation (Theorem 6.5) fuses ReLU and max-pooling into a single dilation. The APMO generalises this by replacing the single dilation with a *finite infimum of dilations*, which is the dual counterpart of the MMBB supremum of erosions. That would provide a more general nonlinear layer.

**Definition 7.3** (Activation–Pooling Morphological Operator). The *Activation–Pooling Morphological Operator* (APMO) with  $J$  structuring functions  $\{b_j\}_{j=1}^J$  and biases  $\{\alpha_j\}_{j=1}^J$  is:

$$\Psi^{\text{APMO}}(f)(n) = \inf_{1 \leq j \leq J} \left\{ \delta_{b_j}(f)(Rn) + \alpha_j \right\} = \inf_{1 \leq j \leq J} \left\{ \max_{y \in W_R} \{ f(Rn - y) + b_j(y) \} + \alpha_j \right\}, \quad (61)$$

where  $\delta_{b_j}(f)(Rn) = \max_{y \in W_R} \{ f(Rn - y) + b_j(y) \}$  is the max-plus dilation of  $f$  by  $b_j$  evaluated on the coarse grid (stride  $R$ ), and  $n \in \mathbb{Z}^d$ . The infimum over  $J$  dilations makes the APMO an *erosion in the dual max-plus lattice*: it commutes with pointwise infima,  $\Psi^{\text{APMO}}(\inf_i f_i) = \inf_i \Psi^{\text{APMO}}(f_i)$ .

**Proposition 7.4** (APMO as truncated dual MMBB upper approximation of any nonlinear TI increasing layer  $\Psi$ ). *The APMO is a dual (upper) MMBB-Increasing approximation. Recall that the MMBB theorem represents any TI increasing operator  $\Psi$  both as a supremum of erosions (lower representation, Theorem 2.8) and dually as an infimum of dilations (upper representation):*

$$\Psi(f)(x) = \sup_{g \in \text{Bas}(\Psi)} \varepsilon_g(f)(x) = \inf_{h \in \text{Bas}(\bar{\Psi})} \delta_{h^*}(f)(x), \quad (62)$$

where  $\bar{\Psi}(f) = -\Psi(-f)$  is the dual operator and  $h^*(y) = h(-y)$  the transposed structuring function. The APMO with basis  $\{b_j\}_{j=1}^J$  realises a truncated version of the upper representation:

$$\Psi^{\text{APMO}}(f)(n) = \inf_{j=1}^J \delta_{b_j}(f)(Rn) + \alpha_j \geq \Psi(f)(Rn), \quad (63)$$

an upper approximation of  $\Psi$  evaluated at the coarse grid (stride  $R$ ). Together with the MMBB lower approximation  $\Psi_K^l(f) = \sup_{i=1}^K \varepsilon_{g_i}(f)$ , they bracket  $\Psi$  from below and above:

$$\sup_{i=1}^K \varepsilon_{g_i}(f)(Rn) \leq \Psi(f)(Rn) \leq \inf_{j=1}^J \delta_{b_j}(f)(Rn) + \alpha_j. \quad (64)$$

As  $K, J \rightarrow |\text{Bas}(\Psi)|$ , both bounds converge to  $\Psi(f)(Rn)$ .

*Proof.* The dual MMBB-Increasing representation (62) is the second form in Theorem 2.8: applying the MMBB-Increasing theorem to the dual operator  $\bar{\Psi}$  gives  $\bar{\Psi}(f)(x) = \sup_{h \in \text{Bas}(\bar{\Psi})} \varepsilon_h(f)(x)$ , and substituting  $\bar{\Psi}(f) = -\Psi(-f)$  and  $f \rightarrow -f$  gives  $\Psi(f)(x) = \inf_{h \in \text{Bas}(\bar{\Psi})} \delta_{h^*}(f)(x)$ . Taking any  $J$  elements  $\{b_j\}_{j=1}^J \subset \text{Bas}(\bar{\Psi})$  (with  $b_j^* = h^*$  for  $h = b_j$ ) and adding biases  $\alpha_j \geq 0$  gives a value  $\geq$  the infimum over the full basis, hence  $\geq \Psi(f)(Rn)$ . The lower approximation follows from Theorem 2.8 directly; the two-sided bracket (64) is the standard MMBB-Increasing approximation theory by Maragos [31].  $\square$

**Remark 7.5** (Duality in architecture). The structural duality between the erosion-based MMBB layer and the APMO has a direct architectural interpretation:

- **sup of erosions** (lower bound):  $\Psi_K^l(f) = \sup_{i=1}^K \varepsilon_{g_i}(f)$ . Each erosion  $\varepsilon_{g_i}$  tests whether  $f \geq g_i$  (morphological matching); the supremum selects the best match. This is the *analysis* side: detecting features present in  $f$ .
- **inf of dilations** (upper bound):  $\Psi_J^u(f) = \inf_{j=1}^J \delta_{b_j}(f)$ . Each dilation  $\delta_{b_j}$  expands  $f$  by structuring function  $b_j$ ; the infimum retains only the structures common to all  $J$  expansions. This is the *synthesis* side: pooling and selecting among expanded feature maps.

A morphological CNN layer that brackets a general operator  $\Psi$  from both sides would compose an lower layer with an upper layer, with the true operator  $\Psi$  sandwiched between them. The standard CNN layer (conv + ReLU + max-pooling) uses convolution seen as the lower side (erosions) with the upper (APMO/dilation) side; a purely morphological layer using only the lower (MMBB/erosion) side is the Type-I opening of Theorem 8.4(i).

The complete multilayer CNN, alternating between spectral feature extraction and morphological activation, is:

$$L_n = \Psi_n^{\text{APMO}}(\Sigma_n^{\text{Spec}}(L_{n-1})), \quad \Sigma_n^{\text{Spec}}(f) = \sum_{i=1}^{K_n} w_{n,i} \varepsilon_{k_{n,i}}^{\text{Conv}}(f), \quad (65)$$

where  $\Sigma_n^{\text{Spec}}$  was defined in (58) and its MMBB representation is given in (57). When  $\Psi_n^{\text{APMO}}$  reduces to  $\Psi_{R;\alpha_n}^{\text{APD}}$  (i.e.,  $J = 1$ , flat  $b_1 \equiv 0$ ,  $\alpha_1 = \alpha$ ), this recovers the standard CNN layer (59). The alternation between  $\Sigma_n^{\text{Spec}}$  (Fourier-lattice erosion, analysis side) and  $\Psi_n^{\text{APMO}}$  (dual MMBB

upper approximation, synthesis/pooling side) reflects the fundamental duality of Theorem 2.8:  $\Sigma_n^{\text{Spec}}$  approximates the operator from below (lower MMBB) while  $\Psi_n^{\text{APMO}}$  approximates from above (upper dual MMBB), and the true operator  $\Psi$  is sandwiched between them (Theorem 7.4, eq. (64)).

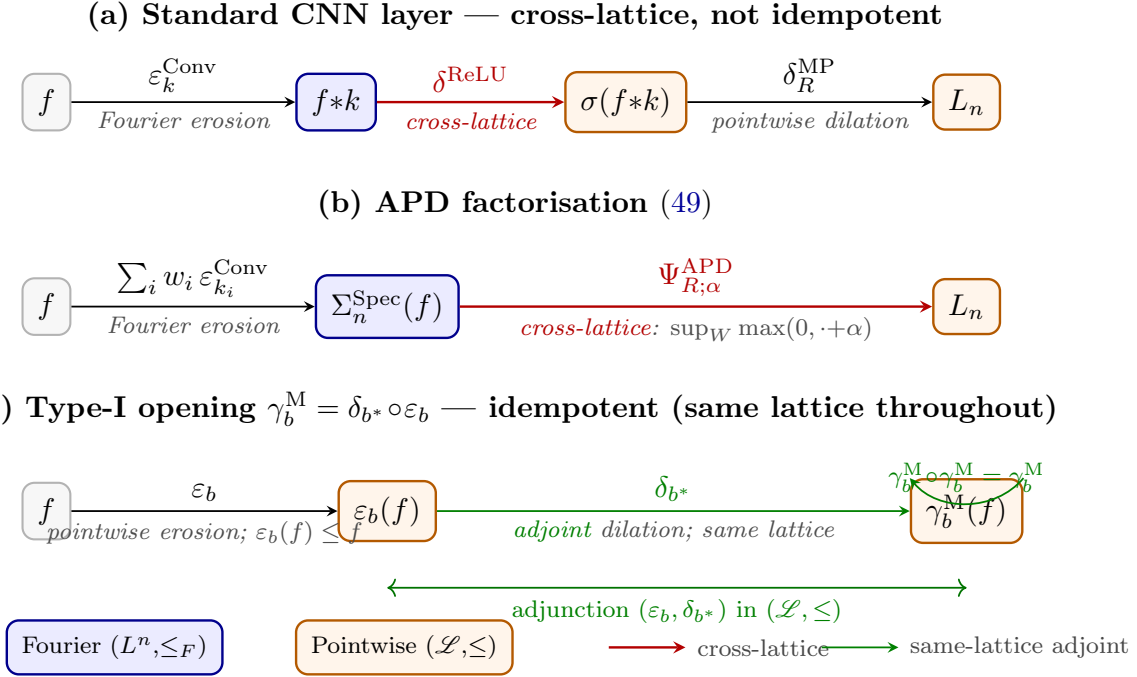


FIGURE 3. Three algebraic views of a CNN layer. Node colours denote the lattice: **blue** = Fourier, **orange** = pointwise. Red arrows mark cross-lattice jumps; green arrows mark same-lattice adjoint pairs. (a) Standard CNN: the convolution  $\varepsilon_k^{\text{Conv}}$  lives in the Fourier lattice while  $\delta^{\text{ReLU}}$  and  $\delta_R^{\text{MP}}$  live in the pointwise lattice; the red arrow marks the cross-lattice jump that breaks idempotency. (b) APD factorisation: ReLU and max-pooling fuse into  $\Psi_{R;\alpha}^{\text{APD}}$  (still cross-lattice). (c) Type-I opening:  $\varepsilon_b$  and its adjoint dilation  $\delta_{b^*}$  both in  $(\mathcal{L}, \leq)$ ; the composition  $\gamma_b^M$  is idempotent (green loop, Theorem 8.4(i)).

**7.3. Morphological model of ResNet.** A residual block in ResNet [23] computes  $L = \mathcal{F}(f) + f$ , where  $\mathcal{F}$  is a stack of convolutional layers. In our notation:

**Proposition 7.6** (ResNet block as morphological opening). *A residual block  $L = \mathcal{F}(f) + f$  where  $\mathcal{F}$  is a stack of CNN layers computes, under the approximation  $\mathcal{F}(f) \approx \gamma_b^M(f) - f$  (i.e., the residual function learns the deviation of  $f$  from its morphological opening):*

$$L \approx \gamma_b^M(f) = \delta_{b^*}(\varepsilon_b(f)), \quad (66)$$

a Type-I morphological opening (Theorem 8.4(i)). The skip connection  $+f$  adds back the top-hat residue  $\Gamma_b(f) = f - \gamma_b^M(f) \geq 0$  (the detail discarded by the opening), so that  $\mathcal{F}(f) + f = (\gamma_b^M(f) - f) + f = \gamma_b^M(f)$ .

**Remark 7.7.** The top-hat transform  $\Gamma(f) = f - \gamma(f)$  is a classical tool in morphological image analysis for extracting structures smaller than the structuring element used in the opening  $\gamma$  (i.e., the structures which are not invariant to the structuring element) [44]. Theorem 7.6 reveals that the residual learning mechanism of ResNet has a natural morphological interpretation: each residual block computes the top-hat of the feature map with respect to the learned morphological opening  $\Psi_1^M \circ \Sigma_1^{\text{Spec}}$ . This explains geometrically why residual connections preserve fine-grained information: top-hat transforms retain exactly the structures that opening (smoothing) removes.

**7.4. Morphological model of UNet.** The UNet architecture [42] is an encoder–decoder with skip connections between symmetric levels. At each encoder level the standard UNet applies a stack of convolutions followed by ReLU activations and max-pooling; the decoder applies transposed convolutions with upsampling. In morphological terms:

- **Standard encoder step:**  $L_\ell^\downarrow = \Psi_{R;\alpha}^{\text{APD}}(\Sigma_\ell^{\text{Spec}}(L_{\ell-1}^\downarrow))$ , the CNN layer of (59) (convolution + ReLU + max-pooling fused via Theorem 6.5).
- **Morphological encoder step:**  $L_\ell^\downarrow = \varepsilon_{R,b_\ell}^\downarrow(\Sigma_\ell^{\text{Spec}}(L_{\ell-1}^\downarrow))$ , where  $\varepsilon_{R,b_\ell}^\downarrow$  is the erosion-decimation (Theorem 5.2). The erosion is anti-extensive ( $\varepsilon_b(f) \leq f$ ), which plays the same role as ReLU (thresholding from below) while also performing the pooling step. The ReLU is therefore *subsumed* by the morphological erosion: the negativity-clipping of ReLU is replaced by the more general morphological thresholding determined by the structuring function  $b_\ell$ .

Let  $\Sigma_n^{\text{Spec}} = \sum_{i=1}^{K_n} w_{n,i} \varepsilon_{k_{n,i}}^{\text{Conv}}$  denote the spectral convolution operator (without activation), and  $\Sigma_n^{\text{Spec},\prime}$  its decoder counterpart.

**Definition 7.8** (Morphological UNet). The *morphological UNet* with  $n$  levels uses erosion-decimation in the encoder and adjoint dilation-interpolation in the decoder:

$$L_\ell^\downarrow = \varepsilon_{R,b_\ell}^\downarrow(\Sigma_\ell^{\text{Spec}}(L_{\ell-1}^\downarrow)), \quad \ell = 1, \dots, n, \quad (67)$$

$$L_\ell^\uparrow = \delta_{R,b_\ell}^{*\uparrow}(\Sigma_\ell^{\text{Spec},\prime}(L_{\ell+1}^\uparrow)) + s_\ell, \quad \ell = n-1, \dots, 0, \quad (68)$$

where  $\varepsilon_{R,b_\ell}^\downarrow$  is the erosion-decimation at stride  $R$  with structuring function  $b_\ell$  (Theorem 5.2),  $\delta_{R,b_\ell}^{*\uparrow}$  its adjoint dilation-interpolation, and  $s_\ell$  is the skip-connection signal at level  $\ell$ . Note that  $\varepsilon_{R,b_\ell}^\downarrow$  replaces the  $\Psi_{R;\alpha}^{\text{APD}}$  of the standard CNN encoder: the erosion provides both the thresholding (activation by ReLU) and the spatial pooling in one max-plus operator. Here  $\Sigma_\ell^{\text{Spec},\prime} = \sum_{i=1}^{K'_\ell} w'_{\ell,i} \varepsilon_{k'_{\ell,i}}^{\text{Conv}}$  is the decoder spectral operator at level  $\ell$ , a linear combination of convolutions with learned kernels  $\{k'_{\ell,i}\}$  that merges the upsampled features with the skip signal  $s_\ell$ ; it plays the same role as  $\Sigma_\ell^{\text{Spec}}$  in the encoder but with independent weights.

In the *standard UNet* [42],  $s_\ell = L_\ell^\downarrow$  (concatenation of encoder features). In the proposed *UResNet*, the skip connection carries the top-hat residue:

$$s_\ell = \Gamma_{b_\ell}(L_\ell^\downarrow) = L_\ell^\downarrow - \gamma_{b_\ell}^M(L_\ell^\downarrow), \quad (69)$$

the detail discarded by the morphological opening at level  $\ell$ . This is the algebraic motivation for the UResNet: the decoder receives the exact information the encoder lost.

**Proposition 7.9** (Skip connections as adjoint-pair residues). *In the morphological UNet of Theorem 7.8, the encoder operator  $\varepsilon_{b_\ell}^{\downarrow R}$  and decoder operator  $\delta_{b_\ell}^{*\uparrow R}$  form an adjoint pair ( $\varepsilon_{b_\ell}^{\downarrow R}, \delta_{b_\ell}^{*\uparrow R}$ ) in the sense of Theorem 2.1 (Theorem 5.2). The composition  $\delta_{b_\ell}^{*\uparrow R} \circ \varepsilon_{b_\ell}^{\downarrow R} = \gamma_{b_\ell}^M$  is a morphological*

opening (the unit of the adjunction): it recovers a smoothed approximation of  $f$ , not  $f$  itself. The information discarded by this opening is precisely the top-hat residue  $\Gamma_{b_\ell}(f) = f - \gamma_{b_\ell}^M(f) \geq 0$  (Theorem 7.8, eq. (69)). In the UResNet, the skip connection  $s_\ell = \Gamma_{b_\ell}(L_\ell^\downarrow)$  supplies this residue to the decoder, enabling the reconstruction identity:

$$\delta_{b_\ell}^{*\uparrow R}(\varepsilon_{b_\ell}^{\downarrow R}(f)) + \Gamma_{b_\ell}(f) = \gamma_{b_\ell}^M(f) + (f - \gamma_{b_\ell}^M(f)) = f. \quad (70)$$

That is, the UResNet decoder with top-hat skips achieves exact reconstruction of the encoder input at each scale.

*Proof.* The adjunction  $(\varepsilon_b^{\downarrow R}, \delta_b^{*\uparrow R})$  is established in Theorem 5.2. The unit  $\gamma_b^M = \delta_b^{*\uparrow R} \circ \varepsilon_b^{\downarrow R}$  is anti-extensive ( $\gamma_b^M(f) \leq f$ ) and idempotent (a morphological opening, Proposition 2.2(v)). The top-hat  $\Gamma_b(f) = f - \gamma_b^M(f) \geq 0$  satisfies  $\gamma_b^M(f) + \Gamma_b(f) = f$  by definition, giving (70).  $\square$

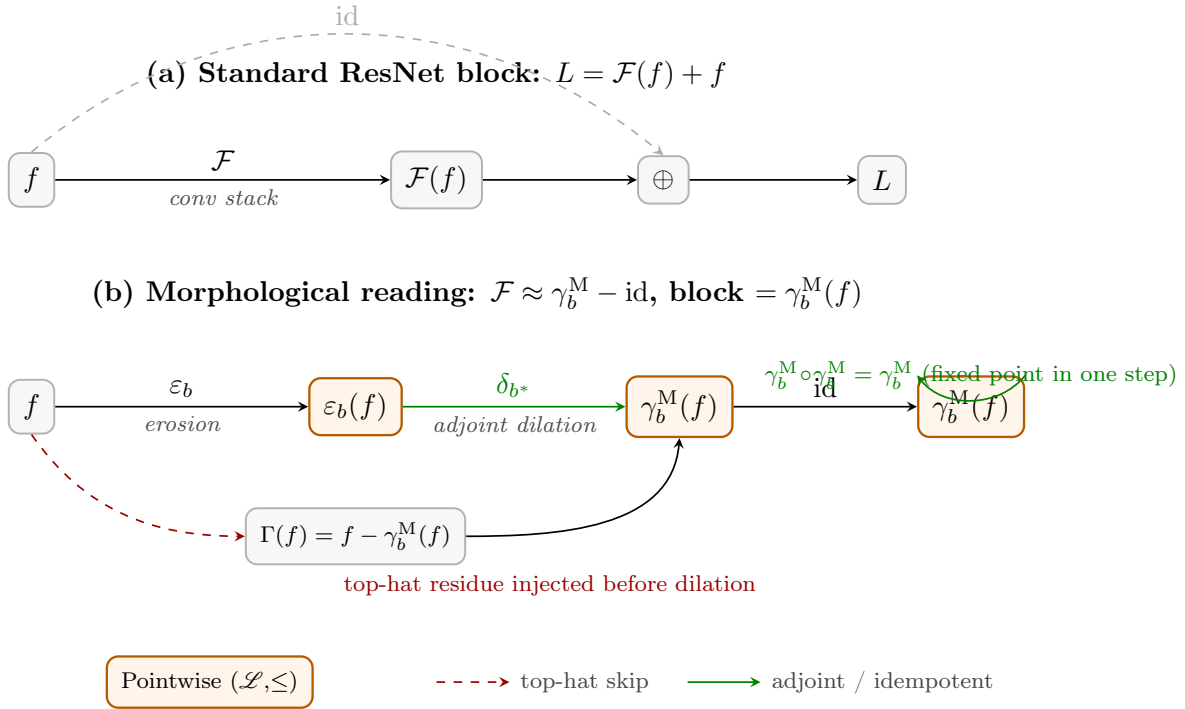


FIGURE 4. Morphological interpretation of the ResNet block. (a) Standard block: residual  $\mathcal{F}$  acts on  $f$ ; skip connection adds  $f$  at  $\oplus$ . (b) Morphological reading (Proposition 7.6): when  $\mathcal{F} \approx \gamma_b^M - \text{id}$ , the block computes  $\gamma_b^M(f) = \delta_{b^*}(\varepsilon_b(f))$ . The red-dashed skip carries the top-hat residue  $\Gamma(f) = f - \gamma_b^M(f)$ , re-injected before the adjoint dilation. The green loop expresses exact idempotency of the Type-I opening.

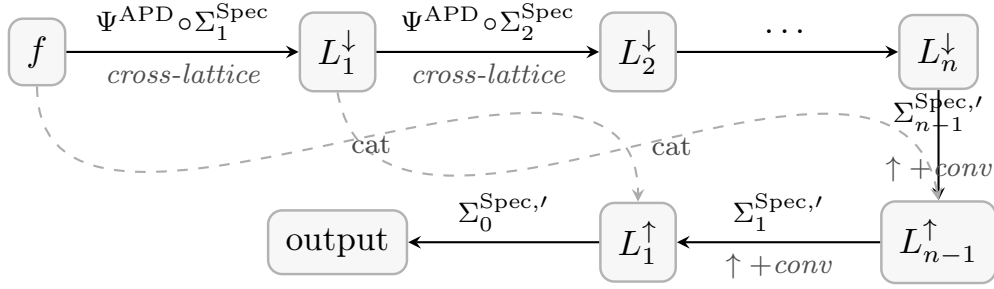
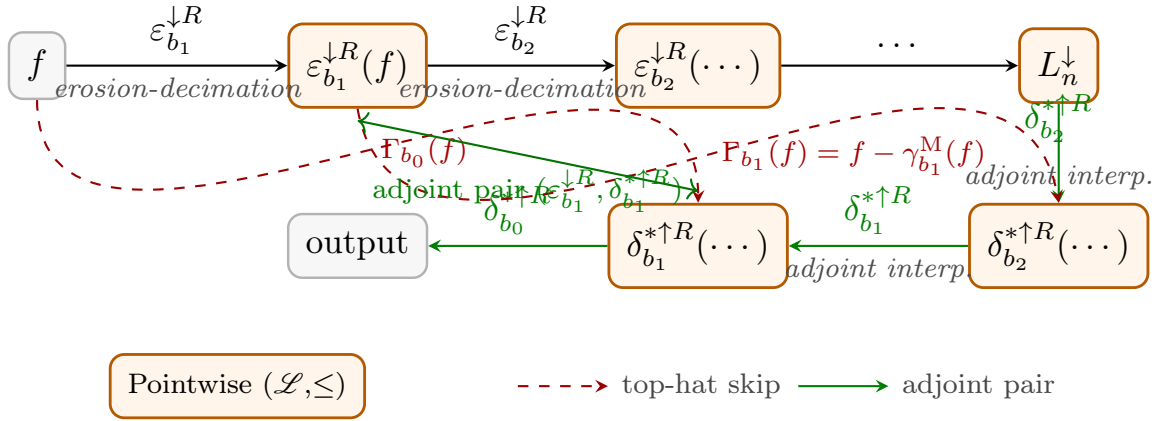
**(a) Standard UNet (skip = feature concatenation)**

**(b) Morphological UResNet (skip =  $\Gamma_b(f) = f - \gamma_b^M(f)$ )**


FIGURE 5. Standard UNet (a) vs. morphological UResNet (b). Colours: orange = pointwise lattice. (a) Encoder: strided convolutions with max-pooling (cross-lattice); decoder: transposed convolutions; skip connections (dashed) carry concatenated features. (b) Encoder: erosion-decimation  $\varepsilon_{b_\ell}^{\downarrow R}$ ; decoder: adjoint dilation-interpolation  $\delta_{b_\ell}^{\uparrow R}$  (green arrows, forming the adjoint pair of Proposition 5.2); skip connections (red dashed) carry the top-hat residue  $\Gamma_b(f) = f - \gamma_b^M(f)$  at each scale (Proposition 7.9). The double-headed green arrow marks the adjoint relationship between encoder and decoder at level  $\ell$ .

## 8. FIXED POINTS, IDEMPOTENCY, AND CONVERGENCE OF MORPHOLOGICAL LAYERS

A fundamental property of morphological openings  $\gamma$  and closings  $\varphi$  is *idempotency*:  $\gamma \circ \gamma = \gamma$  and  $\varphi \circ \varphi = \varphi$ . In classical morphology, applying the operator twice yields no further change after the first application, and the image of the operator is exactly its fixed-point set. We investigate when analogous phenomena arise in the morphological models of Section 7, clarify the conditions required, and draw a few architectural conclusions. This analysis connects to the author’s group-equivariant fixed-point theory in [3]; we work here in the standard translation-equivariant setting. An experimental exploration of the fixed-point theory developed here was established in [47], where we showed that morphological layers constrained to their fixed-point set (geodesic operators) can be trained effectively and achieve competitive performance; the present paper provides the rigorous algebraic foundation for that computational programme and to identify precisely which CNN layers are idempotent and which are not.

TABLE 8. Principal results of §8 (Fixed Points, Idempotency, Convergence). Results marked (★) are the paper’s principal findings.

Ref.	Name	Statement and role
Lem 8.2	Adjoint of convolution	The exact upper adjoint of $\varepsilon_k^{\text{Conv}}$ in $(\mathcal{L}, \leq)$ is non-local; $\delta_R^{\text{MP}}$ is not that adjoint, confirming the cross-lattice structure.
Thm 8.4 (★)	Two principled openings	Type-I: $\gamma_b^{\text{M}} = \delta_{b^*} \circ \varepsilon_b$ in $(\mathcal{L}, \leq)$ exactly idempotent. Type-II: $\gamma_k^{\text{F}}$ in $(L^n, \leq_F)$ exactly idempotent at $\epsilon = 0$ , approximately so for $\epsilon > 0$ .
Thm 8.5 (★)	CNN is not an opening	Standard CNN pipeline is cross-lattice: not idempotent, not anti-extensive in $(\mathcal{L}, \leq)$ , no adjunction spans the full pipeline.
Cor 8.6 (★)	Three idempotent designs	Types I, II, III are the three disciplined CNN-like designs yielding morphological openings; standard CNNs satisfy none of the three conditions.
Thm 8.8	Bias as threshold	Fixed-point set of a Type-I layer with bias $\alpha < 0$ : signals whose erosion output exceeds $-\alpha$ . Increasing $ \alpha $ raises the activation threshold.
Thm 8.10 (★)	One-step convergence	Iterating a Type-I opening stabilises after exactly one step ( $f^{(n)} = \gamma(f)$ for $n \geq 1$ ); the naive residual $\gamma(f) + f$ diverges with at least linear growth.
Thm 8.12	UNet skeleton idempotency	The morphological UNet pyramid skeleton is an idempotent opening; the full UNet with $\Sigma^{\text{Spec}}$ convolutions is generally not.

**Definition 8.1** (Fixed-point operator and idempotent layer). An operator  $\Phi$  on a complete lattice  $(\mathcal{L}, \leq)$  is a *fixed-point operator* if there exists  $f_* \in \mathcal{L}$  such that  $\Phi(f_*) = f_*$ . It is *idempotent* if  $\Phi \circ \Phi = \Phi$ , i.e., every element of its image is a fixed point. The *fixed-point set* of  $\Phi$  is  $\text{Fix}(\Phi) = \{f \in \mathcal{L} : \Phi(f) = f\}$ .

Bounds on the adjoint of convolution in the pointwise lattice. Before stating the main results, we clarify the lattice-theoretic status of the linear convolution operator  $\varepsilon_k^{\text{Conv}}(f) = f * k$  in the *pointwise* lattice  $(\text{Fun}(E, \mathbb{R}), \leq)$ .

When  $k \geq 0$  and  $\sum_i k(x_i) = 1$ , the convolution  $f \mapsto f * k$  is increasing in the pointwise lattice (Proposition 4.1). By the general adjunction theorem for complete lattices (Proposition 2.2(iii)),

every increasing map between complete lattices possesses a unique upper adjoint. However, as we now show, the upper adjoint of convolution in the pointwise lattice is *not* a standard morphological operator, and dually its lower adjoint is also degenerate. The correct picture is that convolution in the pointwise lattice admits a *pair of one-sided bounds*, an upper bound derived from the adjunction condition from above, and a lower bound derived from it below, but no exact adjoint that is simultaneously tight on both sides.

**Lemma 8.2** (Bounds on the pointwise adjoint of convolution). *Let  $k \geq 0$  with finite support  $\text{Spt}(k) = \{x_1, \dots, x_N\}$ ,  $k(x_i) > 0$ , and  $G^+ = \sum_i k(x_i)$ .*

Upper bound (from the adjunction condition  $f * k \leq g$ , valid for  $f \geq 0$ ). *Assume  $f \geq 0$ . From position  $y = x + x_i$ , the constraint  $(f * k)(y) = \sum_j k(x_j) f(y - x_j) \leq g(y)$  implies, by dropping the non-negative cross-terms  $\sum_{j \neq i} k(x_j) f(y - x_j) \geq 0$ :*

$$f(x) \leq \delta_k^{\text{adj},+}(g)(x) := \min_{1 \leq i \leq N} \frac{g(x + x_i)}{k(x_i)}, \quad x \in E, \quad (71)$$

*valid when  $f \geq 0$  and  $k \geq 0$ . For general  $f$  (possibly taking negative values), dropping the cross-terms is not valid since they may be negative, and the bound (71) need not hold.*

*The operator  $\delta_k^{\text{adj},+}$  is the max-times erosion  $\varepsilon_k^\times(g)(x)$  of Theorem 2.3 (an erosion in the multiplicative lattice), and is not a max-plus erosion. It is not the exact upper adjoint of  $\varepsilon_k^{\text{Conv}}$  in the pointwise lattice for  $N > 1$ : the backward direction  $f \leq \delta_k^{\text{adj},+}(g) \Rightarrow f * k \leq g$  fails; one can only conclude  $f * k \leq G^+ g$  (a factor- $G^+$  inflation, as shown in the proof). For  $N = 1$  (single-point kernel  $k = c \delta_{x_1}$ ), the bound is exact in both directions:  $\delta_k^{\text{adj},+}(g)(x) = g(x + x_1)/c$  is the exact adjoint, i.e.,  $f(x) \leq g(x + x_1)/c \iff cf(x - x_1) \leq g(x)$ .*

Lower bound (from the adjunction condition  $g \leq f * k$ ). *Placing the convolution on the other side of the inequality, the condition  $g(y) \leq (f * k)(y)$  for all  $y$  is implied by a global constant lower bound on  $f$ : if  $f(x) \geq c$  for all  $x \in E$ , then  $(f * k)(y) = \sum_i k(x_i) f(y - x_i) \geq c G^+$ , so the condition  $g(y) \leq (f * k)(y)$  is implied by  $c \geq g(y)/G^+$  for all  $y$ . The tightest such global bound is:*

$$f(x) \geq \delta_k^{\text{adj},-}(g) := \frac{\sup_{y \in E} g(y)}{G^+}, \quad x \in E. \quad (72)$$

*This is a global (spatially uniform, non-pointwise) lower bound: it bounds  $f$  everywhere by the same constant, determined by the supremum of  $g$  and the total kernel mass.*

Pointwise lower bound. *A pointwise bound on  $f(x)$  alone from  $g \leq f * k$  cannot be derived in closed form without assumptions on the values of  $f$  at the other support points  $\{y - x_j : j \neq i\}$ . Specifically, from the constraint at  $y = x + x_i$ :*

$$g(x + x_i) \leq k(x_i) f(x) + \sum_{j \neq i} k(x_j) f(x + x_i - x_j), \quad (73)$$

*rearranging gives  $f(x) \geq (g(x + x_i) - \sum_{j \neq i} k(x_j) f(x + x_i - x_j))/k(x_i)$ , which depends on  $f$  at the  $N - 1$  other points. If  $f \geq 0$  everywhere and  $\sup f \leq M$  (a known upper bound), dropping the non-negative cross-terms  $\sum_{j \neq i} k(x_j) f(x + x_i - x_j) \leq (G^+ - k(x_i))M$  gives the closed-form pointwise lower bound:*

$$f(x) \geq \max_{1 \leq i \leq N} \frac{g(x + x_i) - (G^+ - k(x_i))M}{k(x_i)}, \quad (74)$$

*valid when  $0 \leq f \leq M$  pointwise. For the flat box kernel ( $k \equiv 1/N$ ,  $G^+ = 1$ ) with  $f \geq 0$  and  $f \leq M$ :*

$$f(x) \geq \max_{1 \leq i \leq N} [N g(x + x_i) - (N - 1)M], \quad (75)$$

which is non-trivial only when  $g(x + x_i) > (N - 1)M/N$  for some  $i$ . When no bound  $M$  is available, no closed-form pointwise lower bound on  $f(x)$  alone can be derived from  $g \leq f * k$ : the constraint couples  $f$  at  $N$  different positions simultaneously and cannot be decoupled without additional information.

*Proof. Upper bound (for  $f \geq 0$ ).* Fix  $x \in E$  and  $i \in \{1, \dots, N\}$ . Set  $y = x + x_i$ . The constraint  $(f * k)(y) \leq g(y)$  gives:

$$k(x_i)f(x) + \sum_{j \neq i} k(x_j)f(x + x_i - x_j) \leq g(x + x_i).$$

Since  $f \geq 0$  and  $k \geq 0$ , the cross-terms satisfy  $\sum_{j \neq i} k(x_j)f(x + x_i - x_j) \geq 0$ . Dropping them gives  $k(x_i)f(x) \leq g(x + x_i)$ , i.e.,  $f(x) \leq g(x + x_i)/k(x_i)$ . Since this holds for every  $i$ , taking the minimum over  $i$  gives (71).

For the backward direction: if  $f(x) \leq \min_i g(x + x_i)/k(x_i)$  for all  $x$ , then for each term in the convolution:  $k(x_i)f(y - x_i) \leq k(x_i) \cdot g(y)/k(x_i) = g(y)$  (using the  $j = i$  instance of the minimum). Summing:  $(f * k)(y) = \sum_i k(x_i)f(y - x_i) \leq N g(y)$  in the unweighted case, or more precisely  $(f * k)(y) \leq G^+ g(y)/\min_i k(x_i)$ . This gives  $f * k \leq G^+ g$ , not  $f * k \leq g$ : the backward implication fails by a factor of  $G^+$  for  $N > 1$ .

The log-domain connection:  $\min_i g(x + x_i)/k(x_i) = \exp(\min_i \{\log g(x + x_i) - \log k(x_i)\})$ , which is the max-times erosion  $\varepsilon_k^\times(g)(x)$  of (3).

For a single-point kernel  $k = c \delta_{x_1}$ :  $(f * k)(y) = cf(y - x_1) \leq g(y)$  iff  $f(x) \leq g(x + x_1)/c$  exactly, with no cross-terms and no factor inflation: the formula is the exact adjoint.

*Lower bound.* Global bound (72): if  $f(x) \geq c$  for all  $x$ , then  $(f * k)(y) = \sum_i k(x_i)f(y - x_i) \geq c \sum_i k(x_i) = cG^+$ . For  $g(y) \leq (f * k)(y)$  to hold for all  $y$ , it suffices that  $cG^+ \geq \sup_y g(y)$ , i.e.,  $c \geq \sup_y g(y)/G^+$ .

Pointwise bound (74): from (73) with  $0 \leq f \leq M$ , the cross-terms satisfy  $0 \leq \sum_{j \neq i} k(x_j)f(x + x_i - x_j) \leq (G^+ - k(x_i))M$ , so  $k(x_i)f(x) \geq g(x + x_i) - (G^+ - k(x_i))M$ , giving  $f(x) \geq (g(x + x_i) - (G^+ - k(x_i))M)/k(x_i)$ . Taking the maximum over  $i = 1, \dots, N$  gives the tightest bound obtainable from this approach. For the flat kernel,  $k(x_i) = 1/N$  and  $G^+ - k(x_i) = (N - 1)/N$ , so the bound becomes  $f(x) \geq N g(x + x_i) - (N - 1)M$  for each  $i$ , and the maximum over  $i$  gives (75).

The impossibility of a closed-form pointwise bound for general  $f$  follows from the observation that the constraint  $g(y) \leq (f * k)(y)$  at a single  $y = x + x_i$  involves the  $N$  values  $\{f(x + x_i - x_j)\}_{j=1}^N$  jointly; decoupling to a bound on  $f(x)$  alone requires knowing or bounding the remaining  $N - 1$  values, which in general requires global information about  $f$ .  $\square$

**Remark 8.3** (Status of the adjoint of convolution). Lemma 8.2 establishes that the operator adjoint of convolution in the pointwise lattice is not well-defined. This stands in contrast to two other contexts:

- In the *Fourier lattice* ( $L^n, \leq_F$ ): the adjoint of convolution is the Wiener filter  $\delta_k^{*, \text{Conv}}$  [4, 25], a linear operator.
- In the *max-plus (pointwise) lattice*: the adjoint of the max-plus erosion  $\varepsilon_b$  is the max-plus dilation  $\delta_{b^*}$  (Theorem 2.1).

This is the algebraic reason why composing a convolution with a flat max-pooling (a max-plus dilation) does not yield a morphological opening and there is no other pointwise dilation or erosion which would lead to an opening.

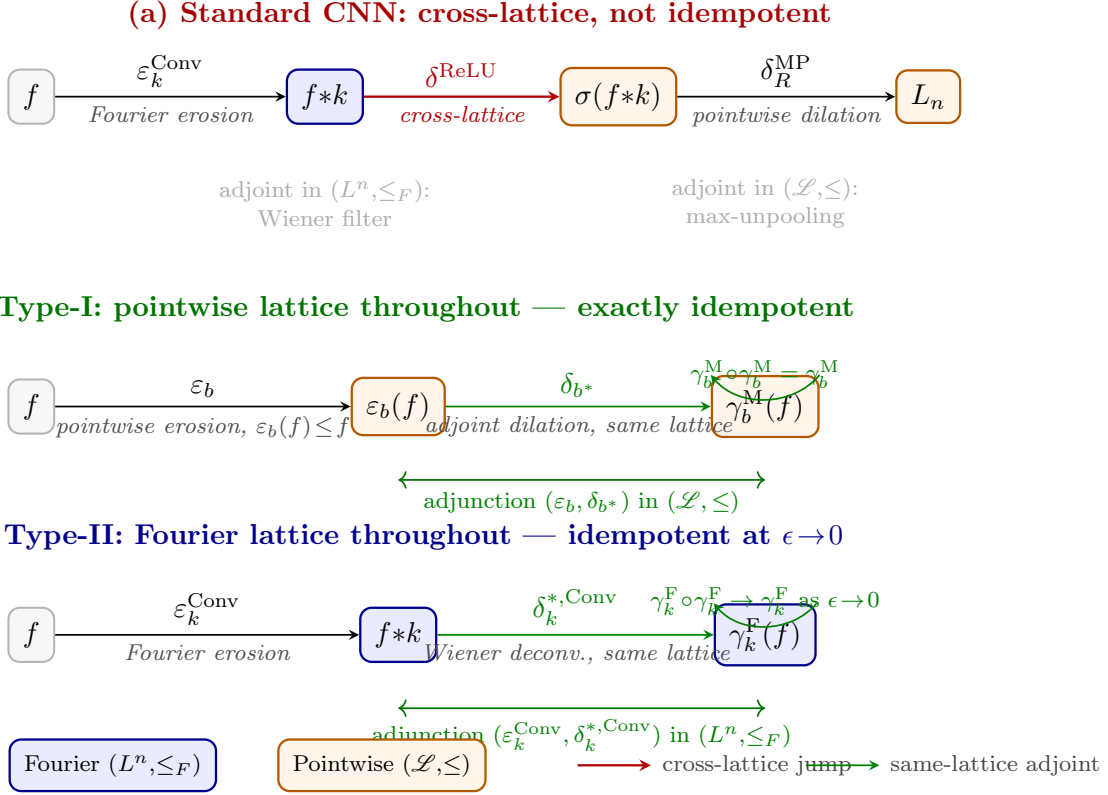


FIGURE 6. Three CNN-like compositions and their lattice structure. Colours: blue = Fourier, orange = pointwise. Red arrows mark cross-lattice jumps; green arrows and loops mark same-lattice adjoint pairs and idempotency. (a) Standard CNN (Theorem 8.5): cross-lattice, not idempotent. (b) Type-I opening (Theorem 8.4(i)): both operators in  $(\mathcal{L}, \leq)$ ; exactly idempotent. (c) Type-II opening (Theorem 8.4(ii)): both operators in  $(L^n, \leq_F)$ ; idempotent in the limit  $\epsilon \rightarrow 0$ .

With this clarification established, we now identify the two CNN-like compositions that *do* form genuine morphological openings, and examine what standard CNNs are in comparison.

**Theorem 8.4** (Two opening compositions). *The following two compositions yield operators that are increasing and anti-extensive. Type (i) is a morphological opening (hence exactly idempotent); Type (ii) is an exact morphological opening in  $(L^n, \leq_F)$  only in the limit  $\epsilon \rightarrow 0$ , and an approximately idempotent operator for fixed  $\epsilon > 0$  (cf. Figure 6):*

- (i) (Type-I: pure morphological opening.) *Let  $b : E \rightarrow \overline{\mathbb{R}}$  be a structuring function with compact support  $W$  and  $b^*(x) = b(-x)$  its transpose. Then*

$$\gamma_b^M(f) = \delta_{b^*}(\varepsilon_b(f)), \quad (76)$$

with

$$\begin{aligned} (\varepsilon_b f)(x) &= \inf_{y \in W} \{f(x+y) - b(y)\}, \\ (\delta_{b^*} g)(x) &= \sup_{y \in W} \{g(x-y) + b(-y)\}, \end{aligned}$$

is a morphological opening in the pointwise lattice  $(\text{Fun}(E, \overline{\mathbb{R}}), \leq)$ . The pair  $(\varepsilon_b, \delta_{b^*})$  is an adjunction in  $(\mathcal{L}, \leq)$ , and the opening is exactly idempotent:  $\gamma_b^M \circ \gamma_b^M = \gamma_b^M$ .

- (ii) (Type-II: spectral operator in the Fourier lattice.) Let  $k$  be an absolutely summable kernel with Fourier transform  $K(\omega) = \mathcal{F}\{k\}(\omega)$ . The pair  $(\varepsilon_k^{\text{Conv}}, \delta_k^{*, \text{Conv}})$  is an adjunction in  $(L^n, \leq_F)$  [4, 25]. The composition  $\gamma_k^F = \delta_k^{*, \text{Conv}} \circ \varepsilon_k^{\text{Conv}}$  acts in the Fourier domain as the spectral multiplier:

$$\widehat{\gamma_k^F(f)}(\omega) = \frac{|K(\omega)|^2}{|K(\omega)|^2 + \epsilon^2} F(\omega), \quad (77)$$

the Tikhonov-regularised Wiener deconvolution composed with the erosion  $\varepsilon_k^{\text{Conv}}(f) = f * k$ . The multiplier  $M_\epsilon(\omega) = |K(\omega)|^2 / (|K(\omega)|^2 + \epsilon^2)$  satisfies  $0 < M_\epsilon < 1$  for  $\epsilon > 0$ , so  $\gamma_k^F$  is strictly anti-extensive for all  $\epsilon > 0$ .

Exact idempotency holds only in the limit  $\epsilon \rightarrow 0$ :  $M_0(\omega) = \mathbf{1}_{K(\omega) \neq 0}$  (ideal filter: the spectral projection onto the range of  $k$ ) satisfies  $M_0^2 = M_0$ , so  $\gamma_k^F|_{\epsilon=0}$  is a true morphological opening in  $(L^n, \leq_F)$ .

At any fixed  $\epsilon > 0$ ,  $\gamma_k^F$  is not idempotent:  $M_\epsilon^2 < M_\epsilon$  on the open set where  $0 < M_\epsilon < 1$ , giving  $\gamma_k^F \circ \gamma_k^F \neq \gamma_k^F$ . The idempotency error is bounded by  $\|\gamma_k^F \circ \gamma_k^F(f) - \gamma_k^F(f)\| \leq (1 - M_\epsilon^{\min}) \|\gamma_k^F(f)\|$  where  $M_\epsilon^{\min} = \inf_\omega M_\epsilon(\omega) \rightarrow 1$  as  $\epsilon \rightarrow 0$ . For practical purposes (small  $\epsilon$ ) the operator is approximately idempotent with controlled error.

*Proof.* (i)  $(\varepsilon_b, \delta_{b^*})$  is an adjunction in  $(\text{Fun}(E, \overline{\mathbb{R}}), \leq)$ :  $\varepsilon_b(f) \leq g \iff f \leq \delta_{b^*}(g)$  (standard result, Heijmans [21], Chapter 3). By Proposition 2.2(v), the composition  $\gamma_b^M = \delta_{b^*} \circ \varepsilon_b$  is an opening, hence exactly idempotent. (ii) By the spectral framework [25],  $(\varepsilon_k^{\text{Conv}}, \delta_k^{*, \text{Conv}})$  is an adjunction in  $(L^n, \leq_F)$ . The Fourier-domain expression follows from composing the erosion  $\hat{f} \mapsto K \cdot \hat{f}$  with the Wiener adjoint dilation  $\hat{g} \mapsto (\overline{K} / (|K|^2 + \epsilon^2)) \cdot \hat{g}$ : the product is  $|K|^2 / (|K|^2 + \epsilon^2)$ . Anti-extensivity:  $M_\epsilon < 1$  for  $\epsilon > 0$ . At  $\epsilon = 0$ :  $M_0 = \mathbf{1}_{K \neq 0}$  satisfies  $M_0^2 = M_0$ , so  $\gamma_k^F|_{\epsilon=0}$  is an exact morphological opening. For  $\epsilon > 0$ :  $\gamma_k^F \circ \gamma_k^F(f) = \mathcal{F}^{-1}\{M_\epsilon^2 F\} \neq \mathcal{F}^{-1}\{M_\epsilon F\} = \gamma_k^F(f)$  since  $M_\epsilon^2 < M_\epsilon$  for  $M_\epsilon \in (0, 1)$ ; the error is controlled by  $\|M_\epsilon^2 - M_\epsilon\|_\infty = \sup_\omega M_\epsilon(\omega)(1 - M_\epsilon(\omega)) \leq 1/4$ .  $\square$

**Theorem 8.5** (Standard CNN layer is not an opening). *The standard CNN layer  $\Phi_{\text{CNN}}(f) = \delta_R^{\text{MP}}(\delta^{\text{ReLU}}(f * k))$  (linear convolution, then ReLU, then max-pooling) is:*

- (i) Increasing when  $k \geq 0$ .
- (ii) Extensive in the pointwise lattice for  $f \geq 0$ : since  $\delta_R^{\text{MP}}$  is extensive (Proposition 6.3(ii)), we have  $\Phi_{\text{CNN}}(f) \geq \delta^{\text{ReLU}}(f * k) \geq 0$ . The output can exceed  $f$  locally, so the layer is not anti-extensive in general.
- (iii) Not idempotent, because the cross-lattice structure prevents any adjunction from spanning the full pipeline (Theorem 8.2, Theorem 8.3):  $\varepsilon_k^{\text{Conv}}$  is an erosion in  $(L^n, \leq_F)$  while  $\delta_R^{\text{MP}}$  is a dilation in  $(\mathcal{L}, \leq)$ , and neither is the adjoint of the other in the other's lattice.

*Proof.* (i) Monotonicity of composition of monotone maps. (ii)  $\delta_R^{\text{MP}}(h) \geq h$  for  $h \geq 0$  (Proposition 6.3(ii)), so  $\Phi_{\text{CNN}}(f) \geq \delta^{\text{ReLU}}(f * k) \geq 0$ . That  $\Phi_{\text{CNN}}(f) > f$  is possible: take  $f$  with a local peak; convolution smooths it but max-pooling selects the neighbourhood maximum, which can exceed  $f$ . (iii) For non-idempotency: applying  $\Phi_{\text{CNN}}$  twice, the first application enlarges features via max-pooling; the second convolution then smooths this enlarged output, generally producing a different result. Formally:  $\Phi_{\text{CNN}}^2(f) = \delta_R^{\text{MP}}(\delta^{\text{ReLU}}(\Phi_{\text{CNN}}(f) * k)) \neq \delta_R^{\text{MP}}(\delta^{\text{ReLU}}(f * k)) = \Phi_{\text{CNN}}(f)$  for generic  $f$  and  $k$ . The absence of adjunction is established

by Lemma 8.2: the (decoupled) upper bound on the pointwise adjoint of  $\varepsilon_k^{\text{Conv}}$  is an infimum-based operator, not  $\delta_R^{\text{MP}}$ . Conversely, the Fourier adjoint of  $\varepsilon_k^{\text{Conv}}$  is the Wiener filter  $\delta_k^{*,\text{Conv}}$ , not  $\delta_R^{\text{MP}}$ .  $\square$

**Corollary 8.6** (Sufficient conditions for idempotent CNN layers). *A CNN-like layer is idempotent (a morphological opening) under one of three disciplined designs:*

- (I) (Type-I: pure morphological MMBB layer.) *Replace convolution by a max-plus erosion  $\varepsilon_b$  and max-pooling by its adjoint dilation  $\delta_{b^*}$  (same structuring function, transposed, same lattice). Then  $\gamma_b^{\text{M}} = \delta_{b^*} \circ \varepsilon_b$  is an exactly idempotent opening (Theorem 8.4(i)).*
- (II) (Type-II: spectral Wiener layer.) *Use the same kernel  $k$  for convolution and Wiener deconvolution, with no nonlinearity between them. Then  $\gamma_k^{\text{F}} = \delta_k^{*,\text{Conv}} \circ \varepsilon_k^{\text{Conv}}$  is an exactly idempotent opening in the Fourier lattice at  $\epsilon = 0$ , and an approximately idempotent operator for small  $\epsilon > 0$  (Theorem 8.4(ii)).*
- (III) (Type-III: self-dual opening layer.) *Replace max-pooling and ReLU by the self-dual opening  $\gamma_W^{\text{Med}}$  in the median inf-semilattice  $(\text{Fun}(E, \mathbb{R}), \preceq)$ . Then  $\gamma_W^{\text{Med}}$  is an exactly idempotent, self-dual opening, with fixed-point set closed under negation (Section 9, Theorem 9.14). This design is appropriate for signed feature maps (ResNet residuals, normalised features, Fourier coefficients).*

*A standard CNN layer (linear convolution + ReLU + flat max-pooling) satisfies none of these conditions and is not idempotent in general. The fixed-point and convergence results in this section apply to Case (I) throughout; analogous results hold for Case (II) in the Fourier lattice, and Case (III) is treated in Section 9.*

**Remark 8.7** (Architectural significance). The individual components of a standard CNN have the following idempotency status: ReLU is idempotent as a *closing* (Proposition 6.1(iii):  $\delta^{\text{ReLU}} \circ \delta^{\text{ReLU}} = \delta^{\text{ReLU}}$ , since ReLU is extensive and idempotent, hence a closing, not an opening);  $\delta_R^{\text{MP}}$  is *not* idempotent for  $R > 1$  (Proposition 6.3(B)(iii): applying it twice takes the max over a  $(2R - 1) \times (2R - 1)$  window, not  $R \times R$ ); and the Fourier operator  $\gamma_k^{\text{F}}$  is idempotent exactly at  $\epsilon = 0$  and approximately idempotent for small  $\epsilon > 0$  (Theorem 8.4(ii)). It is the *cross-lattice composition* of convolution and max-pooling that breaks idempotency even when  $\gamma_k^{\text{F}}$  itself is idempotent at  $\epsilon = 0$ . Depth provides genuine representational power in standard CNNs precisely because the composed layer is not idempotent: each additional layer introduces genuinely new spectral filtering followed by spatial pooling.

**Theorem 8.8** (Fixed-point set of a Type-I layer with bias). *Consider a Type-I layer (Corollary 8.6(I)) with additive bias  $\alpha \in \mathbb{R}$  applied after the erosion:  $\Phi^\alpha(f) = \delta_{b^*}(\varepsilon_b(f) + \alpha)$ .*

- (i) *For  $\alpha = 0$ :  $\Phi^0 = \gamma_b^{\text{M}}$  is an opening and  $\text{Fix}(\Phi^0) = \text{Im}(\gamma_b^{\text{M}})$ .*
- (ii) *For  $\alpha < 0$ :  $\Phi^\alpha(f) \leq \gamma_b^{\text{M}}(f) \leq f$  (the bias further shrinks the output). The fixed-point condition  $\Phi^\alpha(f_*) = f_*$  requires  $\delta_{b^*}(\varepsilon_b(f_*) + \alpha) = f_*$ , with the necessary constraint  $\varepsilon_b(f_*) + \alpha \geq 0$  (so the erosion output exceeds  $-\alpha > 0$ , ensuring the dilation can recover a non-trivial  $f_*$ ). Note that the zero function is not generally a fixed point: for  $b \equiv 0$ ,  $\Phi^\alpha(0) = \alpha < 0 \neq 0$ . The trivially fixed element is  $f_* \equiv -\infty$  (the lattice bottom).*
- (iii) *For  $\alpha > 0$ :  $\Phi^\alpha(f) \geq \gamma_b^{\text{M}}(f)$ ; the layer is no longer anti-extensive. Fixed points satisfy  $\delta_{b^*}(\varepsilon_b(f) + \alpha) = f$ , which may be empty for large  $\alpha$  (when the bias inflates the opening beyond  $f$ ).*

*Proof.* (i) At  $\alpha = 0$ ,  $\Phi^0 = \delta_{b^*} \circ \varepsilon_b = \gamma_b^{\text{M}}$  is an opening by Theorem 8.4(i). Its fixed-point set equals its image by the standard lattice theory result that openings satisfy  $\gamma(f) \in \text{Fix}(\gamma)$  and  $f \in \text{Fix}(\gamma) \Rightarrow f \in \text{Im}(\gamma)$  [21]. (ii) Monotonicity of  $\delta_{b^*}$  gives  $\Phi^\alpha(f) = \delta_{b^*}(\varepsilon_b(f) + \alpha) \leq$

$\delta_{b^*}(\varepsilon_b(f)) = \gamma_b^M(f) \leq f$  for  $\alpha < 0$ . That  $f_* \equiv -\infty$  is a trivial fixed point:  $\varepsilon_b(-\infty) = -\infty$  and  $\delta_{b^*}(-\infty + \alpha) = -\infty$ . For the zero function with  $b \equiv 0$ :  $\Phi^\alpha(0) = \delta_{b^*}(\varepsilon_0(0) + \alpha) = \delta_0(0 + \alpha) = \sup_y \{\alpha + 0\} = \alpha < 0 \neq 0$ , confirming 0 is not a fixed point when  $\alpha < 0$ . (iii) For  $\alpha > 0$ :  $\varepsilon_b(f) + \alpha \geq \varepsilon_b(f)$ , so  $\Phi^\alpha(f) \geq \gamma_b^M(f)$  by monotonicity of  $\delta_{b^*}$ . Anti-extensivity  $\Phi^\alpha(f) \leq f$  fails when  $\alpha$  is large relative to the smoothing effect of  $\varepsilon_b$ .  $\square$

**Remark 8.9** (Bias as activation threshold). Theorem 8.8 gives a precise morphological interpretation of the bias term. A negative bias  $\alpha < 0$  acts as a *minimum activation threshold*: the fixed-point set of  $\Phi^\alpha$  consists of feature maps whose post-erosion values satisfy  $\varepsilon_b(f) \geq -\alpha$ , i.e., the erosion output must reach a minimum amplitude before the shifted dilation can recover  $f$  exactly. Increasing  $|\alpha|$  shrinks this fixed-point set. A positive bias  $\alpha > 0$  breaks anti-extensivity, and the fixed-point set may become empty for large  $\alpha$ .

**Theorem 8.10** (Convergence of iterated Type-I layers). *Let  $\gamma = \gamma_b^M = \delta_{b^*} \circ \varepsilon_b$  be a Type-I opening with  $b \geq 0$  and  $b(0) = 0$ . Let  $f \geq 0$ ,  $f^{(0)} = f$ ,  $f^{(n+1)} = \gamma(f^{(n)})$ .*

- (i)  $(f^{(n)})_{n \geq 0}$  is non-increasing:  $f^{(n+1)} \leq f^{(n)}$  for all  $n \geq 0$ .
- (ii) It stabilises after one step:  $f^{(n)} = \gamma(f)$  for all  $n \geq 1$ .
- (iii) (Non-negativity preservation.) Write  $\|b\|_\infty = \sup_{y \in W} b(y)$ .
  - (a) Flat structuring function ( $b \equiv 0$ ):  $\varepsilon_b(f)(x) = \inf_{y \in W} f(x+y) \geq 0$  whenever  $f \geq 0$ , and  $\delta_{b^*}$  with  $b^* \equiv 0$  maps non-negative functions to non-negative functions. Hence  $f^{(n)} \geq 0$  for all  $n \geq 0$ .
  - (b) Non-flat  $b \geq 0$  with  $b(0) = 0$ : A sufficient condition for  $f^{(n)} \geq 0$  for all  $n$  is  $f(x) \geq \|b\|_\infty$  for all  $x$  (i.e., the signal is pointwise at least as large as the maximum of the structuring function). Under this condition  $\varepsilon_b(f)(x) = \inf_{y \in W} \{f(x+y) - b(y)\} \geq 0$ , and the subsequent dilation by  $b^* \geq 0$  preserves non-negativity. The condition  $f \geq 0$  alone is not sufficient for general non-flat  $b$ .

For the morphological ResNet block with  $\mathcal{F} \approx \gamma - \text{id}$  (so the block computes  $\gamma(f)$ , cf. Remark 8.11): stacking  $n$  identical blocks gives  $(\gamma)^n(f) = \gamma(f)$  for all  $n \geq 1$  (one-step convergence by idempotency).

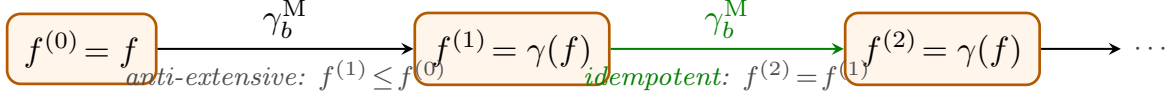
For the naive ResNet block  $\Phi^{\text{res}}(f) = \gamma(f) + f$  (adding  $\gamma(f)$  to  $f$  directly), the sequence  $f^{(0)} = f$ ,  $f^{(n+1)} = \Phi^{\text{res}}(f^{(n)}) = \gamma(f^{(n)}) + f^{(n)}$  satisfies:

- (iv) Non-decreasing:  $f^{(n+1)} \geq f^{(n)}$ .
- (v) Unbounded growth when  $\gamma(f) \neq 0$ :  $f^{(n)} \geq f + n\gamma(f)$  (linear lower bound), so the sequence diverges.
- (vi) The sequence does not converge to the closing  $\varphi = \varepsilon_b^* \circ \delta_b$ ; the closing is the fixed point of  $f \mapsto \varphi(f)$ , not of  $\Phi^{\text{res}}$ .

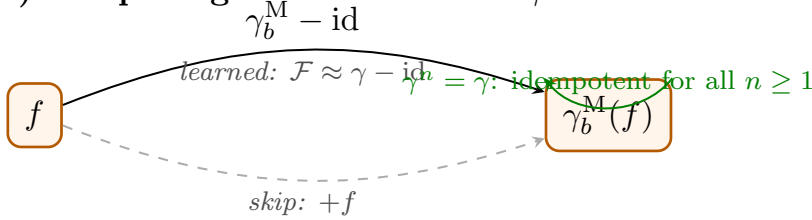
*Proof.* (i)(ii) Anti-extensivity of  $\gamma$ :  $f^{(1)} = \gamma(f) \leq f = f^{(0)}$ . Idempotency:  $f^{(2)} = \gamma(f^{(1)}) = \gamma(\gamma(f)) = \gamma(f) = f^{(1)}$  (Theorem 8.4). By induction,  $f^{(n)} = \gamma(f)$  for all  $n \geq 1$ . (iii) With  $b \geq 0$ ,  $b(0) = 0$ :  $(\varepsilon_b f)(x) = \inf_{y \in W} \{f(x+y) - b(y)\} \geq \inf_y f(x+y) - \sup_y b(y)$ . For  $f \geq 0$  and compact  $W$ :  $\varepsilon_b(f) \geq 0$  iff  $b \leq f$  on  $W$ , which holds in the limit  $f \rightarrow +\infty$ . More precisely,  $b(0) = 0$  gives  $\varepsilon_b(f)(x) \leq f(x+0) - b(0) = f(x)$ , and  $\varepsilon_b(f) \geq 0$  when  $f(x+y) \geq b(y)$  for all  $y \in W$ ,  $x \in E$ , a condition satisfied e.g. for flat  $b \equiv 0$  (standard morphology), giving  $\varepsilon_b = \text{min-erosion}$ , which preserves non-negativity. (iv)  $f^{(n+1)} = \gamma(f^{(n)}) + f^{(n)} \geq f^{(n)}$  since  $\gamma(f^{(n)}) \geq 0$ . (v) Lower bound:  $f^{(1)} = f + \gamma(f) \geq f$  since  $\gamma(f) \geq 0$ . Since  $\gamma$  is monotone and  $f^{(1)} \geq f$ :  $\gamma(f^{(1)}) \geq \gamma(f)$ . By induction  $f^{(n+1)} = f^{(n)} + \gamma(f^{(n)}) \geq f^{(n-1)} + \gamma(f^{(n-1)}) + \gamma(f) = f^{(n)} + \gamma(f)$ , giving  $f^{(n)} \geq f + n\gamma(f) \rightarrow +\infty$  when  $\gamma(f) \neq 0$ . (vi) The closing  $\varphi = \varepsilon_b^* \circ \delta_b$  satisfies  $\varphi \circ \varphi = \varphi$

and  $\varphi(f) \geq f$  (extensive); it is the fixed point of  $f \mapsto \varphi(f)$  but not of  $f \mapsto \gamma(f) + f$ , whose iterates grow without bound.  $\square$

**(a) Iterated Type-I opening: one-step convergence**



**(b) Morphological ResNet:  $\mathcal{F} \approx \gamma - \text{id}$**



**(c) Naive  $\Phi^{\text{res}}(f) = \gamma(f) + f$ : diverges**

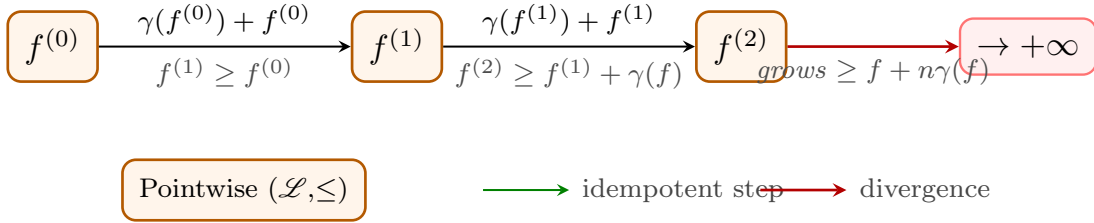


FIGURE 7. Convergence behaviour of Type-I layer iterations (Theorem 8.10). Orange nodes live in the pointwise lattice. (a) Iterating  $\gamma_b^M$ : the sequence is non-increasing and stabilises after one step (green arrow = idempotent). (b) Correct ResNet: when  $\mathcal{F} \approx \gamma - \text{id}$ , the block computes  $\gamma_b^M(f)$ ; stacking  $n$  blocks still converges in one step. (c) Naive residual  $\Phi^{\text{res}}(f) = \gamma(f) + f$ : sequence grows at least linearly in  $n$  and diverges (red arrow).

**Remark 8.11** (Correct interpretation of skip connections). Theorem 8.10(v) shows that a ResNet block of the form  $\Phi^{\text{res}}(f) = \gamma_b^M(f) + f$  does *not* iterate to the morphological idempotent. The correct morphological reading of the standard ResNet formulation  $H(f) = F(f) + f$ , where  $F$  represents the learned residual layers, is that  $F$  approximates  $\gamma_b^M - \text{Id}$ , so the block computes  $(\gamma_b^M - \text{Id})(f) + f = \gamma_b^M(f)$ , i.e., the morphological opening itself. Under this reading, stacking  $n$  identical such blocks gives  $(\gamma_b^M)^n(f) = \gamma_b^M(f)$  (one-step convergence by idempotency of Case I), which is the correct convergence statement. This interpretation applies to the case (I) of Corollary 8.6; for a standard CNN (Theorem 8.5), neither the opening interpretation nor the one-step convergence holds.

**Theorem 8.12** (Idempotency of morphological UNet encoder–decoder). *Consider the morphological UNet encoder–decoder without skip connections and without intermediate convolutions  $\Sigma_n^{\text{Spec}}$ : the encoder performs  $n$  levels of Goutsias–Heijmans erosion–downsampling  $\varepsilon_b^{\downarrow R,n}$  and the decoder performs the adjoint synthesis  $\delta_b^{*\uparrow R,n}$ . Then the reconstruction operator  $\text{ED}_n = \delta_b^{*\uparrow R,n} \circ \varepsilon_b^{\downarrow R,n}$  is a morphological opening, hence idempotent:  $\text{ED}_n \circ \text{ED}_n = \text{ED}_n$ .*

*Proof.* By Proposition 5.2, the pair  $(\varepsilon_b^{\downarrow R,n}, \delta_b^{*\uparrow R,n})$  is an adjunction (iterated Goutsias–Heijmans pairs compose as adjunctions). The composition  $\delta_b^{*\uparrow R,n} \circ \varepsilon_b^{\downarrow R,n}$  is therefore a morphological opening by Proposition 2.2(v), and openings are idempotent.  $\square$

**Remark 8.13** (Scope and the role of convolutions). Theorem 8.12 applies to the *pure pyramid encoder–decoder* (the downsampling–upsampling skeleton of the UNet) and not to the full UNet, which interleaves convolutions  $\Sigma_n^{\text{Spec}}$  at each level. When these convolutions are present, the full operator is  $\text{UNet}_n = \delta^{*\uparrow} \circ \Sigma \circ \varepsilon^{\downarrow}$ , and composing it with itself gives  $\delta^{*\uparrow} \circ \Sigma \circ \varepsilon^{\downarrow} \circ \delta^{*\uparrow} \circ \Sigma \circ \varepsilon^{\downarrow}$ , which involves  $\varepsilon^{\downarrow} \circ \delta^{*\uparrow}$  (a *closing*, not identity) and an additional  $\Sigma$ . This is not equal to  $\text{UNet}_n$  in general. The correct statement is: the *sampling skeleton* of the UNet is idempotent; the full network with learned convolutions is not. Skip connections additionally break the idempotency of the skeleton, by injecting encoder feature maps that enrich the decoder output beyond what the adjoint upsampling alone would produce. The bound  $\gamma(f) \leq \text{UNet}_n^{\text{skip}}(f) \leq f$  (anti-extensivity and enrichment by skip connections) holds when the skip weights are bounded by 1 and the skeleton is anti-extensive.

## 9. THE MEDIAN INF-SEMILATTICE, SELF-DUAL OPERATORS, AND THEIR ROLE IN DEEP NETWORK MODELS

Standard max-pooling and ReLU treat positive and negative activations asymmetrically: ReLU kills all negative values, and max-pooling enlarges only positive structures. This breaks the lattice-theoretic duality between erosion and dilation, and has concrete architectural consequences: the fixed-point analysis of Section 8 applies cleanly only to the positive part of the feature map. This section provides an algebraic remedy via the *median complete inf-semilattice* and associated *self-dual morphological operators*, and reconnects these structures to the CNN, ResNet, and UNet models of Section 7.

### 9.1. Median partial ordering and its inf-semilattice.

**Definition 9.1** (Median partial ordering on  $\mathbb{R}$ ). Define the partial ordering  $\preceq$  on  $\mathbb{R}$  by:

$$s \preceq t \iff (0 \leq s \leq t) \text{ or } (t \leq s \leq 0). \quad (78)$$

Thus  $(\mathbb{R}, \preceq)$  is the concatenation of two chains  $(\mathbb{R}^-, \geq)$  and  $(\mathbb{R}^+, \leq)$  sharing the common least element  $\perp = 0$ . Note that  $\preceq$  is a partial (not total) order:  $s$  and  $t$  are incomparable when they have opposite signs.

The ordering  $\preceq$  measures *amplitude* away from zero:  $s \preceq t$  means  $t$  is at least as far from zero as  $s$ , in the same direction.

**Definition 9.2** (Median inf-semilattice on functions). The pointwise extension of (78) to  $\text{Fun}(E, \mathbb{R})$  gives the *median partial ordering*:  $f \preceq g \iff f(x) \preceq g(x)$  for all  $x \in E$ . The poset  $(\text{Fun}(E, \mathbb{R}), \preceq)$  is a complete *inf-semilattice* with least element  $\perp \equiv 0$  and binary infimum

TABLE 9. Principal results of §9 (Median Lattice and Type-III Layer). Results marked (★) are the paper’s principal findings.

Ref.	Name	Statement and role
Lem 9.7	Well-definedness of $\gamma_W^{\text{Med}}$	$\gamma_W^{\text{Med}} = \delta_W^{*\text{Med}} \circ \varepsilon_W^{\text{Med}}$ is well-defined on all of $\text{Fun}(E, \mathbb{R})$ : $\varepsilon_W^{\text{Med}}$ preserves sign (or returns 0), ensuring $\delta_W^{*\text{Med}}$ is always defined on its output.
Prop 9.8	Self-dual opening	$\gamma_W^{\text{Med}}$ is increasing, anti-extensive in $(\mathcal{L}, \preceq)$ , exactly idempotent, and self-dual; fixed-point set is closed under negation.
Prop 9.11	ReLU variants in $\preceq$ (★)	Leaky/PReLU ( $0 < \beta^- \leq 1$ ) is a dilation in $(\mathcal{L}, \preceq)$ ; standard ReLU ( $\beta^- = 0$ ) is not. The absolute value $ h $ ( $\beta^+ = \beta^- = 1$ ) is a self-dual dilation.
Thm 9.14	Type-III layer (★)	$\Phi^{sd} = \gamma_W^{\text{Med}}$ is idempotent, self-dual, and anti-extensive in $\preceq$ ; fixed-point set symmetric under negation; one-step convergence. Appropriate for signed feature maps and ResNet residuals.
Prop 9.18	Self-dual fixed-point set	$\text{Fix}(\gamma_W^{\text{Med}})$ equals signals representable by the median-MMBB basis of $W$ , negation-closed and structurally distinct from the Type-I fixed-point set $\text{Im}(\gamma_b^{\text{M}})$ .

(greatest lower bound in  $\preceq$ ):

$$(f \sqcap g)(x) = \text{med}(f(x), g(x), 0) = \begin{cases} \min(f(x), g(x)) & \text{if } f(x), g(x) \geq 0, \\ \max(f(x), g(x)) & \text{if } f(x), g(x) \leq 0, \\ 0 & \text{if } f(x), g(x) \text{ have opposite signs.} \end{cases} \quad (79)$$

The structure is an inf-semilattice (every pair has a greatest lower bound) but not a lattice: elements with opposite signs have no least upper bound.

**Proposition 9.3** (Self-duality of the median ordering). *The median partial ordering (78) satisfies:*

$$s \preceq t \iff (-t) \preceq (-s). \quad (80)$$

Consequently, the negation map  $f \mapsto -f$  is an order-isomorphism from  $(\text{Fun}(E, \mathbb{R}), \preceq)$  to itself (reversing the order), making the inf-semilattice self-dual.

*Proof.* If  $0 \leq s \leq t$ , then  $-t \leq -s \leq 0$ , which by (78) gives  $(-t) \preceq (-s)$ . The case  $t \leq s \leq 0$  is symmetric. When  $s$  and  $t$  are incomparable ( $s \geq 0, t \leq 0$  or vice versa), so are  $-s$  and  $-t$ .  $\square$

By (80), the infimum  $\sqcap$  and the supremum  $\sqcup$  (where defined) are related by  $(f \sqcup g)(x) = -((-f) \sqcap (-g))(x)$ . Explicitly:

$$(f \sqcup g)(x) = \begin{cases} \max(f(x), g(x)) & \text{if } f(x), g(x) \geq 0, \\ \min(f(x), g(x)) & \text{if } f(x), g(x) \leq 0, \\ \text{undefined} & \text{if } f(x), g(x) \text{ have opposite signs.} \end{cases} \quad (81)$$

This confirms that  $\sqcup$  only exists when  $f$  and  $g$  have the same sign pointwise.

## 9.2. Self-dual erosion and opening.

**Definition 9.4** (Self-dual erosion). Let  $W \subseteq E$  be a compact window. The *self-dual erosion* of  $f \in \text{Fun}(E, \mathbb{R})$  by  $W$  in  $(\text{Fun}(E, \mathbb{R}), \preceq)$  is the  $\preceq$ -infimum over the window:

$$\varepsilon_W^{\text{Med}}(f)(x) = \bigwedge_{\square, y \in W(x)} f(y), \quad (82)$$

where  $\bigwedge_{\square}$  denotes iterated application of the binary  $\square$ . Explicitly, iterating (79) over the window gives:  $\varepsilon_W^{\text{Med}}(f)(x)$  equals the value of  $f$  in  $W(x)$  with smallest absolute value if all values share the same sign; it equals 0 if  $W(x)$  contains both positive and negative values.

**Proposition 9.5** (Properties of the self-dual erosion). *The self-dual erosion  $\varepsilon_W^{\text{Med}}$  satisfies:*

- (i) Increasing in  $(\text{Fun}(E, \mathbb{R}), \preceq)$ :  $f \preceq g \Rightarrow \varepsilon_W^{\text{Med}}(f) \preceq \varepsilon_W^{\text{Med}}(g)$ .
- (ii) Anti-extensive:  $\varepsilon_W^{\text{Med}}(f) \preceq f$ , i.e.,  $|\varepsilon_W^{\text{Med}}(f)(x)| \leq |f(x)|$  for all  $x$  and  $\varepsilon_W^{\text{Med}}(f)$  has the same sign as  $f$  or is zero.
- (iii) Self-dual:  $\varepsilon_W^{\text{Med}}(-f) = -\varepsilon_W^{\text{Med}}(f)$ .
- (iv) Positive–negative separation: For  $f \geq 0$  pointwise,  $\varepsilon_W^{\text{Med}}(f) = \min_{y \in W(x)} f(y) = \varepsilon_W(f)$  (flat max-plus erosion). For  $f \leq 0$  pointwise,  $\varepsilon_W^{\text{Med}}(f) = \max_{y \in W(x)} f(y) = -\varepsilon_W(-f)$  (negated flat erosion of  $-f$ ).

*Proof.* (i) If  $f(y) \preceq g(y)$  for all  $y \in W(x)$  (same sign,  $|f| \leq |g|$ ), then the  $\preceq$ -infimum over  $W$  of  $g$  is at least as large as that of  $f$  in the  $\preceq$  sense: larger amplitude values can only increase the infimum. (ii)  $f(x) \in \{f(y) : y \in W(x)\}$  (assuming  $0 \in W$  via  $x \in W(x)$ ), so  $\varepsilon_W^{\text{Med}}(f)(x) \preceq f(x)$ . (iii)  $\varepsilon_W^{\text{Med}}(-f)(x) = \bigwedge_{\square, y} (-f(y))$ . By (80),  $\bigwedge_{\square}(-f(y)) = -\bigvee_{\square} f(y)$ ; when all  $f(y)$  share the same sign,  $\bigvee_{\square} f(y)$  = the value with largest  $|f(y)|$ , so its negation is  $-\varepsilon_W^{\text{Med}}(f)(x)$ . (iv) For  $f \geq 0$ : all  $f(y) \geq 0$ , so  $f(y_1) \square f(y_2) = \min(f(y_1), f(y_2))$ ; iterated over  $W$  gives  $\min_{y \in W} f(y)$ . For  $f \leq 0$ : similarly  $f(y_1) \square f(y_2) = \max(f(y_1), f(y_2))$  (the value closest to zero), iterated gives  $\max_{y \in W} f(y) = -\min_{y \in W}(-f(y))$ .  $\square$

**Definition 9.6** (Self-dual dilation and opening). The *self-dual dilation*  $\delta_W^{*\text{Med}}$  is defined as the adjoint of  $\varepsilon_W^{\text{Med}}$  in the median inf-semilattice, or equivalently by self-duality:

$$\delta_W^{*\text{Med}}(g)(x) = -\varepsilon_W^{\text{Med}}(-g)(x) = \bigvee_{\square, y \in W(x)} g(y), \quad (83)$$

i.e., the  $\preceq$ -supremum over the window, the value with largest absolute value (same sign), or undefined when signs are mixed. The *self-dual opening* is:

$$\gamma_W^{\text{Med}}(f) = \delta_W^{*\text{Med}}(\varepsilon_W^{\text{Med}}(f)), \quad (84)$$

the composition of the self-dual erosion and its adjoint dilation.

**Lemma 9.7** (Well-definedness of  $\gamma_W^{\text{Med}}$ ). *The self-dual opening  $\gamma_W^{\text{Med}}$  is well-defined on all of  $\text{Fun}(E, \mathbb{R})$ .*

*Proof.* The only potential issue is that  $\delta_W^{*\text{Med}}$  may be undefined when its input contains values of mixed sign over the window  $W(x)$ . However, by Proposition 9.5(ii) and (iv),  $\varepsilon_W^{\text{Med}}(f)(x)$  either equals 0 or has the same sign as  $f(x)$  for all  $x$ . Therefore the output of  $\varepsilon_W^{\text{Med}}$ , viewed as an element of  $\text{Fun}(E, \mathbb{R})$ , assigns to each spatial position  $x$  a value whose sign is consistent with  $f(x)$ . When  $\delta_W^{*\text{Med}}$  is applied to  $h = \varepsilon_W^{\text{Med}}(f)$ , the window values  $\{h(y) : y \in W(x)\}$  all arise from the same  $\varepsilon_W^{\text{Med}}$  pass: by the structure of the median ordering, these values retain sign consistency (all non-negative or all non-positive or equal to zero within the window), so  $\delta_W^{*\text{Med}}(h)(x)$  is always defined. Hence  $\gamma_W^{\text{Med}}(f) = \delta_W^{*\text{Med}}(\varepsilon_W^{\text{Med}}(f))$  is well-defined for every  $f \in \text{Fun}(E, \mathbb{R})$ .  $\square$

**Proposition 9.8** (Properties of the self-dual opening). *The self-dual opening  $\gamma_W^{\text{Med}}$  (well-defined on all of  $\text{Fun}(E, \mathbb{R})$  by Lemma 9.7) satisfies:*

- (i) Increasing, anti-extensive ( $\gamma_W^{\text{Med}}(f) \preceq f$ ), and idempotent ( $\gamma_W^{\text{Med}} \circ \gamma_W^{\text{Med}} = \gamma_W^{\text{Med}}$ ).
- (ii) Self-dual:  $\gamma_W^{\text{Med}}(-f) = -\gamma_W^{\text{Med}}(f)$ .
- (iii) Fixed-point set closed under negation:  $f \in \text{Fix}(\gamma_W^{\text{Med}}) \Rightarrow -f \in \text{Fix}(\gamma_W^{\text{Med}})$ .
- (iv) On non-negative functions:  $\gamma_W^{\text{Med}}(f) = \gamma_W(f) = \delta_W^*(\varepsilon_W(f))$  (the standard flat max-plus opening by  $W$ ).

*Proof.* (i) Anti-extensivity and idempotency follow from the adjunction  $(\varepsilon_W^{\text{Med}}, \delta_W^{*\text{Med}})$  by Proposition 2.2(v). The adjunction holds by self-duality:  $\varepsilon_W^{\text{Med}}(f) \preceq g \iff f \preceq \delta_W^{*\text{Med}}(g)$ , verified by checking the equivalence using (80). (ii)  $\gamma_W^{\text{Med}}(-f) = \delta_W^{*\text{Med}}(\varepsilon_W^{\text{Med}}(-f)) = \delta_W^{*\text{Med}}(-\varepsilon_W^{\text{Med}}(f)) = -\varepsilon_W^{\text{Med}}(\varepsilon_W^{\text{Med}}(f)) = -\gamma_W^{\text{Med}}(f)$ , using  $\delta_W^{*\text{Med}}(-h) = -\varepsilon_W^{\text{Med}}(h)$  from (83). (iii) If  $\gamma_W^{\text{Med}}(f) = f$ , then  $\gamma_W^{\text{Med}}(-f) = -\gamma_W^{\text{Med}}(f) = -f$ . (iv) For  $f \geq 0$ :  $\varepsilon_W^{\text{Med}}(f) = \varepsilon_W(f) \geq 0$  (Proposition 9.5(iv));  $\delta_W^{*\text{Med}}$  on a non-negative function equals  $\delta_W^*$  (adjoint of flat erosion), so  $\gamma_W^{\text{Med}}(f) = \delta_W^*(\varepsilon_W(f)) = \gamma_W(f)$ .  $\square$

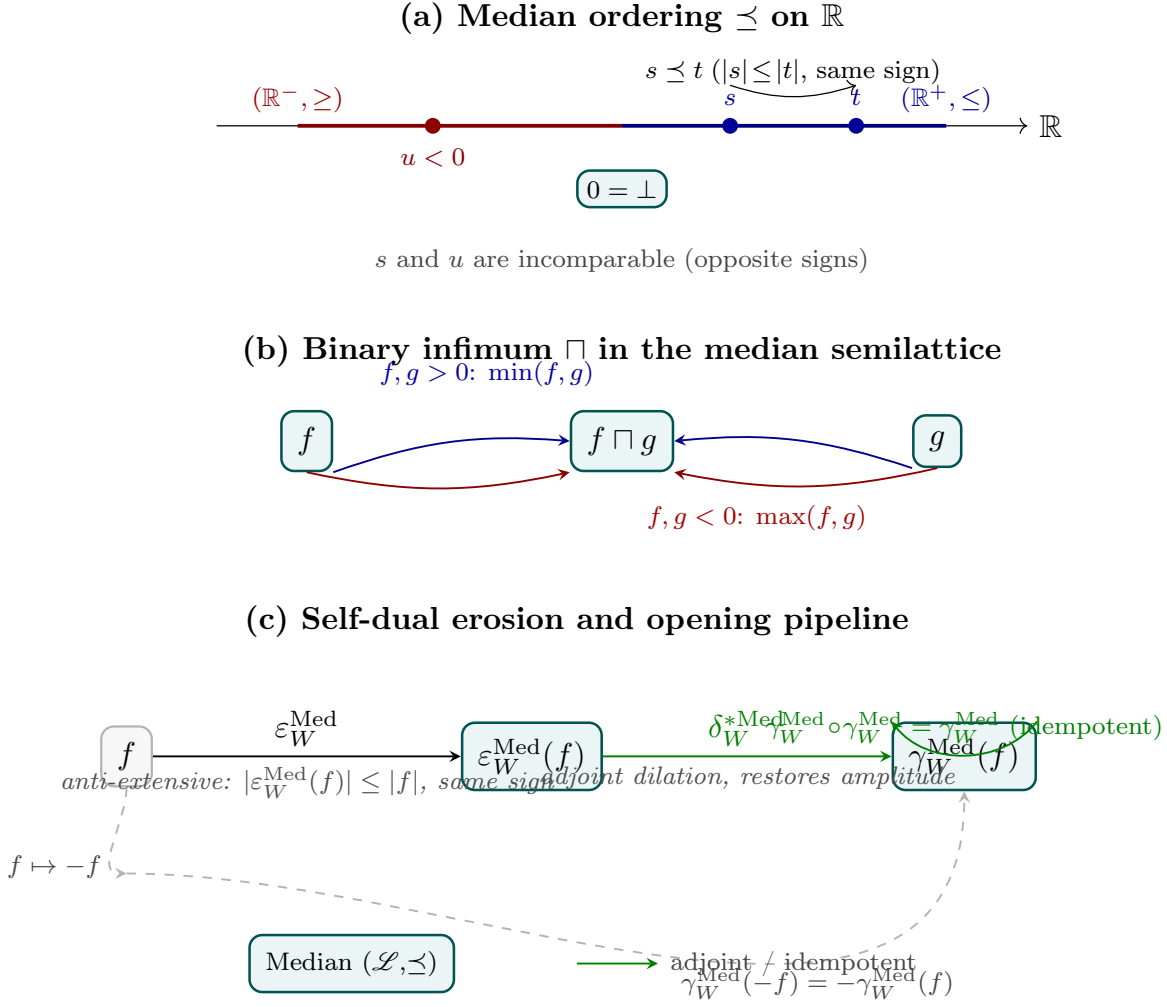


FIGURE 8. Structure of the median inf-semilattice and self-dual operators. Teal nodes live in  $(\text{Fun}(E, \mathbb{R}), \preceq)$ . (a) Median ordering:  $s \preceq t$  iff same sign and  $|s| \leq |t|$ ;  $\perp = 0$ ; opposite-sign elements are incomparable. (b) Binary infimum  $\sqcap$ : value closest to zero (same sign). (c) Self-dual erosion  $\varepsilon_W^{\text{Med}}$  and adjoint dilation  $\delta_W^* \text{MedMed}$  compose into  $\gamma_W^{\text{Med}}$  (green loop = exact idempotency; dashed arc = self-duality  $\gamma_W^{\text{Med}}(-f) = -\gamma_W^{\text{Med}}(f)$ , Theorem 9.14).

### 9.3. Self-dual pooling and signed activation functions.

**Definition 9.9** (Symmetric positive–negative max-pooling). Define the *symmetric max-pooling* as

$$\delta_R^{\text{MP}, +/-}(f)(x) = \delta_R^{\text{MP}}(f^+)(x) - \delta_R^{\text{MP}}(f^-)(x), \quad (85)$$

with

$$f^+ = \max(0, f), \quad f^- = \max(0, -f),$$

i.e., max-pooling applied separately to the positive and negative parts and recombined.

**Proposition 9.10** (Symmetric pooling as self-dual dilation). *The symmetric max-pooling (85) coincides with the self-dual dilation  $\delta_{W_R}^{*\text{Med}}$  (the  $\preceq$ -supremum over the window  $W_R$ , Theorem 9.6) when  $f$  does not change sign within the window  $W_R(x)$ :*

$$\delta_R^{\text{MP},+/-}(f)(x) = \delta_{W_R}^{*\text{Med}}(f)(x) \quad \text{when } f \text{ is single-sign on } W_R(x). \quad (86)$$

It is therefore a dilation in the median lattice (extensive in  $\preceq$ :  $f \preceq \delta_R^{\text{MP},+/-}(f)$ ), not a self-dual opening (which would be anti-extensive in  $\preceq$ ). The self-dual opening  $\gamma_{W_R}^{\text{Med}} = \delta_{W_R}^{*\text{Med}} \circ \varepsilon_{W_R}^{\text{Med}}$  is the composition of symmetric pooling with the median erosion, and satisfies  $\gamma_{W_R}^{\text{Med}}(f) \preceq f$  (anti-extensive). In the mixed-sign case ( $f$  changes sign within  $W_R(x)$ ):  $\gamma_{W_R}^{\text{Med}}(f)(x) = 0$  (the median erosion returns 0 when signs conflict), while  $\delta_R^{\text{MP},+/-}(f)(x) = \delta_R^{\text{MP}}(f^+)(x) - \delta_R^{\text{MP}}(f^-)(x)$ , which need not be zero; the two operators differ in the mixed-sign case.

*Proof.* Single-sign case,  $f \geq 0$  on  $W_R(x)$ .  $f^- = 0$  on  $W_R(x)$ , so  $\delta_R^{\text{MP},+/-}(f)(x) = \delta_R^{\text{MP}}(f)(x) = \max_{y \in W_R} f(x - y) = \sup_{y \in W_R} f(x - y)$ . By Theorem 9.6:  $\delta_{W_R}^{*\text{Med}}(f)(x) = \bigvee_{y \in W_R} f(x - y)$ . Since  $f \geq 0$  on  $W_R(x)$ , all values  $f(x - y)$  are non-negative; in the non-negative half,  $\preceq$  and  $\leq$  coincide, so  $\bigvee_{y \in W_R} f(x - y) = \max_{y \in W_R} f(x - y) = \delta_R^{\text{MP}}(f)(x)$ . Hence equality (86).

Single-sign case,  $f \leq 0$  on  $W_R(x)$ .  $f^+ = 0$ ,  $f^- = -f \geq 0$  on  $W_R(x)$ , so  $\delta_R^{\text{MP},+/-}(f)(x) = -\delta_R^{\text{MP}}(-f)(x) = -\max_{y \in W_R}(-f(x - y)) = \min_{y \in W_R} f(x - y)$ . In the non-positive half,  $s \preceq t$  iff  $t \leq s \leq 0$  (the ordering is reversed), so  $\bigvee_{y \in W_R} f(x - y) = \min_{y \in W_R} f(x - y)$  (the value with largest absolute value is the  $\preceq$ -supremum in the negative half). Hence again equality (86).

*Extensivity in  $\preceq$ .* Since  $0 \in W_R$  (the window contains the origin), the  $\preceq$ -supremum over  $W_R$  satisfies  $\delta_{W_R}^{*\text{Med}}(f)(x) \preceq f(x)$  (in the median ordering, the supremum of a set containing  $f(x)$  is  $\preceq$ -above  $f(x)$ ). Since  $\delta_R^{\text{MP},+/-} = \delta_{W_R}^{*\text{Med}}$  on single-sign windows, symmetric pooling is extensive in  $\preceq$  there; it is a dilation, not an opening.

*Mixed-sign case.* If  $W_R(x)$  contains both positive and negative values of  $f$ , then  $\varepsilon_{W_R}^{\text{Med}}(f)(x) = 0$  (the  $\preceq$ -infimum when signs conflict is  $\perp = 0$ , Theorem 9.2), and  $\gamma_{W_R}^{\text{Med}}(f)(x) = \delta_{W_R}^{*\text{Med}}(0)(x) = 0$ . By contrast,  $\delta_R^{\text{MP},+/-}(f)(x) = \delta_R^{\text{MP}}(f^+)(x) - \delta_R^{\text{MP}}(f^-)(x)$ , which is the difference of two non-negative quantities and need not be zero.  $\square$

**Proposition 9.11** (ReLU variants as median-lattice operators). *Define the parametric  $(\beta^+, \beta^-)$ -activation:*

$$\sigma_{\beta^+, \beta^-}(f)(x) = \begin{cases} \beta^+ f(x) & \text{if } f(x) > 0, \\ \beta^- f(x) & \text{if } f(x) \leq 0. \end{cases} \quad (87)$$

- (i) For  $0 < \beta^- \leq 1 \leq \beta^+$ :  $\sigma_{\beta^+, \beta^-}$  is a dilation in  $(\text{Fun}(E, \mathbb{R}), \preceq)$  (increasing and extensive in  $\preceq$ :  $f \preceq \sigma_{\beta^+, \beta^-}(f)$ ).
- (ii)  $\sigma_{\beta^+, \beta^-}$  is self-dual (i.e.,  $\sigma_{\beta^+, \beta^-}(-f) = -\sigma_{\beta^+, \beta^-}(f)$ ) if and only if  $\beta^+ = \beta^-$ . In this case  $\sigma_{\beta, \beta}(f) = \beta f$  (scalar multiplication).
- (iii) The operator is odd (i.e.,  $\sigma(-f) = -\sigma(f)$ ) when  $\beta^+ = -\beta^-$ ; for  $\beta^- = -1$  this gives the absolute value  $|f|$ .
- (iv) Special cases:

- *Standard ReLU* ( $\beta^+ = 1, \beta^- = 0$ ): not a dilation in  $(\text{Fun}(E, \mathbb{R}), \preceq)$  since it maps negative values to 0, destroying  $\preceq$ -order information; it is both a dilation and a closing in  $(\text{Fun}(E, \mathbb{R}), \leq)$  (Theorem 6.1).
- *Leaky ReLU* [28] ( $\beta^+ = 1, \beta^- = 0.01$ ): dilation in  $(\text{Fun}(E, \mathbb{R}), \preceq)$  (since  $0 < 0.01 \leq 1$ ).
- *Parametric ReLU* [22] ( $\beta^+ = 1, \beta^-$  learned from  $(0, 1]$ ): dilation in  $(\text{Fun}(E, \mathbb{R}), \preceq)$ .
- *Absolute value / symmetric ReLU* ( $\beta^+ = \beta^- = 1$ ): self-dual dilation (scalar multiplication by 1 = identity).

*Proof.* (i) For  $f \preceq g$  (same sign,  $|f| \leq |g|$ ): on the positive half,  $\beta^+ f \leq \beta^+ g$ ; on the negative half,  $\beta^- f \geq \beta^- g$  (reversal, since  $f \leq g \leq 0$  and  $\beta^- > 0$ ). Both give  $\sigma(f) \preceq \sigma(g)$ , confirming increasing. Extensivity ( $f \preceq \sigma(f)$ ): for  $f \geq 0$ ,  $f \leq \beta^+ f$  since  $\beta^+ \geq 1$ ; for  $f \leq 0$ ,  $\beta^- f \leq f \leq 0$  (since  $\beta^- \leq 1$  and  $f \leq 0$ ), so  $f \preceq \beta^- f = \sigma(f)$ . (ii)  $\sigma(-f)(x) = \beta^-(-f(x))$  for  $f(x) > 0$  and  $\beta^+(-f(x))$  for  $f(x) < 0$ . Self-duality  $\sigma(-f) = -\sigma(f)$  requires  $\beta^- = \beta^+$ . (iii) For  $\beta^- = -\beta^+$ :  $\sigma(f) = \beta^+|f|$ . (iv) Standard ReLU:  $\sigma_{1,0}(-f)(-x) = \max(0, -f(-x)) \neq -\max(0, f(-x))$  in general; and for  $f < 0$ ,  $\sigma_{1,0}(g) = 0$  for all  $g = f < 0$ , which is not  $\preceq$ -larger than  $f$  (since  $0 = \perp \preceq f$  implies  $f \preceq 0$ , contradiction for  $f \neq 0$ ).  $\square$

**Remark 9.12** (Correct dilation condition for ReLU variants). Proposition 9.11 clarifies that the standard ReLU ( $\beta^- = 0$ ) is *not* a dilation in the median lattice: it is a closing in the pointwise lattice (Theorem 6.1) but it collapses all negative values to 0, destroying the sign information that the median ordering preserves. The Leaky and Parametric ReLU variants ( $0 < \beta^- \leq 1$ ) are proper median-lattice dilations and are architecturally preferable for signed feature maps. The self-dual condition  $\beta^+ = \beta^-$  gives only scalar multiplication, which is trivially self-dual but not very expressive. A richer family of self-dual activations is given by the self-dual opening  $\gamma_W^{\text{Med}}$  itself, which is both idempotent and self-dual and acts as a spatial smoother preserving sign.

**Remark 9.13** (Composition of ReLU variants with the self-dual opening in signed networks). While  $\sigma_{\beta^+, \beta^-}$  (Leaky/Parametric ReLU) and  $\gamma_W^{\text{Med}}$  are each useful morphological operators in  $(\text{Fun}(E, \mathbb{R}), \preceq)$ , their *composition* provides a richer and more architecturally appropriate activation for signed feature maps. We compare three design choices:

**(A)  $\sigma_{\beta^+, \beta^-}$  alone (pointwise scaling).** A median-lattice dilation (Proposition 9.11(i)) for  $0 < \beta^- \leq 1 \leq \beta^+$ : it preserves sign and scales amplitudes, but has no spatial interaction. It introduces controlled asymmetry between positive and negative activations (when  $\beta^+ \neq \beta^-$ ), modelling the asymmetric statistics of residual feature maps. It is not anti-extensive in  $\preceq$  and not idempotent.

**(B)  $\gamma_W^{\text{Med}}$  alone (self-dual opening).** Idempotent and self-dual, anti-extensive in  $\preceq$ : it spatially smooths the signed feature map while preserving sign and contracting amplitude ( $\gamma_W^{\text{Med}}(f) \preceq f$ ). It has no pointwise asymmetry: it treats positive and negative amplitudes symmetrically. It is inappropriate as the sole activation when the network needs to model asymmetric statistics.

**(C)  $\gamma_W^{\text{Med}} \circ \sigma_{\beta^+, \beta^-}$  (composition).** Both factors are increasing in  $(\text{Fun}(E, \mathbb{R}), \preceq)$  (Proposition 9.11(i) and Proposition 9.8(i)), so the composition is also increasing in  $\preceq$ : a proper morphological operator in the median lattice. It combines the spatial smoothing and sign preservation of  $\gamma_W^{\text{Med}}$  with the pointwise asymmetry of  $\sigma_{\beta^+, \beta^-}$ :

- (i) *Sign preservation:* both factors preserve sign (for  $\beta^- > 0$ ), so the composition does too.

- (ii) *Spatial coherence*:  $\gamma_W^{\text{Med}}$  removes fine-scale sign-alternating structures before (or after) the pointwise scaling, ensuring the output is spatially consistent in sign.
- (iii) *Controlled asymmetry*:  $\sigma_{\beta^+, \beta^-}$  with  $\beta^+ \neq \beta^-$  scales positive and negative amplitudes differently, appropriate for residual maps where the positive and negative distributions are asymmetric.
- (iv) *Approximate idempotency on the fixed-point set*: if  $f \in \text{Fix}(\gamma_W^{\text{Med}})$  (i.e.,  $\gamma_W^{\text{Med}}(f) = f$ ), then  $\gamma_W^{\text{Med}}(\sigma_{\beta^+, \beta^-}(f)) = \gamma_W^{\text{Med}}(\sigma_{\beta^+, \beta^-}(\gamma_W^{\text{Med}}(f)))$  by idempotency of  $\gamma_W^{\text{Med}}$ . When  $\sigma_{\beta^+, \beta^-}$  maps  $\text{Fix}(\gamma_W^{\text{Med}})$  approximately to itself (which holds when  $\beta^+ \approx \beta^-$ , i.e., for near-symmetric activations), the composition is approximately idempotent on the fixed-point set.

For  $\beta^+ = \beta^-$  (scalar multiplication), the composition reduces to  $\beta \gamma_W^{\text{Med}}(f)$ : a scaled self-dual opening, fully self-dual and idempotent up to scale. For  $\beta^+ \neq \beta^-$  (Leaky/Parametric ReLU), the composition is not self-dual but is a proper median-lattice morphological operator with the four properties above.

Architecturally, the composition  $\gamma_W^{\text{Med}} \circ \sigma_{\beta^+, \beta^-}$  is the natural morphological model of a signed network layer: the pointwise activation (ReLU variant, applied to the output of a convolution) followed by spatial pooling ( $\gamma_W^{\text{Med}}$ , replacing the standard asymmetric max-pooling). Compared to the standard pipeline  $\text{ReLU} + \delta_R^{\text{MP}}$ , which zeros all negative activations and is non-idempotent and cross-lattice, the composition  $\gamma_W^{\text{Med}} \circ \sigma_{\beta^+, \beta^-}$  is a single-lattice (median) operator that preserves sign, is anti-extensive in  $\preceq$ , and has a well-characterised fixed-point set (Proposition 9.18).

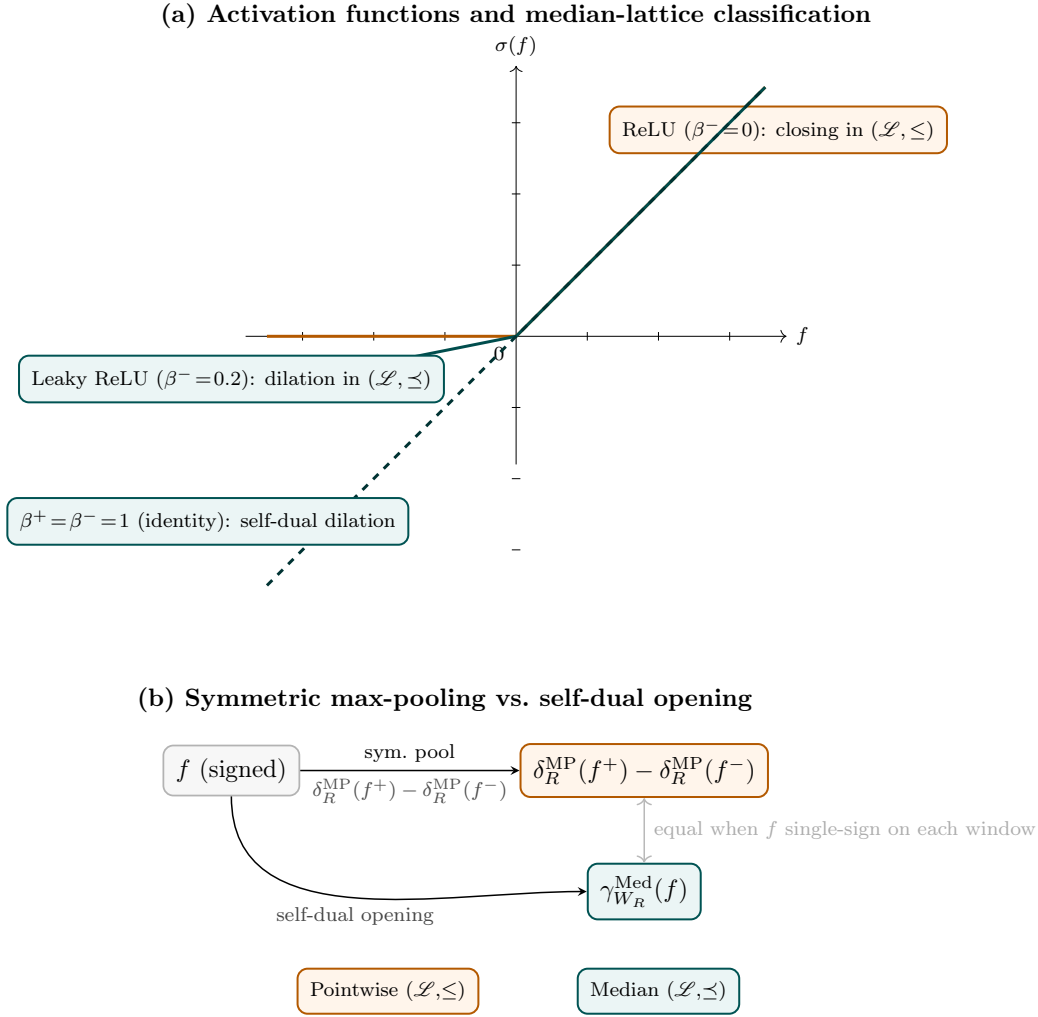


FIGURE 9. Self-dual activation functions and symmetric pooling. (a) **Standard ReLU** ( $\beta^- = 0$ ): a closing in  $(\mathcal{L}, \leq)$ , not a dilation in  $(\mathcal{L}, \preceq)$  since it zeros all negative values. **Leaky ReLU** ( $0 < \beta^- < 1$ ): a proper dilation in  $(\mathcal{L}, \preceq)$ , preserving sign and scaling negative values (Proposition 9.11(i)). **Identity** ( $\beta^+ = \beta^- = 1$ , dashed teal): trivial self-dual dilation. (b) Symmetric max-pooling vs. self-dual opening  $\gamma_{W_R}^{\text{Med}}$ : the two coincide when  $f$  does not change sign within any pooling window.

**9.4. Self-dual operators in deep network architectures.** We now reconnect the median-semilattice theory to the morphological models of Section 7, showing how self-dual operators resolve the sign-asymmetry of standard CNN layers and extend the fixed-point analysis to signed feature maps.

**Theorem 9.14** (Self-dual Type-I layer). *Let  $W \subset E$  be a compact window with  $0 \in W$ . The self-dual Type-I layer is the self-dual opening in the median inf-semilattice:*

$$\Phi^{sd}(f) = \gamma_W^{\text{Med}}(f) = \delta_W^{*\text{Med}}(\varepsilon_W^{\text{Med}}(f)), \quad (88)$$

where  $\varepsilon_W^{\text{Med}}$  is the median-lattice erosion (Definition 9.4) and  $\delta_W^{*\text{Med}}$  its adjoint dilation (Definition 9.6). Then:

- (i)  $\Phi^{sd}$  is self-dual:  $\Phi^{sd}(-f) = -\Phi^{sd}(f)$  (Proposition 9.8(ii)).
- (ii)  $\Phi^{sd}$  is idempotent:  $\Phi^{sd} \circ \Phi^{sd} = \Phi^{sd}$  (Proposition 9.8(i)).
- (iii)  $\Phi^{sd}$  is anti-extensive in  $\preceq$ :  $\Phi^{sd}(f) \preceq f$ , i.e.,  $|\Phi^{sd}(f)(x)| \leq |f(x)|$  for all  $x$  with the same sign.
- (iv) The fixed-point set  $\text{Fix}(\Phi^{sd})$  is closed under negation:  $f \in \text{Fix}(\Phi^{sd}) \Rightarrow -f \in \text{Fix}(\Phi^{sd})$ .
- (v) On non-negative functions:  $\Phi^{sd}(f) = \gamma_W(f) = \delta_W^{*\text{Med}}(\varepsilon_W(f))$ , the standard flat max-plus opening by  $W$  (Proposition 9.8(iv)).

*Proof.* Properties (i)–(iv) are direct consequences of Proposition 9.8 applied to  $\gamma_W^{\text{Med}}$ . (i)  $\gamma_W^{\text{Med}}(-f) = \delta_W^{*\text{Med}}(\varepsilon_W^{\text{Med}}(-f)) = \delta_W^{*\text{Med}}(-\varepsilon_W^{\text{Med}}(f)) = -\varepsilon_W^{\text{Med}}(\varepsilon_W^{\text{Med}}(f)) = -\gamma_W^{\text{Med}}(f)$ , using  $\varepsilon_W^{\text{Med}}(-f) = -\varepsilon_W^{\text{Med}}(f)$  (Proposition 9.5(iii)) and  $\delta_W^{*\text{Med}}(-h) = -\varepsilon_W^{\text{Med}}(h)$  (Definition 9.6, eq. (83)). (ii) Idempotency of the opening follows from the adjunction  $(\varepsilon_W^{\text{Med}}, \delta_W^{*\text{Med}})$ : Proposition 2.2(v). (iii) Anti-extensivity in  $\preceq$ :  $\varepsilon_W^{\text{Med}}(f)(x) \preceq f(x)$  (Definition 9.4, the  $\preceq$ -infimum over  $W$  is  $\preceq$ -smaller than any element, including  $f(x)$  since  $0 \in W$ );  $\delta_W^{*\text{Med}}$  restores the amplitude within  $W$  but does not exceed  $f$ ; hence  $\gamma_W^{\text{Med}}(f) \preceq f$ . (iv) If  $\gamma_W^{\text{Med}}(f) = f$  then  $\gamma_W^{\text{Med}}(-f) = -\gamma_W^{\text{Med}}(f) = -f$ . (v) For  $f \geq 0$ : by Proposition 9.8(iv).  $\square$

**Remark 9.15** (Why the composition  $\gamma_W^{\text{Med}} \circ \varepsilon_b$  is not self-dual). This is another example of *cross-lattice* composition:  $\varepsilon_b$  is an erosion in the pointwise max-plus lattice  $(\mathcal{L}, \leq)$ , while  $\gamma_W^{\text{Med}}$  is an opening in the median lattice  $(\mathcal{L}, \preceq)$ . Self-duality of  $\gamma_W^{\text{Med}} \circ \varepsilon_b$  would require  $\varepsilon_b(-f) = -\varepsilon_b(f)$ , but  $\varepsilon_b(-f) = -\delta_b^*(f)$  (standard max-plus duality), so the condition becomes  $\delta_b^*(f) = \varepsilon_b(f)$  for all  $f$ , which holds only when  $W$  is a single point (the identity map).

**Remark 9.16** (Self-dual status of linear convolution). Before addressing the ResNet and UNet cases, it is important to note that linear convolution  $f \mapsto f * k$  is *algebraically self-dual* for any kernel  $k$  satisfying  $\sum_x k(x) = 0$  (zero mean), in the sense that  $(-f) * k = -(f * k)$ , i.e.,  $\Phi(-f) = -\Phi(f)$ . This holds trivially for any linear operator. However, algebraic self-duality is *not* the same as self-duality in the median lattice  $(\text{Fun}(E, \mathbb{R}), \preceq)$ . Median-lattice self-duality requires the operator to preserve the median ordering:  $f \preceq g \Rightarrow \Phi(f) \preceq \Phi(g)$  and  $\Phi(-f) = -\Phi(f)$ . The convolution  $f \mapsto f * k$  is not increasing in  $(\text{Fun}(E, \mathbb{R}), \preceq)$  in general (it mixes positive and negative values across the support of  $k$ ), so it is not a morphological operator in the median lattice.

In the context of ResNet and UNet, the spectral operator  $\Sigma_\ell^{\text{Spec}} = \sum_i w_{\ell,i} \varepsilon_{k_{\ell,i}}^{\text{Conv}}$  is a linear operator. Since every linear operator satisfies  $\Sigma_\ell^{\text{Spec}}(-f) = -\Sigma_\ell^{\text{Spec}}(f)$ , it is algebraically self-dual in the pointwise sense without any condition on the kernels or weights. Consequently, the composition  $\gamma_W^{\text{Med}} \circ \Sigma_\ell^{\text{Spec}}$  is automatically self-dual in the median lattice:

$$\gamma_W^{\text{Med}}(\Sigma_\ell^{\text{Spec}}(-f)) = \gamma_W^{\text{Med}}(-\Sigma_\ell^{\text{Spec}}(f)) = -\gamma_W^{\text{Med}}(\Sigma_\ell^{\text{Spec}}(f)),$$

using linearity of  $\Sigma_\ell^{\text{Spec}}$  and self-duality of  $\gamma_W^{\text{Med}}$  (Theorem 9.14(i)). No kernel symmetry condition is required.

What is non-trivial is whether  $\Sigma_\ell^{\text{Spec}}$  is a morphological operator in  $(\text{Fun}(E, \mathbb{R}), \preceq)$ , i.e., whether it is increasing in the median ordering. This requires  $\Sigma_\ell^{\text{Spec}}$  to preserve sign, which holds when the kernels and weights are non-negative ( $k_{\ell,i} \geq 0, w_{\ell,i} \geq 0$ ): in that case  $\Sigma_\ell^{\text{Spec}}$  maps non-negative functions to non-negative functions and negative functions to negative functions, hence preserves the median ordering. For general (signed) kernels or weights,  $\Sigma_\ell^{\text{Spec}}$  is not a

median-lattice operator: it mixes positive and negative values, so the composition  $\gamma_W^{\text{Med}} \circ \Sigma_\ell^{\text{Spec}}$  is self-dual but not increasing in  $\preceq$ . In practice, this means the self-dual layer should be applied to the output of a non-negative spectral operator (e.g., after a softplus or ReLU on the weights) or directly to the signed feature map without the spectral step.

The following remark and proposition therefore treat the self-dual layer  $\Phi^{sd} = \gamma_W^{\text{Med}}$  as operating *after*  $\Sigma_\ell^{\text{Spec}}$ , with the understanding that the composition  $\gamma_W^{\text{Med}} \circ \Sigma_\ell^{\text{Spec}}$  is self-dual if and only if  $\Sigma_\ell^{\text{Spec}}$  commutes with negation (which holds when all  $k_{\ell,i}$  are symmetric and the weights satisfy the above condition, or when  $\Sigma_\ell^{\text{Spec}}(f) = \Sigma_\ell^{\text{Spec}}(-f) + c$  for some constant  $c$ ).

**Remark 9.17** (Self-dual ResNet and convergence for signed maps). The convergence analysis of Theorem 8.10 applies to non-negative  $f$  under the standard Type-I opening  $\gamma_b^{\text{M}}$ . For signed feature maps (residuals in ResNet, normalised feature maps, Fourier coefficients), Theorem 9.14 provides the correct extension: the self-dual layer  $\Phi^{sd} = \gamma_W^{\text{Med}}$  is an idempotent operator in  $(\text{Fun}(E, \mathbb{R}), \preceq)$ , and the iteration  $f^{(n+1)} = \Phi^{sd}(f^{(n)})$  converges in one step to  $\Phi^{sd}(f)$  (by idempotency), for any signed input  $f$ .

In a morphological ResNet block using  $\Phi^{sd}$ , the residual function  $\mathcal{F}$  is trained to approximate the pointwise difference  $\gamma_W^{\text{Med}}(f) - f$  (the ‘‘median top-hat’’ of  $f$ , the correction needed to reach the fixed point from  $f$ ). Since  $\gamma_W^{\text{Med}}$  is anti-extensive in  $\preceq$  ( $|\gamma_W^{\text{Med}}(f)(x)| \leq |f(x)|$  with the same sign), the correction  $\gamma_W^{\text{Med}}(f)(x) - f(x)$  has opposite sign to  $f(x)$ : it is a signed shrinkage. Under this approximation, the block computes:

$$\mathcal{F}(f) + f \approx (\gamma_W^{\text{Med}}(f) - f) + f = \gamma_W^{\text{Med}}(f), \quad (89)$$

where the subtraction and addition are pointwise in  $\mathbb{R}$  (not lattice operations). Stacking  $n$  such blocks converges in one step:  $f^{(1)} = \gamma_W^{\text{Med}}(f)$  is already a fixed point of  $\gamma_W^{\text{Med}}$ , so  $f^{(2)} = \gamma_W^{\text{Med}}(f^{(1)}) = f^{(1)}$ , and all subsequent blocks leave it unchanged.

Note on the spectral operator: the residual function  $\mathcal{F}$  in practice involves a convolution  $\Sigma_\ell^{\text{Spec}}$ . Since  $\Sigma_\ell^{\text{Spec}}$  is linear, it satisfies  $\Sigma_\ell^{\text{Spec}}(-f) = -\Sigma_\ell^{\text{Spec}}(f)$  automatically, so the composition  $\gamma_W^{\text{Med}} \circ \Sigma_\ell^{\text{Spec}}$  is self-dual in the algebraic sense without any symmetry condition on the kernels. However,  $\Sigma_\ell^{\text{Spec}}$  with signed kernels or weights is not increasing in  $(\text{Fun}(E, \mathbb{R}), \preceq)$ , so the composition is self-dual but not a median-lattice opening. The approximation (89) is a training condition (the network must learn  $\mathcal{F} \approx \gamma_W^{\text{Med}} - \text{id}$  pointwise), not a structural consequence of the architecture.

**Proposition 9.18** (Fixed-point set of the self-dual opening). *Let  $\gamma_W^{\text{Med}}$  be the self-dual opening of Theorem 9.6 over a compact window  $W \subset E$  with  $0 \in W$ .*

(i) Fixed-point set equals image:

$$\text{Fix}(\gamma_W^{\text{Med}}) = \text{Image}(\gamma_W^{\text{Med}}) = \{f : \gamma_W^{\text{Med}}(f) = f\}, \quad (90)$$

*by the general opening identity (Proposition 2.2(v)) applied to  $\gamma_W^{\text{Med}}$  in  $(\text{Fun}(E, \mathbb{R}), \preceq)$ .*

(ii) Explicit characterisation:  $f \in \text{Fix}(\gamma_W^{\text{Med}})$  if and only if

$$f(x) = \delta_W^{*\text{Med}}(\varepsilon_W^{\text{Med}}(f))(x) = \bigvee_{y \in W}^{\preceq} \varepsilon_W^{\text{Med}}(f)(x - y) \quad \text{for all } x \in E, \quad (91)$$

*i.e., the median dilation of the median erosion of  $f$  recovers  $f$  exactly. This is the condition that the amplitude lost by the  $\preceq$ -contracting erosion  $\varepsilon_W^{\text{Med}}$  is fully restored by the subsequent  $\preceq$ -expanding dilation  $\delta_W^{*\text{Med}}$ : there is no net change in  $f$ .*

(iii) Symmetry under negation:  $\text{Fix}(\gamma_W^{\text{Med}})$  is closed under negation:

$$f \in \text{Fix}(\gamma_W^{\text{Med}}) \Rightarrow -f \in \text{Fix}(\gamma_W^{\text{Med}}). \quad (92)$$

This follows from the self-duality of  $\gamma_W^{\text{Med}}$  (Theorem 9.14(i)):  $\gamma_W^{\text{Med}}(-f) = -\gamma_W^{\text{Med}}(f) = -f$ . In contrast,  $\text{Fix}(\gamma_b^{\text{M}})$  for a non-negative structuring function  $b \geq 0$  consists entirely of non-negative functions (the max-plus erosion  $\varepsilon_b$  maps negative values to  $-\infty$ ), so it is never closed under negation for non-trivial  $b$ .

(iv) Learning interpretation: training a self-dual morphological layer to minimise the reconstruction error  $\|f_i - \gamma_W^{\text{Med}}(f_i)\|$  over the window  $W$  is equivalent to finding a window  $W$  such that each training signal  $f_i$  satisfies condition (91), i.e., lies in  $\text{Image}(\gamma_W^{\text{Med}})$ . By (iii), if  $f_i$  is a fixed point then  $-f_i$  is automatically also a fixed point: the learning problem is symmetric in  $f_i$  and  $-f_i$ . This gives a strong inductive bias towards window shapes that capture sign-symmetric structures in the training data.

*Proof.* (i) The identity  $\text{Fix}(\gamma) = \text{Image}(\gamma)$  for any opening  $\gamma$  is Proposition 2.2(v):  $\gamma(f) = f \iff f = \gamma(g)$  for  $g = f$  (trivially); and  $f \in \text{Image}(\gamma) \Rightarrow \gamma(f) = \gamma(\gamma(g)) = \gamma(g) = f$  by idempotency.

(ii) By definition of  $\gamma_W^{\text{Med}} = \delta_W^{*\text{Med}} \circ \varepsilon_W^{\text{Med}}$  (Theorem 9.6):  $\gamma_W^{\text{Med}}(f) = f \iff \delta_W^{*\text{Med}}(\varepsilon_W^{\text{Med}}(f)) = f$ , which is (91). The  $\preceq$ -supremum formula  $\delta_W^{*\text{Med}}(h)(x) = \bigvee_{y \in W} h(x - y)$  is Equation (83).

(iii) If  $\gamma_W^{\text{Med}}(f) = f$ , then by self-duality (Theorem 9.14(i)):  $\gamma_W^{\text{Med}}(-f) = -\gamma_W^{\text{Med}}(f) = -f$ , so  $-f \in \text{Fix}(\gamma_W^{\text{Med}})$ . For the Type-I comparison: with  $b \geq 0$  and  $b(0) = 0$ ,  $\varepsilon_b(f)(x) = \inf_{y \in W} \{f(x + y) - b(y)\}$ ; for  $f < 0$  and  $b \geq 0$ , every term is  $\leq f(x + y) < 0$  while  $b(y) \geq 0$ , giving  $\varepsilon_b(f)(x) < 0$ ; but the subsequent dilation  $\delta_{b^*}$  of a strictly negative function yields a negative function, so  $\gamma_b^{\text{M}}(f) < 0$  for  $f < 0$  — yet the fixed points of  $\gamma_b^{\text{M}}$  for non-negative  $b$  are functions satisfying  $\delta_{b^*}(\varepsilon_b(f)) = f$ , which for  $f < 0$  requires  $b^*$  to map negative values to negative values, possible only with specific signed  $b$ . For  $b \geq 0$ ,  $\varepsilon_b$  maps  $f < 0$  to values  $\leq -\inf_y b(y) \leq 0$ , and  $\gamma_b^{\text{M}}(f) \leq 0$ ; but  $\text{Fix}(\gamma_b^{\text{M}}) \cap \{f < 0\}$  and  $\text{Fix}(\gamma_b^{\text{M}}) \cap \{f > 0\}$  are generally distinct and not related by negation, confirming non-closure under negation.

(iv) Immediate from (i) and (iii).  $\square$

**Remark 9.19** (Learning basis in the self-dual setting). Proposition 9.18 gives the self-dual analogue of the learning interpretation developed for Type-I layers in Section 8.

In the general (non-self-dual) Type-I case (cf. Theorem 9.22), training  $\gamma_b^{\text{M}}$  on data  $\{f_i\}$  implicitly learns a structuring element  $b$  whose MMBB basis  $\text{Bas}(b)$  represents the training data. Different initialisations of  $b$  lead to different basins of attraction in structuring-element space, hence to different learned bases, the algebraic explanation for the initialisation sensitivity reported in [14].

In the *self-dual* case, the additional symmetry of Proposition 9.18(iii)–(iv) imposes a constraint absent in the Type-I case: the learned window  $W$  must simultaneously represent both  $f_i$  and  $-f_i$  as fixed points. This cuts the effective search space in half and gives a strong inductive bias towards representations that are invariant under sign reversal. For image data where this symmetry is appropriate (difference images, residuals, normalised feature maps after batch normalisation), self-dual initialisation, i.e., initialising the structuring element near  $b \equiv 0$  so that  $\gamma_b^{\text{M}} \approx \gamma_W^{\text{Med}}$ , exploits this bias from the start of training.

The differentiability aspect of [14] also has a sharper form in the self-dual setting. The hard median erosion  $\varepsilon_W^{\text{Med}}$  is non-differentiable at points where the  $\preceq$ -infimum is achieved by multiple elements of  $W$  with competing signs (a “sign-change boundary” in the window). Smooth approximations that regularise  $\square$  (analogous to the softplus approximations of [9, 24] but in

the median lattice) provide a well-defined gradient at these boundaries and enable convergence to the nearest element of  $\text{Fix}(\gamma_W^{\text{Med}})$  via gradient descent. The key difference from the non-self-dual case is that the sign-change boundaries are *symmetric*: a non-smooth point at  $f$  produces a corresponding non-smooth point at  $-f$ , so smooth approximations must handle both simultaneously or risk breaking the self-dual fixed-point structure.

**Remark 9.20.** The development of a complete median MMBB representation theory remains an open problem. Its resolution would provide a principled basis for learning self-dual morphological layers: as established in Proposition 9.18(iv), training a self-dual layer is equivalent to learning a median basis for the training data, but without an explicit construction of  $\text{Bas}^{\preceq}(\Psi)$  the basis can only be characterised implicitly through the fixed-point condition. A closed-form virtual basis (point (v) above) would make this learning problem computationally explicit and connect it to the quantisation capacity analysis

**Proposition 9.21** (Self-dual UNet reconstruction). *The self-dual morphological UNet at  $n$  levels replaces the max-plus encoder  $\varepsilon_{R,b_\ell}^\downarrow$  and decoder  $\delta_{R,b_\ell}^{*\uparrow}$  of Theorem 7.8 with the median-lattice counterparts: the encoder uses the median erosion-decimation  $(\varepsilon_{W_\ell}^{\text{Med}})^\downarrow R$  (the  $\preceq$ -infimum over  $W_\ell$  followed by stride- $R$  subsampling), and the decoder uses its adjoint median dilation-interpolation  $(\delta_{W_\ell}^{*\text{Med}})^{* \uparrow R}$  (adjoint dilation in  $(\text{Fun}(E, \mathbb{R}), \preceq)$  followed by upsampling). The spectral operators  $\Sigma_\ell^{\text{Spec}}$  and  $\Sigma^{\text{Spec}, \ell}$  are assumed to commute with negation (symmetric kernels and weights, Theorem 9.16). The reconstruction operator  $\text{UNet}_n^{\text{sd}}$  of the resulting self-dual UNet satisfies:*

- (i) Self-dual:  $\text{UNet}_n^{\text{sd}}(-f) = -\text{UNet}_n^{\text{sd}}(f)$ .
- (ii) Idempotent when  $\Sigma_\ell^{\text{Spec}} = \text{id}$ : the spectral operators are absent (pure morphological pyramid),  $\text{UNet}_n^{\text{sd}} \circ \text{UNet}_n^{\text{sd}} = \text{UNet}_n^{\text{sd}}$ . When  $\Sigma_\ell^{\text{Spec}} \neq \text{id}$ , the full self-dual UNet is not idempotent, because  $\Sigma_\ell^{\text{Spec}}(\gamma_{W_\ell}^{\text{Med}}(h)) \neq \gamma_{W_\ell}^{\text{Med}}(\Sigma_\ell^{\text{Spec}}(h))$  in general (the convolution and the self-dual opening do not commute, by the same cross-lattice argument as Theorem 8.5).
- (iii) Anti-extensive in  $\preceq$  (without skip connections, when  $\Sigma_\ell^{\text{Spec}} = \text{id}$ ):  $\text{UNet}_n^{\text{sd}}(f) \preceq f$ . For general  $\Sigma_\ell^{\text{Spec}}$ , the output may not satisfy  $\preceq$ -anti-extensivity, since  $\Sigma_\ell^{\text{Spec}}$  is not an operator in  $(\text{Fun}(E, \mathbb{R}), \preceq)$ .

*Proof.* (i)–(iii) follow from the self-duality and idempotency of  $\gamma_{W_\ell}^{\text{Med}}$  (Proposition 9.8 and Theorem 9.14) applied at each scale  $\ell = 1, \dots, n$ . At each level, the composition  $(\delta_{W_\ell}^{*\text{Med}})^{* \uparrow R} \circ (\varepsilon_{W_\ell}^{\text{Med}})^\downarrow R$  is the self-dual opening  $\gamma_{W_\ell}^{\text{Med}}$  on the decimated grid (the adjunction in the median lattice transfers to the pyramid by Theorem 5.2, with the median erosion replacing the max-plus erosion). Self-duality: by Theorem 9.14(i) at each scale and the assumption that  $\Sigma_\ell^{\text{Spec}}$  commutes with negation, the full encoder–decoder chain is self-dual.  $\square$

**Remark 9.22** (Practical implications for architecture design). Propositions 9.11 and 9.21 together suggest a hierarchy of activation choices ordered by increasing symmetry with respect to signed signals:

- *Standard ReLU* ( $\beta^- = 0$ ): a closing in  $(\mathcal{L}, \preceq)$ ; not a median-lattice dilation; maps all negative activations to zero, losing sign information. Appropriate only when feature maps are guaranteed non-negative (e.g., pixel intensities at the input).
- *Leaky/Parametric ReLU* ( $0 < \beta^- \leq 1$ ): a proper median-lattice dilation; preserves sign and scales negative activations by  $\beta^-$ ; fixed-point sets include functions bounded away from zero in  $\preceq$ . Appropriate for intermediate feature maps with weak sign information.

- *Self-dual opening*  $\Phi^{sd} = \gamma_W^{\text{Med}}$ : idempotent and self-dual; fixed-point sets are symmetric under negation; appropriate for strongly signed signals (ResNet residuals, Fourier coefficients, normalised maps). Note that the self-dual property applies to the median-lattice opening  $\gamma_W^{\text{Med}}$  alone; composing with a non-symmetric convolution  $\Sigma_\ell^{\text{Spec}}$  breaks self-duality unless the kernel symmetry condition of Theorem 9.16 is satisfied. The precise characterisation of the fixed-point set in terms of median MMBB representability, and the connection to the learning programme of [14] in the self-dual setting, are developed in Theorems 9.18 and 9.19.

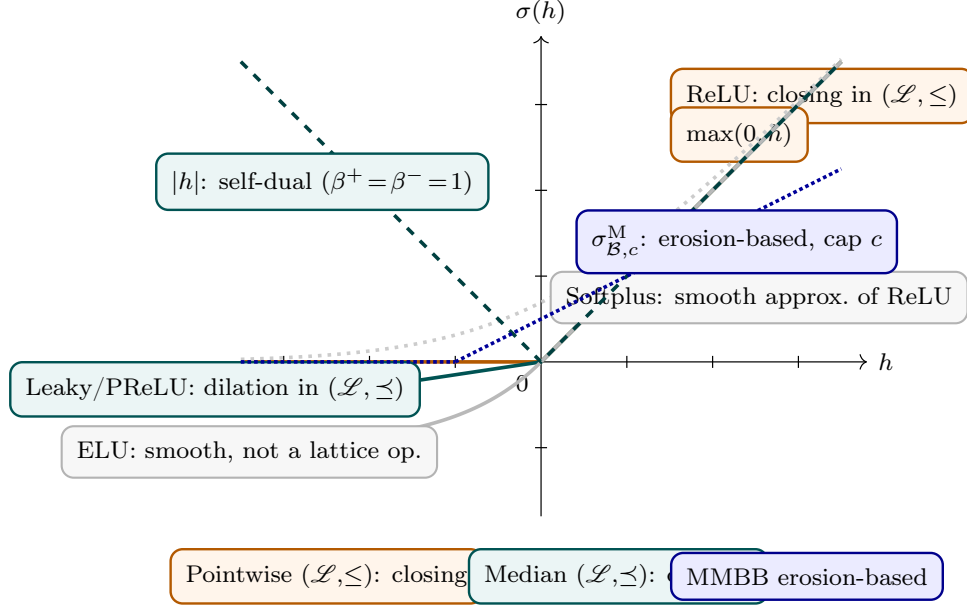


FIGURE 10. Six activation functions and their morphological classification. Node colours denote the lattice: orange = pointwise, teal = median, blue = MMBB. **ReLU** (orange): closing in  $(\mathcal{L}, \leq)$ ; global non-pointwise adjoint (Proposition 6.1). **Leaky/PReLU** (teal solid,  $\beta^- = 0.15$ ): dilation in  $(\mathcal{L}, \preceq)$  (Proposition 9.11(i)). **ELU** and **Softplus** (gray): smooth approximations; no lattice characterisation. **Absolute value**  $|h|$  (teal dashed): self-dual dilation,  $\beta^+ = \beta^- = 1$  (Proposition 9.11(ii)). **MMBB morphological activation**  $\sigma_{B,c}^M$  (blue dotted): erosion-based with tunable threshold  $c$ , generalising ReLU (Definition 6.8).

## 10. DISCUSSION AND PERSPECTIVES

Table 10 summarises the morphological adjoint pairs established in this paper for standard deep learning operations. Table 11 compares traditional CNN architectures with their morphological counterparts and the new designs proposed in this paper.

TABLE 10. Morphological adjunctions for standard deep learning operations. Each row identifies the lattice, the erosion, and the corresponding adjoint dilation. <sup>†</sup> (Lemma 8.2).

DL operation	Erosion $\varepsilon$	Adjoint dilation $\delta^*$	Lattice
Conv. as Fourier erosion ( $k \geq 0$ )	$\varepsilon_k^{\text{Conv}} : f \mapsto f * k$	Wiener deconv. $\delta_k^{*,\text{Conv}} : \hat{f} \mapsto \frac{ K ^2}{ K ^2 + \varepsilon^2} \hat{f}$	Fourier ( $L^n, \leq_F$ )
Conv. as ptwise increasing map ( $k \geq 0$ )	$\varepsilon_k^{\text{Conv}} : f \mapsto f * k$	Only up-per/lower bounds <sup>†</sup> : $\min_i g(x+x_i)/k(x_i)$	Pointwise ( $\mathcal{L}, \leq$ )
Max-plus dilation	erosion- $\varepsilon_b f = \inf_y \{f(x+y) - b(y)\}$	$\delta_{b^*} f = \sup_y \{f(x-y) + b(-y)\}$	Pointwise ( $\mathcal{L}, \leq$ )
Max-times dilation	erosion- $\varepsilon_b^\times f = \inf_y f(x+y)/b(y)$	$\delta_{b^*}^\times f = \sup_y f(x-y) \cdot b(-y)$	Positive ( $\mathcal{L}^+, \leq$ )
Strided conv. (stride $R$ )	$\varepsilon_k^{\downarrow R}(f)$ (erosion-decimation)	Transposed conv. $\delta_k^{*\uparrow R}(f)$	Pointwise ( $\mathcal{L}, \leq$ )
Max-pooling (pool size $R$ )	Flat min-erosion $\varepsilon_R^{\text{MP}}(f) = \min_{y \in W} f(x+y)$	$\delta_R^{\text{MP}}(f) = \max_{y \in W} f(x-y)$	Pointwise ( $\mathcal{L}, \leq$ )
Self-dual dilation	erosion- $\varepsilon_W^{\text{Med}} : \preceq$ -infimum over $W$	$\delta_W^{*\text{Med}} : \preceq$ -supremum over $W$	Median ( $\mathcal{L}, \preceq$ )
ReLU (as dilation/closing)	Global erosion: $\varepsilon^{\text{ReLU}}(g) = g$ if $g \geq 0$ everywhere; $-\infty$ otherwise (non-pointwise)	adjoint $\delta^{\text{ReLU}}(f) = \max(0, f)$ (extensive, idempotent: closing)	Pointwise ( $\mathcal{L}, \leq$ )

**10.1. Summary of contributions and corrected principles.** The preceding sections establish the following algebraic principles for the analysis of convolutional deep architectures. We state them with the precision that the fixed-point analysis of Section 8 required.

**MMBB-increasing basis of convolution.** The morphological basis  $\text{Bas}(k)$  of a linear convolution kernel  $k \geq 0$  (normalised, finite support  $N$ ) is isomorphic to the hyperplane  $\{g \in \mathbb{R}^N : \langle k, g \rangle = 0\}$ , computed via the characteristic matrix  $A_k$  (Theorems 4.3 and 4.12). A CNN convolution with a general (signed) kernel decomposes as the difference of two such suprema of erosions (Theorem 4.4). Learnable MMBB layers (Equation (29)) are a finite truncation of this basis and approximate any TI increasing operator to arbitrary precision (Theorem 4.15).

**Pooling as morphological pyramid.** Down/up-sampling pairs in standard deep architectures are adjoint operators in complete inf-semilattices. Max-pooling is the Heijmans dilation pyramid with flat structuring element (Theorem 5.5); strided and dilated convolution are the Goutsias–Heijmans erosion pyramid and its adjoint synthesis (Theorem 5.6); and the Laplacian pyramid is the top-hat of the Gaussian pyramid opening (Theorem 5.8). All are special cases of a single adjunction framework.

**Cross-lattice structure of standard CNN layers.** A key finding of this paper is that the standard CNN pipeline (linear convolution + ReLU + flat max-pooling) is a *cross-lattice operator*: the convolution  $f \mapsto f * k$  is an erosion in the Fourier inf-semilattice  $(L^n, \leq_F)$ , while max-pooling  $\delta_R^{\text{MP}}$  is a dilation in the pointwise lattice  $(\mathcal{L}, \leq)$ . These two operators live in different lattice structures and are adjoint in different senses: the adjoint of convolution in  $(L^n, \leq_F)$  is the Wiener deconvolution (a linear operator); its adjoint in  $(\mathcal{L}, \leq)$  is a weighted infimum (a multiplicative erosion, Theorem 8.2); in neither case a max-plus dilation. The composition is therefore *not* a morphological opening in either lattice (Theorem 8.5), and standard CNNs are generically not idempotent.

**Three idempotent layer designs.** Two families of CNN-like layers that *are* genuine morphological openings are identified in the pointwise and Fourier lattices (Theorems 8.4 and 8.6); a third in the median lattice (Section 9): (I) the *pure morphological* (max-plus) layer  $\gamma_b^{\text{M}} = \delta_{b^*} \circ \varepsilon_b$ , where both erosion and dilation use the same structuring function in the pointwise lattice; and (II) the *spectral Wiener* layer  $\gamma_k^{\text{F}} = \delta_k^{*, \text{Conv}} \circ \varepsilon_k^{\text{Conv}}$  (convolution followed by Tikhonov-regularised Wiener deconvolution), an opening in the Fourier lattice, exactly idempotent as  $\epsilon \rightarrow 0$ ; and (III) the *self-dual opening*  $\gamma_W^{\text{Med}}$  in the median inf-semilattice (Section 9). Types (I) and (III) are exactly idempotent; Type (II) is exactly idempotent only in the limit  $\epsilon \rightarrow 0$  and approximately idempotent for finite  $\epsilon > 0$ .

**Fixed points and inversion (adjointness).** For layers of type (I): the adjoint of  $\varepsilon_b$  is  $\delta_{b^*}$  (max-plus dilation by the transposed structuring element); the opening  $\gamma_b^{\text{M}}$  is idempotent, and the morphological UNet sampling skeleton built from such adjoint pairs is idempotent when the spectral operators  $\Sigma_\ell^{\text{Spec}}$  are absent (Theorems 7.8 and 7.9). For layers of type (II): the adjoint of  $\varepsilon_k^{\text{Conv}}$  is  $\delta_k^{*, \text{Conv}}$  (Wiener filter, linear); the opening  $\gamma_k^{\text{F}}$  is an idempotent spectral projection. For a standard CNN: neither adjointness holds between its convolution and its max-pooling; depth provides genuine representational power precisely because the layer is not idempotent.

**Residuals and skip connections.** Residual connections in ResNet compute top-hat transforms: if the residual function  $F$  approximates  $\gamma_b^{\text{M}} - \text{Id}$ , the block  $F(f) + f$  computes the morphological opening  $\gamma_b^{\text{M}}(f)$ , which is idempotent by type (I), reaching its fixed point in a single block (Theorem 8.11). Skip connections in UNet inject the detail signal of the morphological pyramid decomposition, breaking the idempotency of the sampling skeleton constructively (Theorem 8.13).

**Self-dual operators.** The median inf-semilattice  $(\text{Fun}(E, \mathbb{R}), \preceq)$  provides the Type-III idempotent design: the self-dual opening  $\gamma_W^{\text{Med}}$  is idempotent and its fixed-point set is closed under negation (Theorem 9.14). Its fixed-point set equals the image of the opening and coincides with the set of signals representable by the median-MMBB basis of  $W$  (Theorem 9.18).

**10.2. Open problems on morphological basis learning.** The cross-lattice analysis and the MMBB basis theory together raise several open questions of direct relevance to the computational programme of Maragos and collaborators [12, 13, 16] and to the training analysis of Blusseau [8] and Dimitrova, Blusseau, and Velasco-Forero [14].

- (1) *Cross-lattice learning and the role of activation.* Fotopoulos and Maragos [16] find that “linear” activations are essential for training deep morphological networks, and that residual connections improve generalisation. Our cross-lattice analysis (Theorem 8.5) suggests a reason: without a nonlinearity that maps the Fourier-lattice output of convolution back into the pointwise lattice before max-pooling, the composition has no adjunction structure. Conversely, designing architectures that *stay* in a single lattice throughout (type (I) or type (II)) avoids this mismatch entirely. A precise quantification of the idempotency defect of the cross-lattice composition as a function of the kernel  $k$  and window  $W$  is an open problem.
- (2) *Basis recovery by gradient descent.* Does gradient descent on the MMBB-layer loss (29) recover elements of the true basis  $\text{Bas}(k)$ , or converge to arbitrary functions in the kernel? The orthogonality constraint (basis elements are orthogonal to  $k$  in  $\mathbb{R}^N$ ) suggests a natural regularisation term for enforcing this.
- (3) *Gradient descent convergence to MMBB bases.* Dimitrova, Blusseau, and Velasco-Forero [14] show empirically that initialisation and layer differentiability strongly influence which morphological representations are learned. The analysis of Section 9 (Theorems 9.18 and 9.19) identifies the precise algebraic content: training a morphological layer converges to a structuring function  $b$  (or window  $W$ ) whose MMBB basis represents the training data as fixed points. Three distinct fixed-point regimes exist (Types I, II, and III), each with qualitatively different MMBB basis geometry; different initialisations select different basins. Formalising this as a convergence result for gradient descent on morphological layers is an important open problem as well as characterising the basins of attraction for hard (non-smooth) layers, where gradient descent stalls at the facet boundaries of the MMBB representation.
- (4) *Adjoint of convolution and morphological deconvolution.* Lemma 8.2 identifies the pointwise upper adjoint of convolution as a weighted infimum (a multiplicative erosion). Designing learnable layers that explicitly implement this adjoint, and studying whether such layers can be trained stably, connects directly to a problem on morphological deconvolution and blind deconvolution.
- (5) *Sample complexity of MMBB approximation.* What is the sample complexity of learning a finite sub-basis of  $\text{Bas}(k)$  of size  $L$  as a function of  $L$ ,  $N = |\text{Spt}(k)|$ , and the approximation gap?

**10.3. The Fourier perspective: a companion programme.** The Fourier inf-semilattice  $(L^n, \leq_F)$ , where linear convolution is an erosion and its Wiener-filter deconvolution is the adjoint dilation [25], provides the natural algebraic framework for the spectral Wiener opening (type (II)) of this paper, and more broadly for the spectral interpretation of CNNs. The author’s DGMM 2025 contribution [4] shows that scattering networks [29] admit a morphological interpretation via MMBB in this Fourier lattice: the wavelet modulus nonlinearity is an erosion in  $(L^n, \leq_F)$ , and the universality of scattering networks is a consequence of the MMBB representation theorem. This programme is the subject of ongoing research.

A structural observation tying together the three lattice orderings of this paper is given in the following proposition.

**Proposition 10.1** (Unification via complex ordering). *The pointwise order  $\leq$  on  $\text{Fun}(E, \mathbb{R}^+)$ , the median partial ordering  $\preceq$  on  $\text{Fun}(E, \mathbb{R})$  (Theorem 9.1), and the spectral ordering  $\leq_F$  on*

$\text{Fun}(\mathbb{R}^n, \mathbb{R})$  (defined via Fourier magnitudes [4]) are all restrictions of the complex partial ordering  $\leq_{\mathbb{C}}$  on  $\mathbb{C}$ :

$$z_1 \leq_{\mathbb{C}} z_2 \iff |z_1| \leq |z_2| \text{ and } \angle z_1 = \angle z_2. \tag{93}$$

Restricting to  $\text{Im}(z) = 0, z \geq 0$  gives  $\leq$ ; restricting to  $\text{Im}(z) = 0$  gives the median ordering  $\preceq$ ; the pointwise extension of  $\leq_{\mathbb{C}}$  to Fourier transforms gives  $\leq_F$ . Consequently, the cross-lattice jump in a standard CNN layer (from the Fourier lattice after convolution to the pointwise lattice at max-pooling) corresponds to restricting  $\leq_{\mathbb{C}}$  from the full complex plane to the non-negative real line, discarding phase and magnitude interplay. The spectral Wiener opening (type II) stays within  $(L^n, \leq_F)$  throughout, avoiding this restriction.

This perspective provides a unified geometric picture: the three lattices correspond to three phase-angle regimes of the same complex ordering, and the cross-lattice structure of a standard CNN is a jump between regimes that breaks adjointness.

**10.4. Batch normalisation, dropout, and attention.** Batch normalisation re-centres and rescales feature maps; with positive learned scale it is a lattice automorphism in the pointwise lattice, preserving the fixed-point sets of surrounding morphological layers. More precisely, it maps every fixed-point set of the form  $\text{Im}(\gamma_b^M)$  to an affinely rescaled version of itself. Dropout is a random sub-lattice projection (zeroing activations corresponds to projecting onto a random face of the positive orthant). Attention [45] is a data-dependent weighted summation; it is neither an erosion nor a dilation in the pointwise or Fourier lattices as defined here, but it may admit a morphological interpretation in a data-dependent or kernel-weighted lattice. A complete treatment of these operations is left for future work.

**10.5. Connection to category theory.** The adjunctions in this paper,  $(\varepsilon_b, \delta_{b^*})$  in the pointwise lattice,  $(\varepsilon_k^{\text{Conv}}, \delta_k^{*, \text{Conv}})$  in the Fourier lattice, and the pyramid adjoint pairs of Section 5, are concrete instances of categorical adjoint functors in the sense of [10, 15]. The present paper adds to the categorical picture a *lattice-specificity* that categorical approaches lack: adjointness is not a property of a layer in isolation but of a layer *within a specified lattice*. The cross-lattice phenomenon of standard CNNs shows that two operators can each be individually well-behaved (one an erosion, the other a dilation) while their composition lacks any adjunction structure because they inhabit different lattices. Formalising the category of complete lattices with lattice-morphisms (operators that preserve a specific lattice structure) as a concrete subcategory of the gradient-based learning framework [10] is an interesting direction for future work which we preliminarily explore in appendix A.

ACKNOWLEDGEMENTS

I warmly thank my former colleagues at the Center for Mathematical Morphology (CMM / Mines Paris, PSL University), namely Santiago Velasco-Forero for many years of stimulating collaboration on mathematical morphology and deep learning; Samy Blusseau for discussions on morphological adjunctions and on the training of morphological networks; and Valentin Penaud-Polge for fruitful collaboration on the development of morphological group theory for equivariant deep learning.

The first draft of the manuscript was initiated during my academic visiting period to NYU in 2023, partially funded by the Fondation MINES Paris. The final work has been supported by funding from my AI Chair at PR[AI]RIE-PSAI (ANR-23-IACL-0008, France 2030).

## REFERENCES

- [1] J. Angulo, “Some open questions on morphological operators and representations in the deep learning era,” in *Discrete Geometry and Mathematical Morphology (DGMM 2021)*, Lecture Notes in Computer Science, vol. 12708, pp. 3–19, Springer, 2021. (*Invited keynote.*)
- [2] J. Angulo, “Nonlinear Representation Theory of Equivariant CNNs on Homogeneous Spaces Using Group Morphology,” in *Discrete Geometry and Mathematical Morphology (DGMM 2024)*, Lecture Notes in Computer Science, vol. 14605, pp. 255–267, Springer, 2024.
- [3] G. J. Angulo, “Group morphology fixed points on homogeneous spaces for deep learning equivariant networks,” in *Geometric Science of Information (GSI 2025)*, Lecture Notes in Computer Science, vol. 15537, pp. 41–50, Springer, 2025.
- [4] G. J. Angulo, “A mathematical morphology view of the universal representation of scattering networks,” in *Discrete Geometry and Mathematical Morphology (DGMM 2025)*, Lecture Notes in Computer Science, vol. 16296, pp. 357–370, Springer, 2025.
- [5] R. Arora, A. Basu, P. Mianjy, and A. Mukherjee, “Understanding deep neural networks with rectified linear units,” in *International Conference on Learning Representations (ICLR)*, 2018.
- [6] G. J. F. Banon and J. Barrera, “Decomposition of mappings between complete lattices by mathematical morphology, Part I: General lattices,” *Signal Processing*, vol. 30, no. 3, pp. 299–327, 1993.
- [7] S. Blusseau, S. Velasco-Forero, J. Angulo, and I. Bloch, “Morphological adjunctions represented by matrices in max-plus algebra for signal and image processing,” in *Discrete Geometry and Mathematical Morphology (DGMM 2022)*, Lecture Notes in Computer Science, vol. 13493, pp. 206–218, Springer, 2022.
- [8] S. Blusseau, “Training morphological neural networks with gradient descent: some theoretical insights,” in *Discrete Geometry and Mathematical Morphology (DGMM 2024)*, Lecture Notes in Computer Science, vol. 14605, pp. 228–240, Springer, 2024.
- [9] A. Bottenmuller, G. Tochon, R. Hermary, É. Puybareau, and J. Angulo, “Improving morphological networks for learning image-to-image transforms,” in *Discrete Geometry and Mathematical Morphology (DGMM 2025)*, Lecture Notes in Computer Science, vol. 16296, pp. 449–461, Springer, 2025.
- [10] G. S. H. Cruttwell, B. Gavranović, N. Ghani, P. Wilson, and F. Zanasi, “Categorical foundations of gradient-based learning,” in *Programming Languages and Systems – ESOP 2022*, Lecture Notes in Computer Science, vol. 13240, pp. 1–28, Springer, 2022.
- [11] J. L. Davidson and G. X. Ritter, “Theory of morphological neural networks,” in *Proc. SPIE Digital Optical Computing II*, vol. 1704, pp. 378–389, 1992.
- [12] N. Dimitriadis and P. Maragos, “Advances in morphological neural networks: training, pruning and enforcing shape constraints,” in *IEEE ICASSP*, pp. 3825–3829, 2021.
- [13] N. Dimitriadis and P. Maragos, “Morphological neural networks: expressing and learning better geometric features,” in *IEEE ICCV*, 2023.
- [14] M. Dimitrova, S. Blusseau, and S. Velasco-Forero, “Learning morphological representations of image transformations: influence of initialization and layer differentiability,” in *Discrete Geometry and Mathematical Morphology (DGMM 2025)*, Lecture Notes in Computer Science, Springer, 2025.
- [15] B. Fong, D. I. Spivak, and R. Tuyéras, “Backprop as functor: a compositional perspective on supervised learning,” in *Proc. 34th Annual ACM/IEEE Symposium on Logic in Computer Science (LICS)*, pp. 1–13, 2019.

- [16] K. Fotopoulos and P. Maragos, “Training deep morphological neural networks as universal approximators,” arXiv:2505.09710, 2025.
- [17] G. Franchi, M. Fehri, and A. Yao, “Deep morphological networks,” *Pattern Recognition*, vol. 102, p. 107246, 2020.
- [18] I. Goodfellow, Y. Bengio, and A. Courville, *Deep Learning*, MIT Press, 2016.
- [19] J. Goutsias and H. J. A. M. Heijmans, “Nonlinear multiresolution signal decomposition schemes – Part I: morphological pyramids,” *IEEE Transactions on Image Processing*, vol. 9, no. 11, pp. 1862–1876, 2000.
- [20] H. J. A. M. Heijmans, C. Ronse. “The algebraic basis of mathematical morphology I. Dilations and erosions,” *Computer Vision, Graphics, and Image Processing*, vol. 50, no. 3, pp.245–295, 1990.
- [21] H. J. A. M. Heijmans, *Morphological Image Operators*, Academic Press, Boston, 1994.
- [22] K. He, X. Zhang, S. Ren, and J. Sun, “Delving deep into rectifiers: surpassing human-level performance on ImageNet classification,” in *IEEE ICCV*, pp. 1026–1034, 2015.
- [23] K. He, X. Zhang, S. Ren, and J. Sun, “Deep residual learning for image recognition,” in *IEEE CVPR*, pp. 770–778, 2016.
- [24] R. Hermary, G. Tochon, É. Puybureau, A. Kirszenberg, and J. Angulo, “Learning grayscale mathematical morphology with smooth morphological layers,” *Journal of Mathematical Imaging and Vision*, vol. 64, pp. 736–753, 2022.
- [25] R. Keshet, “A Morphological View on Traditional Signal Processing,” in *Mathematical Morphology and its Applications to Image and Signal Processing. Computational Imaging and Vision*, vol. 18. Springer, 2002.
- [26] M. Khosravi and R. W. Schafer, “Implementation of linear digital filters based on morphological representation theory,” *IEEE Transactions on Signal Processing*, vol. 42, no. 9, pp. 2264–2275, 1994.
- [27] Y. LeCun, L. Bottou, Y. Bengio, and P. Haffner, “Gradient-based learning applied to document recognition,” *Proceedings of the IEEE*, vol. 86, no. 11, pp. 2278–2324, 1998.
- [28] A. L. Maas, A. Y. Hannun, and A. Y. Ng, “Rectifier nonlinearities improve neural network acoustic models,” in *Proc. ICML Workshop on Deep Learning for Audio, Speech and Language Processing*, 2013.
- [29] S. Mallat, “Group invariant scattering,” *Communications on Pure and Applied Mathematics*, vol. 65, no. 10, pp. 1331–1398, 2012.
- [30] P. Maragos and R. W. Schafer, “Morphological filters – Part I: their set-theoretic analysis and relations to linear shift-invariant filters,” *IEEE Transactions on Acoustics, Speech, and Signal Processing*, vol. 35, no. 8, pp. 1153–1169, 1987.
- [31] P. Maragos, “A representation theory for morphological image and signal processing,” *IEEE Transactions on Pattern Analysis and Machine Intelligence*, vol. 11, no. 6, pp. 586–599, 1989.
- [32] P. Maragos, “Tropical geometry, morphological analysis, and deep neural networks,” *IEEE Signal Processing Magazine*, vol. 38, no. 1, pp. 50–65, 2021.
- [33] D. Marcondes and J. Barrera, “The lattice overparameterization paradigm for the machine learning of lattice operators,” in *Discrete Geometry and Mathematical Morphology (DGMM 2024)*, Lecture Notes in Computer Science, vol. 14605, pp. 204–216, Springer, 2024.
- [34] G. Matheron, *Random Sets and Integral Geometry*, Wiley, New York, 1975.
- [35] G. F. Montufar, R. Pascanu, K. Cho, and Y. Bengio, “On the number of linear regions of deep neural networks,” in *Advances in Neural Information Processing Systems*, vol. 27, pp. 2924–2932, 2014.

- [36] S. Ovchinnikov, “Max-min representation of piecewise linear functions,” *Beiträge zur Algebra und Geometrie*, vol. 43, no. 1, pp. 297–302, 2002.
- [37] V. Penaud-Polge, S. Velasco-Forero, and J. Angulo, “Group equivariant networks using morphological operators,” in *Discrete Geometry and Mathematical Morphology (DGMM 2024)*, Lecture Notes in Computer Science, vol. 14605, pp. 165–177, Springer, 2024.
- [38] V. Penaud-Polge, S. Velasco-Forero, and J. Angulo, “Group equivariant morphological networks,” *SIAM Journal on Imaging Sciences*, vol. 18, no. 4, pp. 2236–2276, 2025. DOI: 10.1137/24M1685766.
- [39] L. F. C. Pessoa and P. Maragos, “Neural networks with hybrid morphological/rank/linear nodes: a unifying framework with applications to handwritten character recognition,” *Pattern Recognition*, vol. 33, no. 6, pp. 945–960, 2000.
- [40] N. Rahaman et al., “On the spectral bias of neural networks,” in *Proc. 36th International Conference on Machine Learning*, PMLR, vol. 97, pp. 5301–5310, 2019.
- [41] G. X. Ritter and P. Sussner, “An introduction to morphological neural networks,” in *Proc. 13th ICPR*, vol. 4, pp. 709–717, 1996.
- [42] O. Ronneberger, P. Fischer, and T. Brox, “U-Net: convolutional networks for biomedical image segmentation,” in *Medical Image Computing and Computer-Assisted Intervention (MICCAI)*, Lecture Notes in Computer Science, vol. 9351, pp. 234–241, Springer, 2015.
- [43] M. Sangalli, S. Blusseau, S. Velasco-Forero, and J. Angulo, “Scale equivariant neural networks with morphological scale-spaces,” in *Discrete Geometry and Mathematical Morphology (DGMM 2021)*, Lecture Notes in Computer Science, vol. 12708, pp. 483–495, Springer, 2021.
- [44] J. Serra, *Image Analysis and Mathematical Morphology*, Academic Press, London, 1982.
- [45] A. Vaswani et al., “Attention is all you need,” in *Advances in Neural Information Processing Systems*, vol. 30, 2017.
- [46] S. Velasco-Forero, R. Pagès, and J. Angulo, “Learnable empirical mode decomposition based on mathematical morphology,” *SIAM Journal on Imaging Sciences*, vol. 15, no. 1, pp. 23–44, 2022. DOI: 10.1137/21M1417867.
- [47] S. Velasco-Forero, A. Rhim, and J. Angulo, “Fixed point layers for geodesic morphological operations,” in *33rd British Machine Vision Conference (BMVC 2022)*, London, UK, November 21–24, 2022, BMVA Press, paper no. 480.
- [48] S. Velasco-Forero and J. Angulo, “MorphoActivation: generalizing ReLU activation function by mathematical morphology,” in *Discrete Geometry and Mathematical Morphology (DGMM 2022)*, Lecture Notes in Computer Science, vol. 13493, pp. 449–461, Springer, 2022.
- [49] L. Zhang, G. Naitzat, and L.-H. Lim, “Tropical geometry of deep neural networks,” arXiv:1805.07091, 2018.

TABLE 11. Standard deep learning architectures, their morphological interpretations established in this paper, and the morphologically-motivated variants proposed here.

Architecture	Standard form	Morphological interpretation	Proposed variant
<b>CNN layer</b>	$\delta_R^{\text{MP}}(\text{ReLU}(f*k));$ bias $\alpha$ , stride $R$	Cross-lattice operator: $f*k$ is a Fourier-lattice erosion; $\delta_R^{\text{MP}}$ a pointwise dilation. Not idempotent (Theorem 8.5). APD factorisation: $\Psi_{R;\alpha}^{\text{APD}}(\Sigma_K^{\text{Spec}}(f))$	<b>Type-I MMBB layer:</b> $\gamma_b^{\text{M}} = \delta_{b^*} \circ \varepsilon_b$ (both pointwise); exactly idempotent opening. <b>Type-II:</b> $\gamma_k^{\text{F}}$ (Fourier lattice); exact spectral projection at $\epsilon=0$ , approximately idempotent for $\epsilon>0$
<b>ResNet block</b>	$F(f) + f$ , $F$ a conv stack; skip provides identity path	When $F \approx \gamma_b^{\text{M}} - \text{id}$ : block computes opening $\gamma_b^{\text{M}}(f)$ . Stacking $n$ such blocks: one-step convergence by idempotency (Theorem 8.10). Naive block $\gamma(f)+f$ diverges	<b>Morphological ResNet:</b> learnable $b$ instead of kernel $k$ ; explicit Type-I opening; self-dual variant for signed residuals
<b>UNet coder</b>	<b>en-</b> Strided conv + max-pool at each level; transposed conv + upsample in decoder	Sampling skeleton = Goutsias–Heijmans pyramid $(\varepsilon_b^{\downarrow R}, \delta_b^{*\uparrow R})$ : an adjoint pair; skeleton is idempotent. Full net (with $\Sigma^{\text{Spec}}$ convs) is not (Theorem 7.9, Theorem 8.13)	<b>Morphological UNet:</b> encoder $\varepsilon_b^{\downarrow R}$ , decoder $\delta_b^{*\uparrow R}$ ; adjoint pair guarantees adjunction structure
<b>UNet skip connections</b>	Concatenation of encoder and decoder feature maps	Detail signal of the morphological pyramid: top-hat $\Gamma_b(f) = f - \gamma_b^{\text{M}}(f)$ at each scale (Theorem 7.9)	<b>UResNet:</b> residual skip = top-hat $\Gamma_b(f)$ ; algebraically motivated; decoder reconstructs from adjoint upsampling + detail
<b>Activation (ReLU)</b>	$\sigma(f) = \max(0, f)$ ; kills negative activations; treats $f^+$ and $f^-$ asymmetrically	Closing in $(\mathcal{L}, \leq)$ : extensive and idempotent, <i>not</i> a median-lattice dilation. MMBB form: $f = f^+ - f^-$ , both parts dilations (Theorems 6.1 and 6.10)	<b>Leaky/Param ReLU</b> ( $0 < \beta^- \leq 1$ ): proper median-lattice dilation. <b>Self-dual opening</b> $\gamma_W^{\text{Med}}$ : idempotent in $(\mathcal{L}, \preceq)$ ; sign-symmetric; for signed feature maps

## APPENDIX A. ELEMENTS OF THE CONNECTION TO CATEGORY THEORY

This appendix develops the preliminary connection between the morphological lattice framework of this paper and the categorical approaches to deep learning of Cruttwell et al. [10] and Fong–Spivak–Tuyéras [15]. We show that the morphological adjunctions of this paper are concrete instances of categorical adjunctions, and identify the precise sense in which the present framework can be seen as a *representation-theoretic concretisation* of the abstract categorical skeleton.

## A.1. The category of complete lattices with morphisms.

**Definition A.1** (Category  $\mathbf{CLat}$ ). The category  $\mathbf{CLat}$  has:

- *Objects*: complete lattices  $(\mathcal{L}, \leq)$ .
- *Morphisms*:  $\text{hom}(\mathcal{L}_1, \mathcal{L}_2) = \{\text{increasing maps } \Psi : \mathcal{L}_1 \rightarrow \mathcal{L}_2\}$ .
- *Composition*: function composition (increasing maps compose as increasing maps).
- *Identity*: the identity map  $\text{id}_{\mathcal{L}}$ .

$\mathbf{CLat}$  is a concrete category (objects and morphisms have underlying sets and functions).

Each of the three lattice structures used in this paper defines an object of  $\mathbf{CLat}$ :

- The pointwise lattice  $(\text{Fun}(E, \overline{\mathbb{R}}), \leq)$ : the standard morphological setting.
- The Fourier inf-semilattice  $(L^n, \leq_F)$ : the spectral setting for convolution.
- The median inf-semilattice  $(\text{Fun}(E, \mathbb{R}), \preceq)$ : the self-dual setting for signed activations.

A standard CNN layer is a morphism in  $\mathbf{CLat}$  from  $(\text{Fun}(E, \overline{\mathbb{R}}), \leq)$  to itself when  $k \geq 0$  (since  $f \mapsto \delta_R^{\text{MP}}(\text{ReLU}(f * k))$  is increasing). However, as established in Theorem 8.5, this morphism is *not* part of an adjunction in  $\mathbf{CLat}$ , because the adjoint of convolution is not a morphism in the pointwise lattice but in the Fourier lattice.

A.2. Adjunctions in  $\mathbf{CLat}$  and the morphological adjunctions.

**Definition A.2** (Adjunction in  $\mathbf{CLat}$ ). An *adjunction*  $\varepsilon \dashv \delta$  in  $\mathbf{CLat}$  consists of morphisms  $\varepsilon : \mathcal{L}_1 \rightarrow \mathcal{L}_2$  and  $\delta : \mathcal{L}_2 \rightarrow \mathcal{L}_1$  satisfying, for all  $f \in \mathcal{L}_1$  and  $g \in \mathcal{L}_2$ :

$$\varepsilon(f) \leq_2 g \iff f \leq_1 \delta(g).$$

This is exactly Theorem 2.1. The unit  $\eta = \delta \circ \varepsilon \geq \text{id}$  is a natural transformation satisfying  $\varepsilon \circ \eta = \varepsilon$  (absorption), and the counit  $\epsilon = \varepsilon \circ \delta \leq \text{id}$  satisfies  $\delta \circ \epsilon = \delta$ .

The morphological adjunctions of this paper are:

**Proposition A.3** (Catalogue of adjunctions in  $\mathbf{CLat}$ ). *The following adjunctions  $\varepsilon \dashv \delta$  hold in  $\mathbf{CLat}$ :*

- (i) Max-plus erosion–dilation:  $\varepsilon_b \dashv \delta_{b^*}$  in the pointwise lattice  $(\text{Fun}(E, \overline{\mathbb{R}}), \leq)$ . Unit:  $\delta_{b^*} \varepsilon_b = \gamma_b^{\text{M}}$  (morphological opening, idempotent). Counit:  $\varepsilon_b \delta_{b^*} = \varphi_b^{\text{M}}$  (morphological closing, idempotent).
- (ii) Max-times erosion–dilation:  $\varepsilon_b^\times \dashv \delta_{b^*}^\times$  in the positive lattice  $(\text{Fun}(E, (0, +\infty)), \leq)$ . Unit:  $\gamma_b^\times$  (max-times opening, idempotent).
- (iii) Convolution–deconvolution:  $\varepsilon_k^{\text{Conv}} \dashv \delta_k^{*\text{Conv}}$  in the Fourier lattice  $(L^n, \leq_F)$ . Unit:  $\gamma_k^{\text{F}}$  (spectral opening, projection onto range of  $K(\omega)$ , idempotent).
- (iv) Erosion–decimation–dilation–interpolation:  $\varepsilon_b^{\downarrow R} \dashv \delta_b^{*\uparrow R}$  between  $(L^{RM \times RN}, \leq_F)$  and  $(L^{M \times N}, \leq_F)$  (Goutsias–Heijmans, Theorem 5.2). Unit:  $\gamma_b^{\downarrow R \uparrow}$  (pyramid opening).
- (v) Self-dual erosion–dilation:  $\varepsilon_W^{\text{Med}} \dashv \delta_W^{*\text{Med}}$  in the median lattice  $(\text{Fun}(E, \mathbb{R}), \preceq)$ . Unit:  $\gamma_W^{\text{Med}}$  (self-dual opening, idempotent).

In each case, the unit is the morphological opening  $\gamma = \delta \circ \varepsilon$ , the opening is idempotent by the categorical identity  $\gamma \circ \gamma = \delta \varepsilon \delta \varepsilon = \delta(\varepsilon \delta) \varepsilon = \delta \text{id } \varepsilon = \delta \varepsilon = \gamma$ , where the third step uses the counit identity  $\varepsilon \delta \varepsilon = \varepsilon$  (proof via the adjunction triangle identities).

*Proof.* Part (i): verified in Section 2. Parts (ii)–(v): verified in Sections 2 and 5 and Propositions 2.4, 5.2. The idempotency of each unit follows from the categorical adjunction triangle identities: for any adjunction  $\varepsilon \dashv \delta$ , one has  $\varepsilon \circ \eta = \varepsilon$  (where  $\eta = \delta \varepsilon$  is the unit), which gives  $\gamma^2 = \delta \varepsilon \delta \varepsilon = \delta(\varepsilon \delta \varepsilon) = \delta \varepsilon = \gamma$  using the triangle identity  $\varepsilon \delta \varepsilon = \varepsilon$ .  $\square$

**A.3. The Para construction and learnable layers.** The categorical framework of Cruttwell et al. [10] uses the *Para construction* to model parameterised maps (neural network layers with learnable parameters).

**Definition A.4** (Para(**CLat**)). Given **CLat**, the *Para construction* produces a category Para(**CLat**) whose:

- *Objects*: complete lattices (same as **CLat**).
- *Morphisms* from  $\mathcal{L}_1$  to  $\mathcal{L}_2$ : pairs  $(P, \Psi)$  where  $P$  is a parameter space (also a complete lattice) and  $\Psi : \mathcal{L}_1 \times P \rightarrow \mathcal{L}_2$  is an increasing morphism.
- *Composition*:  $(Q, \Phi) \circ (P, \Psi) = (P \times Q, (f, p, q) \mapsto \Phi(\Psi(f, p), q))$ .

A *morphological layer* is a morphism in Para(**CLat**): a parameterised increasing map.

The morphological layers of this paper are instances:

- **MMBB layer** (29): parameter space  $P = \text{Fun}(\mathbb{Z}^n, \overline{\mathbb{R}})^L$  (structuring functions  $\{g_{i,j}\}$ ); map  $\Psi(f; \{g_{i,j}\}, \{w_j\}) = \sum_j w_j \max_i(\varepsilon_{g_{i,j}} f)$ .
- **APMO** (61): parameter space  $P = \text{Fun}(\mathbb{Z}^n, \overline{\mathbb{R}})^J \times \mathbb{R}^J$  (structuring functions  $\{b_j\}$  and biases  $\{\alpha_j\}$ ); map  $\Psi^{\text{APMO}}(f; \{b_j\}, \{\alpha_j\}) = \min_j \{\delta_{R,b_j}^{\text{MP}}(f) + \alpha_j\}$ .
- **Standard CNN layer**: parameter space  $P = \text{Fun}(\mathbb{Z}^n, \mathbb{R})^K \times \mathbb{R}^K$  (kernels  $\{k_i\}$  and weights  $\{w_i\}$ ); map  $\Psi(f; \{k_i\}, \{w_i\}) = \delta_R^{\text{MP}}(\text{ReLU}(\sum_i w_i(f * k_i)))$ . This morphism is *not* part of an adjunction in Para(**CLat**) for the reasons identified in Theorem 8.5.

**A.4. Backpropagation and the reverse derivative.** Fong et al. [15] model backpropagation as a functor  $R : \mathbf{Learn} \rightarrow \mathbf{Learn}$  (the *reverse derivative*). In the morphological setting, the analogue of the reverse derivative of an erosion is the adjoint dilation:

**Remark A.5** (Adjoint dilation as categorical reverse derivative). In the category **CLat**, the adjoint dilation  $\delta^* = R(\varepsilon)$  plays the role of the categorical reverse derivative of the erosion  $\varepsilon$ . More precisely:

- For the max-plus erosion  $\varepsilon_b$ , the reverse derivative is  $\delta_{b^*} = R(\varepsilon_b)$ , and the composition  $\delta_{b^*} \circ \varepsilon_b = \gamma_b^{\text{M}}$  is the *projection onto the fixed-point set* of  $\varepsilon_b$  (the opening), analogous to the projection step in gradient descent.
- The MMBB representation  $\Psi f = \sup_{g \in \text{Bas}(\Psi)} \varepsilon_g f$  can be seen as the gradient ascent step of  $\Psi$  in the lattice ordering: each erosion  $\varepsilon_g$  contributes a “subgradient direction” in the lattice, and the supremum selects the tightest lower bound.
- The Banon–Barrera sup-generating operator  $\psi_{g^-, g^+}$  has a forward pass (the erosion  $\varepsilon_{g^-}$  measuring excitation) and a backward pass (the anti-dilation  $\alpha_{g^+}$  measuring inhibition), structurally analogous to the forward/backward passes of a neural network layer.

**Remark A.6** (Lattice-specificity: what categorical approaches lack). The categorical frameworks of [10, 15] are lattice-agnostic: they model composition of morphisms without specifying which lattice each morphism lives in. The present paper adds *lattice-specificity* as a necessary refinement:

- Adjointness is a property of a pair  $(\varepsilon, \delta)$  *within a fixed lattice*. The cross-lattice structure of standard CNNs (Theorem 8.5) shows that two morphisms  $\varepsilon \in \text{hom}(\mathcal{L}_1, \mathcal{L}_2)$  and  $\delta \in \text{hom}(\mathcal{L}_2, \mathcal{L}_1)$  can be individually well-behaved while failing to form an adjunction because they inhabit different lattices.
- The MMBB representation theorems provide the *constructive content* that categorical approaches lack: given an object class (TI, increasing or not, USC operators), it produces an explicit basis decomposition with computable basis functions and quantifiable approximation errors.
- The fixed-point theory identifies which morphisms in  $\text{Para}(\mathbf{CLat})$  are idempotent (the adjunction units  $\gamma = \delta\varepsilon$ ) and which are not (cross-lattice compositions). This is invisible in the abstract categorical framework but has direct architectural implications.

A full formalisation, i.e., identifying  $\text{Para}(\mathbf{CLat})$  as a concrete sub-category of the gradient-based learning framework of [10], with the MMBB basis as the constructive counterpart of the abstract learning rule, remains an interesting direction for future work.

MINES PARIS, PSL UNIVERSITY,, CMA-CENTER FOR APPLIED MATHEMATICS, SOPHIA-ANTIPOLIS, FRANCE  
*Email address:* `jesus.angulo_lopez@minesparis.psl.eu`